

1998

Ecosystem analysis of water column processes in the York River estuary, Virginia: Historical records, field studies and modeling analysis

Yongsik Sin

College of William and Mary - Virginia Institute of Marine Science

Follow this and additional works at: <https://scholarworks.wm.edu/etd>



Part of the [Ecology and Evolutionary Biology Commons](#), [Environmental Sciences Commons](#), and the [Ocean Engineering Commons](#)

Recommended Citation

Sin, Yongsik, "Ecosystem analysis of water column processes in the York River estuary, Virginia: Historical records, field studies and modeling analysis" (1998). *Dissertations, Theses, and Masters Projects*. Paper 1539616855.

<https://dx.doi.org/doi:10.25773/v5-3k3t-7s21>

This Dissertation is brought to you for free and open access by the Theses, Dissertations, & Master Projects at W&M ScholarWorks. It has been accepted for inclusion in Dissertations, Theses, and Masters Projects by an authorized administrator of W&M ScholarWorks. For more information, please contact scholarworks@wm.edu.

INFORMATION TO USERS

This manuscript has been reproduced from the microfilm master. UMI films the text directly from the original or copy submitted. Thus, some thesis and dissertation copies are in typewriter face, while others may be from any type of computer printer.

The quality of this reproduction is dependent upon the quality of the copy submitted. Broken or indistinct print, colored or poor quality illustrations and photographs, print bleedthrough, substandard margins, and improper alignment can adversely affect reproduction.

In the unlikely event that the author did not send UMI a complete manuscript and there are missing pages, these will be noted. Also, if unauthorized copyright material had to be removed, a note will indicate the deletion.

Oversize materials (e.g., maps, drawings, charts) are reproduced by sectioning the original, beginning at the upper left-hand corner and continuing from left to right in equal sections with small overlaps. Each original is also photographed in one exposure and is included in reduced form at the back of the book.

Photographs included in the original manuscript have been reproduced xerographically in this copy. Higher quality 6" x 9" black and white photographic prints are available for any photographs or illustrations appearing in this copy for an additional charge. Contact UMI directly to order.

UMI

A Bell & Howell Information Company
300 North Zeeb Road, Ann Arbor MI 48106-1346 USA
313/761-4700 800/521-0600

**ECOSYSTEM ANALYSIS OF WATER COLUMN PROCESSES IN THE YORK
RIVER ESTUARY, VIRGINIA: HISTORICAL RECORDS, FIELD STUDIES AND
MODELING ANALYSIS**

A Dissertation

Presented to

The Faculty of the School of Marine Science

The College of William and Mary in Virginia

In Partial Fulfillment

Of the Requirements for the Degree of

Doctor of Philosophy

by

Yongsik Sin

1998

UMI Number: 9918000

UMI Microform 9918000
Copyright 1999, by UMI Company. All rights reserved.

**This microform edition is protected against unauthorized
copying under Title 17, United States Code.**

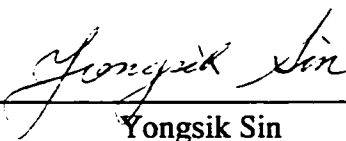
UMI
300 North Zeeb Road
Ann Arbor, MI 48103

APPROVAL SHEET

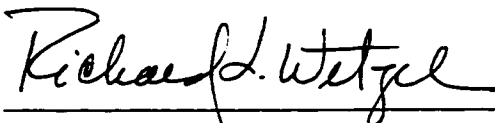
This dissertation is submitted in partial fulfillment of

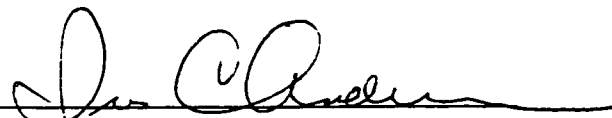
The requirements for the degree of

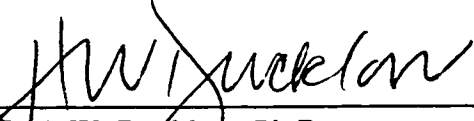
Doctor of Philosophy

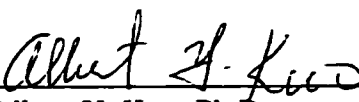

Yongsik Sin

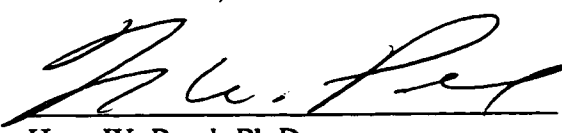
Approved, December 1998


Richard L. Wetzel, Ph.D.
Committee co-chairman/Advisor


Iris C. Anderson, Ph.D.
Committee co-chairman/Advisor


Hugh W. Ducklow, Ph.D.


Albert Y. Kuo, Ph.D.


Hans W. Paerl, Ph.D.
Institute of Marine Sciences
University of North Carolina
Morehead City, North Carolina

DEDICATION

This dissertation is dedicated to my family who supported me with their patience and unconditional love for such a long time.

아버님, 어머님, 그리고 형님, 형수님, 그 기나긴 시간동안 보여주신 끝없는 인내와 사랑이 없었다면 이 논문은 존재하지 않았을 것 입니다. 정말 감사합니다. 특히 물심양면으로 헌신하신 어머님께 이 논문을 바칩니다.

TABLE OF CONTENTS

ACKNOWLEDGMENTS.....	vi
LIST OF TABLES.....	vii
LIST OF FIGURES	viii
ABSTRACT	ix
PROJECT OVERVIEW	
Introduction and Background.....	2
Literature Cited.....	7
SECTION I: Spatial and Temporal Characteristics of Nutrient and Phytoplankton Dynamics in the York River Estuary, Virginia: Analyses of Long Term Data	
Abstract.....	12
Introduction.....	13
Materials and Methods.....	15
Area description and data analyses.....	15
Results.....	19
River discharge and response lag periods.....	19
Seasonality of phytoplankton blooms and productivity.....	22
Effects of river discharge on phytoplankton biomass.....	22
Light limitation, temperature and potential grazing effects.....	27
Nutrient dynamics.....	30
Discussion.....	36
Nutrient limitation.....	36
Seasonal variations in biomass and productivity.....	40
Conclusions.....	47
Literature Cited.....	49
SECTION II: Seasonal Variations of Size Fractionated Phytoplankton along the Salinity Gradient in the York River Estuary, Virginia	
Abstract.....	56
Introduction.....	58
Materials and Methods.....	61

Study site and sample collection.....	61
Chlorophyll <i>a</i> measurement.....	63
Measurement of dissolved inorganic nutrient and physical properties.....	64
Other data collections and statistical analysis.....	65
Results.....	67
River discharge and solar irradiation.....	67
Other physical properties; water depth, temperature, salinity and light attenuation coefficients.....	67
Dissolved inorganic nutrients in the water column.....	71
Temporal and spatial variations of chlorophyll <i>a</i>	77
Linear simple and multiple regression analysis.....	84
Discussion.....	91
Literature Cited.....	101
Appendix I.....	109
Appendix II.....	110
Appendix III.....	111
SECTION III: Ecosystem Modeling Analysis of Size-Structured Phytoplankton Dynamics in the York River Estuary, Virginia	
Abstract.....	113
Introduction.....	115
Materials and Methods.....	117
Area of model application.....	117
Model description.....	117
1. General conceptual structure of the model.....	117
2. Mathematical structure for hydrodynamic processes.....	120
3. Mathematical structure for biological and chemical processes.....	128
Model validation and sensitivity analysis.....	135
Results.....	136
Model validation.....	136
1. Forcing variables.....	136
2. State variables.....	137
Model sensitivity analysis.....	141
1. Model sensitivity: parameter variation.....	141
2. Model sensitivity: forcing variables.....	145
3. Model sensitivity: physical processes.....	149
4. Model sensitivity: boundary conditions.....	153
Discussion.....	158
Conclusions.....	165
Literature Cited.....	167
Appendix I.....	173
PROJECT SUMMARY AND SYNTHESIS.....	176
VITA.....	181

ACKNOWLEDGMENTS

I would like to thank my major advisors, Dr. Richard L. Wetzel and Dr. Iris C. Anderson who provided guidance, motivation and support during the course of this research. I am grateful to Dr. Richard L. Wetzel for his financial and academic assistance which allowed me to complete this study even after 2 years leave of absence. I am indebted to Dr. Iris C. Anderson for her time and efforts which has made this dissertation readable.

I would like to thank the members of my committee for their valuable discussions and insights during both the preparation of my prospectus and the writing of my dissertation. I am especially indebted to Dr. Hugh W. Ducklow for his constructive suggestions and insights which greatly improved the quality of this dissertation and enabled me to publish the first section of this dissertation. I am also grateful to Dr. Albert Y. Kuo for his keen insights, especially on hydrodynamic structure in the ecosystem model of this study. I wish to thank to Dr. Hans W. Paerl for his time and efforts which allowed me to think properly and write this dissertation, in spite of his tight time schedule.

I would like to thank Dr. Leonard W. Haas for his valuable discussions and suggestions which encouraged me to publish the EPA long-term dataset from the York River. He also took me to various meetings so that I could have some inputs from the meetings. I am also grateful to Dr. Ting Dai for his financial support during the final stage of this study. His encouragement and suggestions also were greatly helpful for this study. I would like to thank Dr. Jian Shen and Dr. Kyeong Park for technical assistance at the stage of model development. I wish to thank Dr. Kenneth L. Webb and Dr. Kenneth A. Moore for constructive discussions on nutrient and phytoplankton dynamics. I would like to thank Mr. Gary Anderson for his help with the EPA data set in SAS format. I owe thanks to Dr. Cheol Mo, Dr. Sungchan Kim, Mr. Guan-hong Lee and Dr. Hyeonju Yoon for their help with FORTRAN and life at VIMS. I want to thank William Seufzer, Peter Raymond, David Miller, Craig Tobias, Scott Neubauer and Betty Neikirk for help with field and lab work.

I would like to thank Mrs. Virginia Bray for her constant encouragement and kindness during my stay in a foreign land. I am also deeply grateful to the many friends who encouraged me to survive during my stay at VIMS including the ecosystem process group, Matthew Church, Peter Raymond, Mac Sisson, Jennifer Rhode, Mary Rybitski, Padma Venkatraman, Gary Schultz, Leigh Maccallister, Tami Hutchison, Jacques Oliver, and soccer teams. My special thanks go to Heijin Yun who made my life happier than at any other time.

LIST OF TABLES

SECTION I

1. R^2 for linear regression of surface water salinity vs. river discharge rate.....21
2. R^2 of linear regression analysis.....24

SECTION II

1. Temperature, salinity and light attenuation coefficient..... 70
2. Average ambient concentrations and standard errors of nutrients..... 74
3. Average chlorophyll a concentrations and standard errors..... 83
4. Average chllorophyll:pheopigment ratios and standard errors..... 86
5. Results (r^2) of linear regression analysis on surface water properties..... 88
6. Results (r^2) of linear regression analysis on bottom water properties..... 90

SECTION III

1. Forcing functions, state variables and boundary conditions..... 121
2. The differential equations employed for the state variables..... 124
3. Symbols and units of physical, biological and chemical processes..... 125
4. The results of sensitivity analyses for biological components..... 143
5. The results of sensitivity analyses for chemical components..... 144
6. Average RMS and % change in concentrations of state variables (I)..... 146
7. Average RMS and % change in concentrations of state variables (II)..... 151
8. Percent change in concentrations of state variables when boundary conditions were changed..... 159

LIST OF FIGURES

SECTION I

1. The EPA Chesapeake Bay Monitoring stations in the York River estuary... 16
2. Time series of river discharge rates in the York River estuarine system..... 20
3. Seasonal distributions of chlorophyll *a* and primary production..... 23
4. Correlation between river discharge rates and location of chlorophyll *a* peaks and mean chlorophyll *a* at station LE4.2..... 26
5. Light limitation index..... 29
6. Distributions of N:P molar ratio and chlorophyll *a* 31
7. Salinity dilution curves for water quality properties..... 33
8. Regression of water quality parameters vs. salinity difference..... 35
9. Variations of chlorophyll *a* and salinity difference..... 46

SECTION II

1. Sampling stations in the York River estuary..... 62
2. Time series of river discharge rates from April 1996 to June 1997..... 66
3. Surface daily and monthly PAR at Gloucester Point, Virginia..... 68
4. Temperature, salinity and light attenuation coefficient distributions..... 72
5. Seasonal distributions of ambient nutrients..... 73
6. Temporal variations of molar N:P ratios of ambient nutrients..... 76
7. Seasonal distributions of size fractionated chlorophyll *a*..... 78
8. Percent contributions of three size classes to total chlorophyll *a* in the surface water of the study sites..... 80
9. Percent contributions of three size classes to total chlorophyll *a* in the bottom water of the study sites..... 82
10. Seasonal patterns of acidification ratios..... 85
11. Temporal distributions of chlorophyll *a* at station WE4.2..... 96

SECTION III

1. Study site in the mesohaline zone of the York River estuarine system..... 118
2. Diagram of biological, chemical and physical processes..... 119
3. Geometric structure of the ecosystem model developed in this study..... 122
4. Comparison of predicted values to field data for forcing variables..... 138
5. Validation results for autotrophs and heterotrophs..... 139
6. Validation results for POC, DOC and nutrients..... 140
7. The effects of change in light and temperature on chlorophyll *a* patterns. 147
8. The effects of change in top to bottom salinity difference..... 148
9. The effects of change in top to bottom salinity difference on nutrients.... 150
10. The effects of advection + vertical diffusion on chlorophyll *a* patterns.... 152
11. The effects of advection + vertical diffusion on nutrients..... 154
12. The distributions of diffusion coefficient and chlorophyll *a*..... 155
13. The distributions of diffusion coefficient and nutrients..... 156
14. The distributions of incoming and upward flow and chlorophyll *a*..... 157

ABSTRACT

Analyses of EPA long-term datasets (1985-1994) combined with field studies and ecosystem model development were used to investigate phytoplankton and nutrient dynamics in the York River estuary. Analysis of the EPA dataset showed that algal blooms occurred during winter-spring followed by smaller summer blooms. Peak phytoplankton biomass during the winter-spring blooms occurred in the mid reach of the mesohaline zone whereas during the summer bloom it occurred in the tidal fresh-mesohaline transition zone. River discharge appears to be the major factor controlling the location and timing of the winter-spring blooms and the relative degree of potential nitrogen (N) and phosphorus (P) limitation. Phytoplankton biomass in tidal fresh water regions was limited by high flushing rates. Water residence time was less than cell doubling rate during seasons of high river flow. Positive correlations between PAR at 1m depth and chlorophyll *a* suggested light limitation of phytoplankton in the tidal fresh-mesohaline transition zone. A significant relationship between the delta of salinity between surface and bottom water and chlorophyll *a* distribution suggested the importance of tidal mixing for phytoplankton dynamics in the mesohaline zone. Accumulation of phytoplankton biomass in the mesohaline zone was generally controlled by N with the nutrient supply provided by benthic or bottom water remineralization. In general, phytoplankton dynamics appear controlled to a large extent by resource limitation (bottom-up control) rather than zooplankton grazing (top-down control).

The dynamics of phytoplankton size structure were investigated in the freshwater, transitional and estuarine reaches of the York River over an annual cycle. The contribution of large cells (micro-plankton, $>20 \mu\text{m}$) to total biomass increased downstream during winter whereas that of small cells (nano-, $3 - 20 \mu\text{m}$; pico-plankton, $<3 \mu\text{m}$) increased downstream during summer. I conclude from these studies that spatial and seasonal variations in size structure of phytoplankton observed on the estuarine scale are determined both by the different preferences of micro-, nano-, and picoplankton for nutrients and by their different light requirements. Analyses of phytoplankton size structure are, thus, necessary to better understand phytoplankton dynamics and to better manage water quality in estuarine systems.

An ecosystem model was developed to integrate these data and to investigate mechanisms controlling the size-structured phytoplankton dynamics in the mesohaline zone of the York River estuary. The model developed in Fortran90 included 12 state variables describing the distribution of carbon and nutrients (nitrogen, phosphorus) in the surface mixed layer. Forcing functions included incident radiation, temperature, wind stress, mean flow and tide including advective transport and turbulent mixing. Model results supported the general view that phytoplankton dynamics are controlled by abiotic mechanisms (i.e. bottom-up control) rather than biotic, trophic interactions in the York River estuary. Model sensitivity tests showed that small cells (pico-, nano-sized) are

more likely regulated by temperature and light whereas large cells (micro-sized) are regulated by physical processes such as advection and tidal mixing. Microphytoplankton blooms during winter-spring resulted from a combination of longitudinal advection and vertical diffusion of phytoplankton cells rather than *in-situ* production.

PROJECT OVERVIEW

ECOSYSTEM ANALYSIS OF WATER COLUMN PROCESSES IN THE YORK RIVER ESTUARY, VIRGINIA: HISTORICAL RECORDS, FIELD STUDIES AND MODELING ANALYSIS

INTRODUCTION & BACKGROUND

Estuarine systems are considered to be complicated marine environments for scientists struggling to elucidate the ecology of an organism. On the other hand, they are excellent sites for ecological studies since biotic and abiotic factors, varying spatially and temporally, control the dynamics of organisms in the entire system. In addition to the complexity of the systems, estuaries are productive (Ryther 1969) and play a major role in supporting commercial fisheries since they provide habitats and food resources for juvenile commercial fish and shellfish (Smith 1966, EPA 1982, Levinton 1982).

Understanding the dynamics of phytoplankton is important since as primary producers they are the main source of carbon and nutrients (e.g. N, P) in a food web (Kemp and Boynton 1981, Boynton et al. 1982, Coffin and Sharp 1987, Sundbaeck et al. 1990). Phytoplankton affect water quality, especially dissolved oxygen by photosynthesis and respiration, and can serve as substrates for microbial decomposition resulting in oxygen depletion when their ungrazed biomass has accumulated (Officer et al. 1984, Seliger et al. 1985, Malone et al. 1986, Sundbaeck et al. 1990). In addition, plankton are also light-absorbing particles which can limit their own growth, i.e., self-shading (Kirk 1994), and the depth of light penetration. In eutrophic estuarine environments, characterized by high nutrient input, primary production tends to be unstable, and zooplankton or other higher level organisms typically can not respond

quickly to oscillations in standing stocks of primary producers (biomass), resulting in an accumulation of biomass. Accumulations of ungrazed biomass can modify the composition of the classic food chain that includes phytoplankton, copepods and fishes into a microbially-dominated food chain that includes DOC (from phytoplankton), bacteria, protozoa and copepods. This shift in food chain composition gives rise to enhanced microbial decomposition and oxygen depletion (Sundbäck et al. 1990, Jonas 1992).

Phytoplankton production in aquatic environments may be regulated by bottom-up controls, nutrient fluxes associated with physical variability and top-down controls, biotic, trophic interactions (Carpenter et al. 1987, Day et al. 1989, Alpine and Cloern 1992, Kivi et al. 1993). There has been a controversy over the relative importance of bottom-up vs. top-down control and established concepts of resource competition (Tilman 1982) and trophic cascade (Carpenter et al. 1985) for many years. It is now generally accepted that the relative importance of bottom-up vs. top-down control of structure in phytoplankton is scale-dependent; that is, the structure is determined neither entirely by resource competition nor trophic cascade over time scales of interest. In estuarine environments, these controlling mechanisms interact with phytoplankton in complex ways, mainly because of freshwater and tidal energy inputs into the system (Alpine and Cloern 1992, Pennock and Sharp 1994, Cloern 1996). Temporal variations in river discharge rates into an estuary can affect phytoplankton production and size structure or taxon composition through several processes: 1. altering inputs of nutrients from the surrounding watershed; 2. altering light availability by way of estuarine

gravitational circulation, stratification, and changing the turbidity maximum zone along the estuary; 3. altering rates of dilution or advection of phytoplankton; and, 4. altering the amount of detrital or suspended organic matter supporting heterotrophs in an estuarine system (Malone and Chervin 1979, Malone et al. 1980, Fisher et al. 1988, Malone et al. 1988, Gallegos et al. 1992, Madariaga et al. 1992, Boyer et al. 1993). Whereas seasonal and interannual fluctuations in river discharge rates produce low-frequency oscillations in the phytoplankton community, variations in tides (tidal mixing) result in high-frequency oscillations (Haas 1975, Ray et al. 1989, Aksnes and Lie 1990, Cloern 1991). In estuaries, industries such as sewage treatment plants and power plants also introduce allochthonous inputs into the system. Increasing population and industrial development may contribute to eutrophication through point or non-point sources in estuaries.

It is necessary to fractionate phytoplankton assemblages into different size classes as a way of elucidating phytoplankton dynamics since cell size influences the response of phytoplankton communities to environmental variation (Takahashi & Bienfang 1983, Fogg 1986, Oviatt et al. 1989, Glibert et al. 1992, Armstrong 1994, Hein et al. 1995) thereby impacting aquatic food web structure and fisheries (Lenz 1992, Painting et al. 1993). These changes in size classes and fluctuating biomass, resulting from environmental disturbance, impact nutrient and DO distributions as well as heterotrophic consumers in the water column. Since cell size influences sinking (Michaels and Silver 1988) and transport rates, it will determine where ungrazed biomass accumulates and undergoes microbial processing by bacteria and protozoa which then play a role in

depleting DO (Jonas 1992) and in recycling nutrients (Caron 1991) which can be a major source for primary production (Kemp and Boynton 1984).

The EPA Chesapeake Bay Program has supported biweekly to monthly collections of water quality and biological data along the York River estuary since the mid-1980's. Although a large database now exists for the York River, little has been done to synthesize and use the information to analyze water column processes and especially phytoplankton dynamics. The York River system can be considered as a weakly eutrophic system compared with other tributaries in the Chesapeake Bay. However, nitrate and total phosphorus loads have increased significantly in the Pamunkey River (one of two rivers forming the York) over the period July 1989 to December 1995 (Bell et al. 1996). The York River system may become more eutrophic over the next decade as anthropogenic inputs of nutrients increases due to projected high population growth rates and land use conversions (Corish et al. 1995). Despite the importance of the phytoplankton community in terms of ecological and management issues, mechanisms controlling phytoplankton abundance, production and community composition in the York River estuary have not been well established.

For several decades, simulation models have been used to explore plankton dynamics in aquatic systems due to their ability to integrate and synthesize a tremendous array of information. Models have been used to describe interactions between various plankton components and their physical-chemical environments which would be difficult otherwise due to the complexity of the interactions.

The objectives of this study were to: (1) examine seasonal and spatial variations of the size structure and the biomass of phytoplankton and investigate major controlling factors for the phytoplankton community in the York River estuary by analyzing both historic datasets (10 years of EPA long-term data) as well as field data collected over an annual cycle, (2) develop an ecosystem model describing phytoplankton dynamics and explore the main factors controlling size structure of the phytoplankton community in the York River estuary integrating the existing and field data.

This dissertation is grouped into four chapters, i.e., project overview, three research chapters, and summary and synthesis. Research section one describes spatial and temporal characteristics of phytoplankton and inorganic dissolved nutrients based on EPA long-term datasets (1985-1994). Spatial and temporal characteristics of size fractionated phytoplankton are presented in Section II. Development of an ecosystem model and the ecosystem modeling analyses are presented in Section III.

LITERATURE CITED

- Aksnes, D. L. and Lie, U. 1990. A coupled physical-biological pelagic model of a shallow sill fjord. *Estuar. Coast. and Shelf Sci.* 31:459-486.
- Alpine, A. E. and J. E. Cloern. 1992. Trophic interactions and direct physical effects control phytoplankton biomass and production in an estuary. *Limnol. Oceanogr.* 37(5): 946-955.
- Armstrong, R. A. 1994. Grazing limitation and nutrient limitation in marine ecosystems: Steady state solutions of an ecosystem model with multiple food chains. *Limnol. Oceanogr.* 39(3):597-608.
- Bell, C. F., D. L. Belval, and J. P. Campbell. 1996. Trends in Nutrients and Suspended Solids at the Fall Line of Five Tributaries to the Chesapeake Bay in Virginia, July 1988 through June 1995. Water-Resources Investigations Report 96-4191. U.S. Geological Survey, Richmond, VA.
- Boyer, J. P., R. R. Christian and D. W. Stanley. 1993. Patterns phytoplankton primary productivity in the Neuse River estuary, North Carolina, USA. *Mar. Ecol. Prog. Ser.* 97:287-297.
- Boynton, W. R., W. M. Kemp and C. W. Keefe. 1982. A comparative analysis of nutrients and other factors influencing estuarine phytoplankton production, p. 69-90. *In.* V. Kennedy (ed.), *Estuarine Comparisons*. Academic Press, New York.
- Caron, D. A. 1991. Evolving role of protozoa in aquatic nutrient cycles. *In.* P. C. Ried, C. M. Turley, and P. H. Burkill. (eds.) *Protozoa and their role in marine processes*. NATO ASI, Springer-Verlag Berlin Heidelberg. G 25:387-415 (5.3)
- Carpenter, S. R., J. F. Kitchell, and J. R. Hodgson. 1985. Cascading trophic interactions and lake productivity. *BioScience* 35:634-639.
- Carpenter, S. R., and others. 1987. Regulation of lake primary productivity by food web structure. *Ecology* 68:1863-1876.
- Cloern, J. E. 1996. Phytoplankton bloom dynamics in coastal ecosystems: a review with some general lessons from sustained investigation of San Francisco Bay, California. *Rev. Geophys.* 34(2):127-168.

- Cloern, J. E. 1991. Tidal stirring and phytoplankton bloom dynamics in an estuary. *J. Mar. Res.* 49:203-221.
- Coffin, B. Richard, Sharp, H. Jonathan. 1987. Microbial trophodynamics in the Delaware Estuary. *Estuar. Coast. Shelf Sci.* 41:253-266.
- Corish, K., M. Berman and C. H. Hershner. 1995. An economic analysis of the York River basin. Center for Coastal Management and Policy, Department of Resource Management and Policy, Virginia Institute of Marine Science, College of William and Mary, Gloucester Point, Virginia.
- Day, J. W., Jr., C. A. S. Hall, W. M. Kemp, A. Yanez-Arancibia. 1989. Estuarine Ecology: 4. Estuarine phytoplankton, p. 147-187. John Wiley & Sons, Inc., New York.
- EPA (U.S. Environmental Protection Agency). 1982. Chesapeake Bay: Introduction to an ecosystem. U.S. Environmental Protection Agency, Washington, D.C. 33 p.
- Fisher, T. R., L. W. Harding, Jr., D. W. Stanley, and Larry G. Ward. 1988. Phytoplankton, nutrients, and turbidity in the Chesapeake, Delaware, and Hudson estuaries. *Estuar. Coast. Shelf Sci.* 27:61-93.
- Fogg, G. E. 1986. Light and ultraphytoplankton. *Nature* 319:96.
- Gallegos, C. L., T. E. Jordan, and D. L. Correll. 1992. Event-scale response of phytoplankton to watershed inputs in a subestuary: Timing, magnitude, and location of blooms. *Limnol. Oceanogr.* 37(4):813-828.
- Glibert, P. M., C. A. Miller, C. Garside, M. R. Roman, and G. B. McManus. 1992. NH_4^+ regeneration and grazing: interdependent processes in size-fractionated $^{15}\text{NH}_4^+$ experiments. *Mar. Ecol. Prog. Ser.* 82:65-74.
- Haas, L. W. 1975. Plankton dynamics in a temperate estuary with observations on a variable hydrographic conditions. Doctoral Dissertation, School of Marine Science, College of William and Mary, Gloucester Point, Virginia.
- Hein, M., M. F. Pedersen, and K. Sand-Jensen. 1995. Size-dependent nitrogen uptake in micro- and macroalgae. *Mar. Ecol. Prog. Ser.* 118:247-253.
- Jonas, R. 1992. Microbial processes, organic matter and oxygen demand in the water column. p. 113-148. *In*. D. E. Smith, M. Leffler, and G. Mackiernan, (eds.) *Oxygen Dynamics in the Chesapeake Bay*. Maryland Sea Grant College.
- Kemp, W. M., and W. R. Boynton. 1984. Spatial and temporal coupling of nutrient inputs to estuarine primary production: the role of particulate transport and decomposition. *Bull. Mar. Sci.* 35:522-535.

- Kemp, W. M. and W. R. Boynton. 1981. External and internal factors regulating metabolic roles of an estuarine benthic community. *Oecologia* 51:19-27.
- Kirk, J. T. O. 1994. *Light and Photosynthesis in Aquatic Ecosystems*. p. 75-77. Cambridge University Press, Cambridge, England.
- Kivi, K., S. Kaitala, H. Kuosa, J. Kuparinen, E. Leskinen, R. Lignell, B. Marcussen, and T. Tamminen. 1993. Nutrient limitation and grazing control of the Baltic plankton community during annual succession. *Limnol. Oceanogr.* 38(5):893-905.
- Lenz, J. 1992. Microbial loop, microbial food web and classical food chain: Their significance in pelagic marine ecosystems. *Arch. Hydrobiol. Beih.* 37:265-279.
- Levinton, J. S. 1982. *Marine Ecology*. p. 526. Prentice-Hall, Inc., Englewood Cliffs, New Jersey.
- Madariaga, I. de, Gonzalez-Azpiri, L., Villate, F., and Orive, E. 1992. Plankton responses to hydrological changes induced by freshets in a shallow mesotidal estuary. *Estuar. Coast. Shelf Sci.* 35:425-434.
- Malone, T. C. and M. B. Chervin. 1979. The production and fate of phytoplankton size fractions in the plume of Hudson River, New York Bight. *Limnol. Oceanogr.* 24(4):683-696.
- Malone, T. C., L.H. Crocker, S. E. Pike and B. W. Wendler. 1988. Influences of river flow on the dynamics of phytoplankton production in a partially stratified estuary. *Mar. Ecol. Prog. Ser.* 48:235-249
- Malone, T. C., W. M. Kemp, H. W. Ducklow, W. R. Boynton, J. H. Tuttle, and R. B. Jonas. 1986. Lateral variation in the production and fate of phytoplankton in a partially stratified estuary. *Mar. Ecol. Prog. Ser.* 32:149-160.
- Malone, T. C., P. J. Neale and D. Boardman. 1980. Influences of estuarine circulation on the distribution and biomass of phytoplankton size fractions, p. 249-262. *In*. V. Kennedy (ed.), *Estuarine Perspectives*. Academic Press, New York.
- Michaels, A. E. and M. W. Silver. 1988. Primary production, sinking fluxes and the microbial food web. *Deep-Sea Res.* 35:473-490.
- Officer, C. B., R. B. Biggs, J. L. Taft, L. E. Cronin, M. A. Tyler, and W. R. Boynton. 1984. Chesapeake Bay anoxia: origin, development, significance. *Science* 223:22-27.

- Oviatt, C., P. Lane, F. French III and P. Donaghay. 1989. Phytoplankton species and abundance in response to eutrophication in coastal marine mesocosms. *J. Plankton Res.* 11(6):1223-1244.
- Painting, S. J., C. L. Moloney, and M. I. Lucas. 1993. Simulation and field measurements of phytoplankton-bacteria-zooplankton interactions in the southern Benguela upwelling region. *Mar. Ecol. Prog. Ser.* 100:55-69.
- Pennock, J. R., and Sharp, J. H. 1994. Temporal alternation between light-and nutrient-limitation of phytoplankton in a coastal plain estuary. *Mar. Ecol. Prog. Ser.* 111:275-288
- Ray, T. R., L. W. Haas, and M. E. Sieracki. 1989. Autotrophic picoplankton dynamics in a Chesapeake Bay sub-estuary. *Mar. Ecol. Prog. Ser.* 52:273-285.
- Ryther, J. H. 1969. Photosynthesis and fish production in the sea. *Science* 166:72-76.
- Smith, R. F. 1966. Foreword, pp. vii-viii. *In*. R. F. Smith, A. H. Swartz, and W. H. Massmann (eds.), *A Symposium on Estuarine Fisheries*. Amer. Fish. Soc. Spec. Publ. No. 3. Allen Press, Lawrence, Kansas.
- Seliger, H. H., J. A. Boggs, and W. H. Biggley. 1985. Catastrophic anoxia in the Chesapeake Bay in 1984. *Science* 228:70-73.
- Sundbaeck, K., B. Joensseon, P. Nilsson, and I. Lindstroem. 1990. Impact of accumulating drifting macroalgae on a shallow-water sediment system: An experimental study. *Mar. Ecol. Prog. Ser.* 58(3):261-274.
- Takahashi, M. and P. K. Bienfang. 1983. Size structure of phytoplankton biomass and photosynthesis in subtropical Hawaiian waters. *Mar. Biol.* 76:203-211.
- Tilman, D. 1982. *Resource competition and community structure*. Princeton University Press, Princeton, New Jersey.

SECTION I

Spatial and Temporal Characteristics of Nutrient and Phytoplankton Dynamics in the York River Estuary, Virginia: Analyses of Long Term Data[†]

[†]: Will be appear in *Estuaries* (Vol:22, No:2, June 1999)

ABSTRACT

Ten years (1985-1994) of data were analyzed to investigate general patterns of phytoplankton and nutrient dynamics, and to identify major factors controlling those dynamics in the York River Estuary, Virginia. Algal blooms were observed during winter-spring followed by smaller summer blooms. Peak phytoplankton biomass during the winter-spring blooms occurred in the mid reach of the mesohaline zone whereas peak phytoplankton biomass during the summer bloom occurred in the tidal fresh-mesohaline transition zone. River discharge appears to be the major factor controlling the location and timing of the winter-spring blooms and the relative degree of potential N and P limitation. Phytoplankton biomass in tidal fresh water regions was limited by high flushing rates. Water residence time was less than cell doubling rate during high flow seasons. Positive correlations between PAR at 1m depth and chlorophyll *a* suggested light limitation of phytoplankton in the tidal fresh-mesohaline transition zone. Relationships of salinity difference between surface and bottom water with chlorophyll *a* distribution suggested the importance of tidal mixing for phytoplankton dynamics in the mesohaline zone. Accumulation of phytoplankton biomass in the mesohaline zone was generally controlled by N with the nutrient supply provided by benthic or bottom water remineralization. The implications of limiting factors and river discharge for water quality management in the basin are discussed briefly.

INTRODUCTION

Phytoplankton abundance and primary production in aquatic environments may be regulated by abiotic mechanisms such as nutrient fluxes related to physical-chemical variability (i.e. bottom-up control) and biotic, trophic interactions (i.e. top-down control) (Carpenter et al. 1987; Day et al. 1989; Kivi et al. 1993; Armstrong 1994; Caraco et al. 1997). In fact, there has been continuing controversy and debate over the relative importance of bottom-up vs. top-down controls and established concepts of resource competition (Tilman 1982) and trophic cascade (Carpenter et al. 1985) for many years. It is generally accepted that the relative importance of bottom-up vs. top-down controls of structure in the phytoplankton is scale-dependent; that is, the structure is determined neither entirely by resource competition nor trophic cascade over time scales of interest. In estuarine environments, these controlling mechanisms interact with phytoplankton in complex ways, mainly because of freshwater and tidal energy inputs into the system (Alpine and Cloern 1992; Pennock and Sharp 1994; Cloern 1996). Temporal variations in river discharge to an estuary can affect phytoplankton production and size structure or taxon composition through several processes (e.g. Malone and Chervin 1979; Malone et al. 1980; Cloern et al. 1983; Pennock 1985; Malone et al. 1988; Gallegos et al. 1992; Madariaga et al. 1992; Boyer et al. 1993). While seasonal and interannual fluctuations in river discharge invoke low-frequency oscillations in the phytoplankton community, variations in tides (tidal mixing) result in high-frequency oscillations (Haas 1975; Ray et

al. 1989; Aksnes and Lie 1990; Cloern 1991). In estuaries, facilities such as sewage treatment plants and power plants also introduce allochthonous inputs. Increasing human population densities and industrial development contribute to eutrophication through point and non-point sources in estuaries.

The EPA Chesapeake Bay Program has supported biweekly to monthly collections of water quality and biological data along the York River estuary since the mid-1980's. Although a large database now exists for the York River, little has been done to synthesize and use the information to analyze water column processes and especially phytoplankton dynamics. The York River system can be considered as a weakly eutrophic system compared with other tributaries in the Chesapeake Bay. However, nitrate and total phosphorus loads have increased significantly in the Pamunkey River (one of two rivers forming the York) over the period July 1989 to December 1995 (Bell et al. 1996). The York River system may become more eutrophic over the next decade as anthropogenic input of nutrient increases due to projected high population growth rates and land use conversion (Corish et al. 1995). Despite the importance of the phytoplankton community in terms of ecological and management issues, mechanisms controlling phytoplankton abundance, production and community composition in the York River estuary have not been well established.

The objectives of this study were to: (1) examine seasonal and spatial variations of phytoplankton and nutrient concentrations in the York River over the period 1985-1994; and (2) investigate mechanisms controlling phytoplankton and nutrient dynamics on seasonal, annual, and interannual time scales.

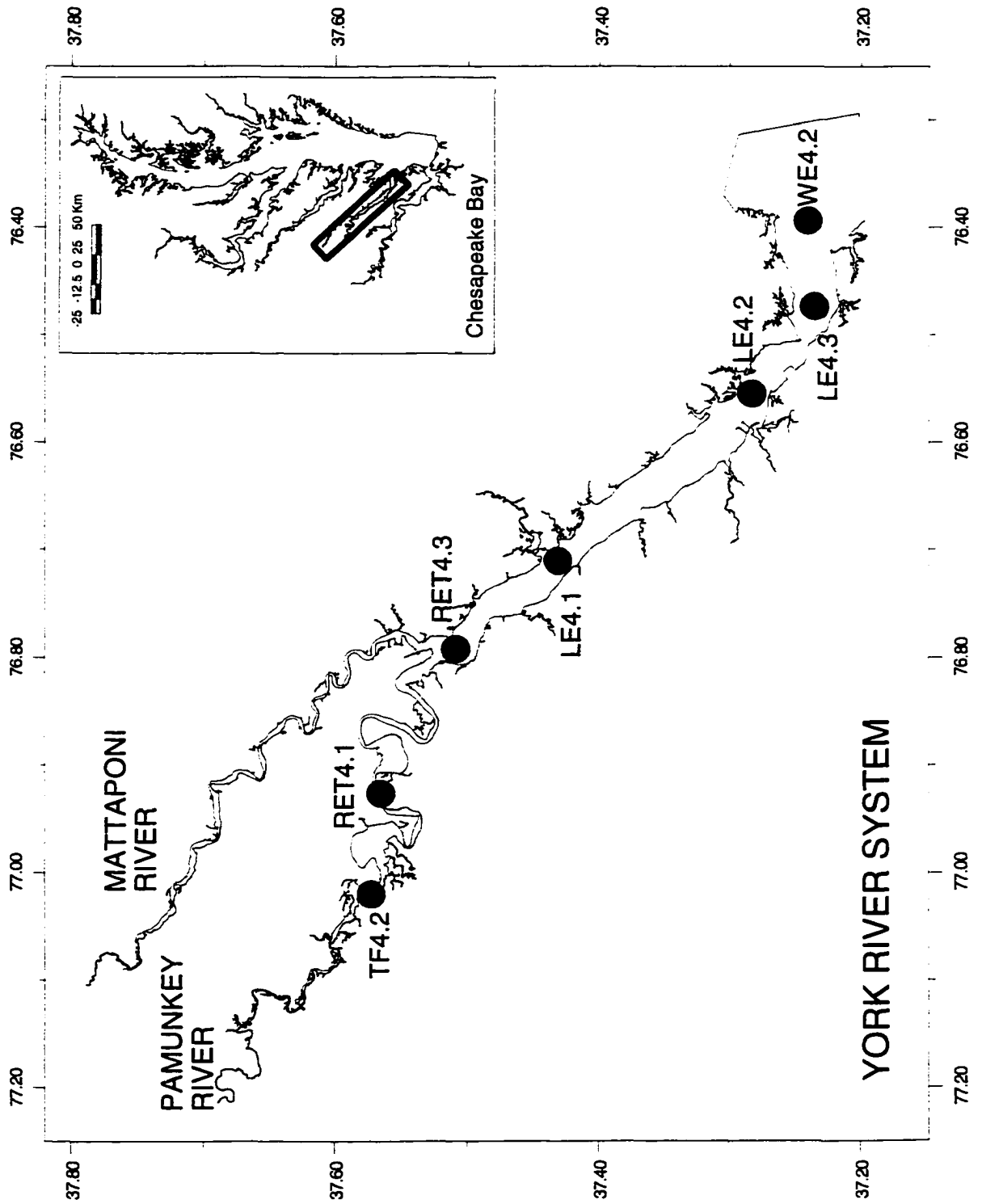
MATERIALS AND METHODS

Area description and data analyses

The York River system, a subestuary of the Chesapeake Bay, is composed of three rivers, i.e. the York, Pamunkey, and Mattaponi (Fig. 1). The York River is formed by the confluence of the Pamunkey and Mattaponi rivers at West Point (48 km from its mouth). Total average freshwater discharge to the river system is $70 \text{ m}^3 \text{ sec}^{-1}$ (Hyer 1977). The salinity distribution of the York River system is affected by the interaction of freshwater, salt water, tidal energy and wind. Salinity gradients between the surface and bottom layers are influenced by neap and spring tidal cycles with destratification of the water column occurring at high spring tides and stratification developing during the intervening periods (Haas 1975). During low flow conditions, salt water extends 21 to 31 km upriver from West Point (Bender 1986).

The EPA Chesapeake Bay Monitoring Program (CBMP) and the Virginia State Water Control Board (VSWCB) have collected water quality data from 10 stations in the York River system over the period 1984 to the present. The results presented here include analyses of the water quality data from 7 stations along the axis of the Pamunkey and York rivers collected between June 1984 and December 1994. Locations of the sampling stations are shown on Fig. 1. The stations represent tidal freshwater, river – estuary transition, and upper, middle and lower estuarine zones. TF4.2 is located in the

Fig. 1. The EPA Chesapeake Bay Monitoring stations in the York River estuary.



tidal freshwater zone. RET4.1 is located upriver of RET4.3 in the transitional zone of the Pamunkey River. LE4.1, LE4.2 and LE4.3 are in the upper, mid, and lower reaches of the mesohaline zone of the York River respectively. WE4.2 is located at the mouth of the estuary (mesohaline). Station designations are those used by the Virginia State Water Control Board (1987). Data were collected monthly between November and February and twice monthly during the periods of March through October, when biological activity was highest and water quality problems most apparent (Virginia Water Control Board 1987).

Biological and other living resources have been assessed at stations TF4.2, RET4.3 and WE4.2 since July 1986 and primary production (estimated by $\text{H}^{14}\text{CO}_3^-$ uptake, $\mu\text{g C l}^{-1} \text{ h}^{-1}$) since January 1989. Mesozooplankton ($> 202 \mu\text{m}$) abundance from July 1986 to December 1994 and microzooplankton (> 73 and $< 202 \mu\text{m}$) abundance from January 1993 to December 1994 were analyzed for this study. Chlorophyll *a* data were collected from surface water only at all stations except station WE4.2 where chlorophyll *a* was measured in both surface water and at 1 m above bottom. Light attenuation coefficients (K_d) were estimated by dividing 1.45 by reported secchi disk depths. PAR (photosynthetically active radiation) at 1 m depth was calculated using Beer's Law, $I_z = I_0 e^{-kz}$, where I_z is the intensity of light at z , the depth of interest, I_0 is the surface intensity, and k is the water column attenuation coefficient. Solar radiation data (1989-1994) measured at the Virginia Institute of Marine Science located ca. 10 km upstream from the York river mouth were used for the I_0 values.

Mean daily river discharge (Q) of the Pamunkey and Mattaponi rivers at the fall line were collected by the U.S. Geological Survey. Only discharge data for the

Pamunkey River were used in these analyses since discharge patterns of the Mattaponi River followed those of the Pamunkey. Monthly means were derived and used for all analyses. To examine the effects of variable river discharge rates three distinct hydrographic years were chosen from the data set. The lowest (1991, $Q = 16.1 \text{ m}^3 \text{ s}^{-1}$) and highest flow years (1994, $Q = 43.9 \text{ m}^3 \text{ s}^{-1}$) over the 10 year period of study were chosen to examine the extremes in river discharge rates. Mean flow ($Q = 28.9 \text{ m}^3 \text{ s}^{-1}$) for 54 years (1941-1994) was determined and 1990 ($Q = 31.9 \text{ m}^3 \text{ s}^{-1}$) was chosen as representative of the mean flow year. To examine the effects of river discharge rates on phytoplankton dynamics at the lower estuary stations (LE4.1, LE4.2, LE4.3 and WE4.2), it was necessary to determine lag time, defined as the time required for transport of a water mass from the fall line to the lower estuary (mesohaline zone). Lag time was determined as the time delay necessary to optimize the R^2 value for regressions of salinity vs. river discharge for low and high flow periods of the year. Two periods were selected: January to May as the high flow period and June to December as the low flow period in a yearly cycle since river discharge rates varied with season. Scenarios of 0, 1, and 2 months were established from the results of running an 1-D hydrodynamic model for the York River developed by Dr. J. Shen at the Virginia Institute of Marine Science (VIMS).

Linear regression was used to investigate statistical correlations between the various water quality parameters and physical factors. Raw data or monthly averages were used in the regression analysis without log transformations.

RESULTS

River discharge and response lag periods

Figure 2 shows the seasonality of river discharge measured at the fall line in the Pamunkey and Mattaponi rivers. Periods of high discharge occur in winter and spring followed by reduced or low discharge during the summer and fall. Discharge rates near the fall line on the Pamunkey at Hanover, Virginia average 28.6 and on the Mattaponi at Beulaville Virginia 15.0 m³ s⁻¹ over the period 1985 to 1994. Peak discharge rates were extraordinarily high during the years, 1993 and 1994.

Table 1 shows R² values for regressions of surface salinity vs. river discharge and indicates the importance of considering lag time for stations in the lower estuary (stations LE4.1, LE4.2, LE4.3). For example, when salinity at station LE4.3 (lower estuary) was regressed against river discharge with no lag time included, the R² value for the regression was the minimum. For the low flow period of June to December, inclusion of a 2 month lag improved the R² for the regression from 0.07 (no lag) to 0.39 (2 month lag). For stations LE4.2, LE4.3 and WE4.2 lag times of 1 and 2 months were chosen for the periods January to May and June to December, respectively in the following analyses. At station LE4.1 no lag was used for the high flow period and a 1 month lag during the low flow period.

Fig. 2. Time series of river discharge rates of the Pamunkey and Mattaponi River in the York River estuarine system from 1985 to 1994.

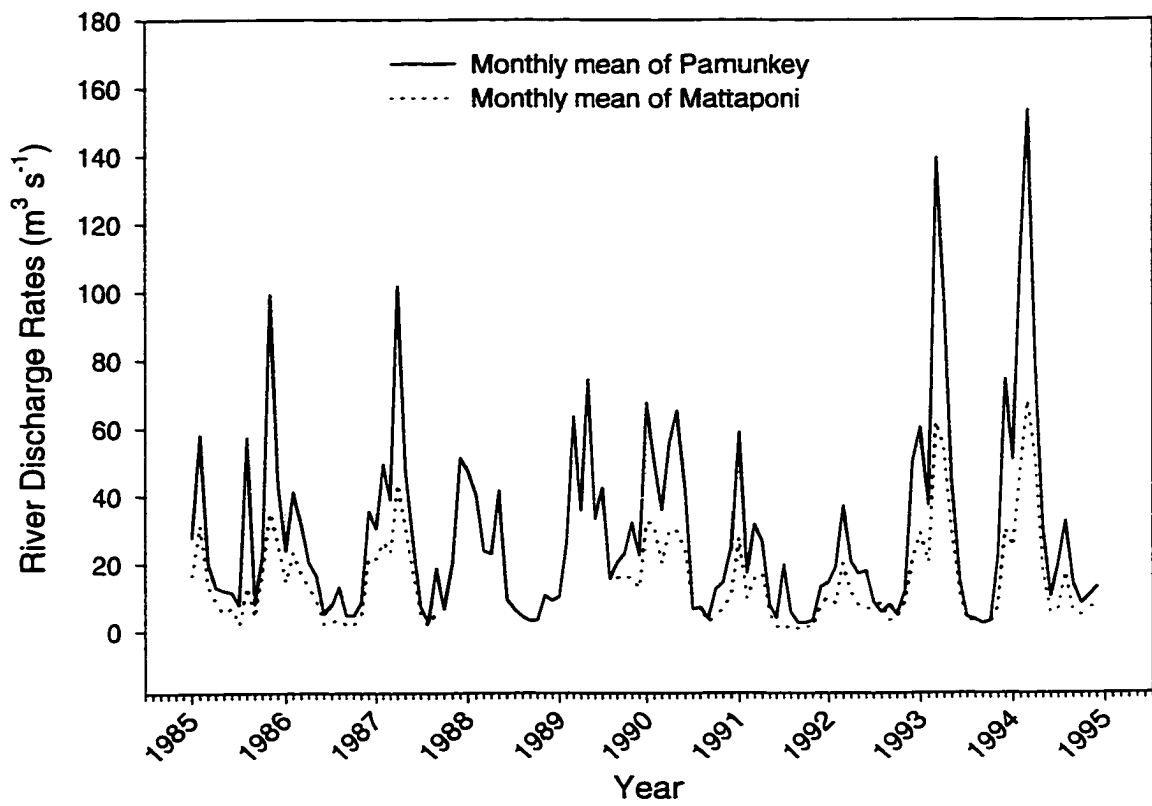


Table 1. R^2 for linear regression of surface water salinity vs. river discharge rates measured at the fall line in the Pamunkey River. Ten years (1985-1994) of monthly mean data were used for the analysis.

Station: Period: Scenario	LE4.1		LE4.2		LE4.3	
	Jan-May	Jun-Dec	Jan-May	Jun-Dec	Jan-May	Jun-Dec
No lag	0.47 ^b	0.33 ^b	0.45 ^b	0.21 ^b	0.34 ^b	0.07 ^a
1 month-lag	0.26 ^a	0.45 ^b	0.34 ^b	0.36 ^b	0.52 ^b	0.28 ^b
2 month-lag	0.20 ^a	0.40 ^b	0.29 ^a	0.38 ^b	0.52 ^b	0.39 ^b

^a: $P < 0.05$, ^b: $P < 0.0001$

Seasonality of phytoplankton blooms and productivity

Over the 10 year period, each station showed a repeating pattern of seasonal phytoplankton blooms (Fig. 3). Blooms were arbitrarily designated as episodes when chlorophyll *a* exceeded $10 \mu\text{g l}^{-1}$. In tidal freshwater regions (TF4.2, RET4.1), maximum chlorophyll concentrations usually occurred during the summer, low flow period but were generally short in duration and less than $15 \mu\text{g l}^{-1}$ chlorophyll (Fig. 3A, 3B). At the lower transition station (RET4.3), two bloom periods were evident; a short, winter bloom followed by a more intense late spring-summer bloom (Fig. 3B, 3C). The upper and mid reaches of the mesohaline zone (LE4.1, LE4.2) had winter-spring blooms and smaller summer blooms (Fig. 3D, 3E) while the lower reach (LE4.3) experienced smaller winter-spring and no apparent summer blooms (Fig. 3F). The transitional station RET4.3 had relatively high concentrations of chlorophyll *a* during the summer at a time when nitrite + nitrate input from freshwater was low.

Seasonal and spatial characteristics of primary production were similar to those of phytoplankton biomass (Fig. 3). Phytoplankton production was high during summer and low during winter at the tidal freshwater station (Fig. 3A). At transition station RET4.3, two peaks were observed; a short, winter peak followed by a higher and prolonged summer peak (Fig. 3B). The station at the mouth of the estuary showed a spring peak and relatively high production during summer (Fig. 3C).

Effects of river discharge on phytoplankton biomass

Table 2 gives the results of regression analyses of chlorophyll *a* or primary production versus river discharge, K_d , PAR and temperature for low, mean and high flow

Fig. 3. Seasonal distributions of chlorophyll *a* and primary production in the York River system; monthly means and standard errors were calculated from the 10 years data (1985-1994) for chlorophyll *a* and from 7 years data (1988-1994) for primary production. Dashed line at 10 $\mu\text{g l}^{-1}$ indicates our criterion for algal blooms and primary production shown in Fig. 3F was measured at WE4.2.

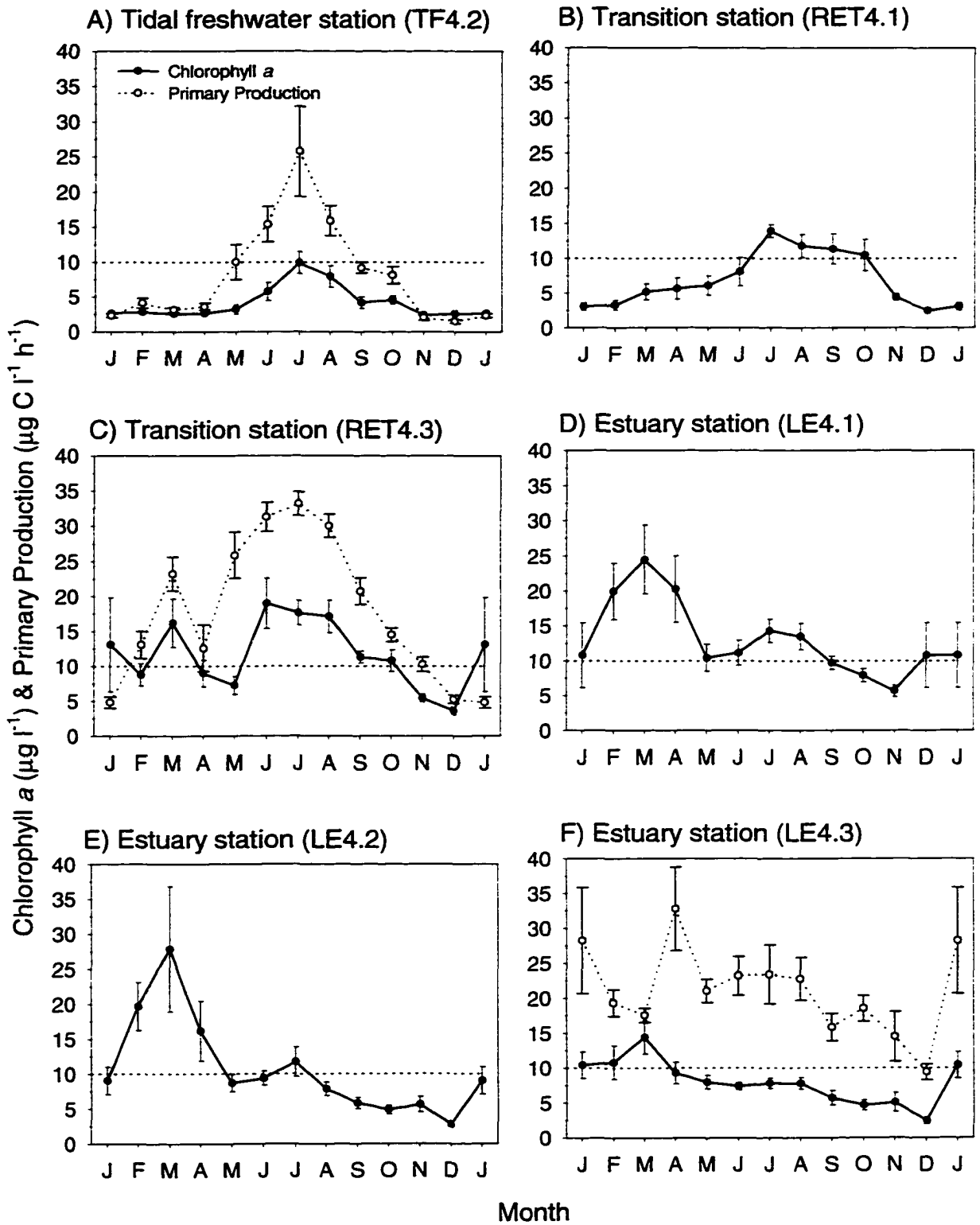


Table 2. Results (R^2) of linear regression analysis of chlorophyll a ($\mu\text{g l}^{-1}$) or primary production ($\mu\text{g C l}^{-1} \text{h}^{-1}$) vs. river discharge rates (Q , $\text{m}^3 \text{s}^{-1}$), light attenuation coefficients (K_d , m^{-1}), PAR at 1 m depth (PAR, $\mu\text{Ein m}^{-2} \text{s}^{-1}$) and temperature (T , $^{\circ}\text{C}$) during the low (1991), mean (1990) and high (1994) flow years. R^2 less than 0.1 omitted and denoted by ' '. R^2 in parentheses represents correlation for primary production and negative values represent negative relationships.

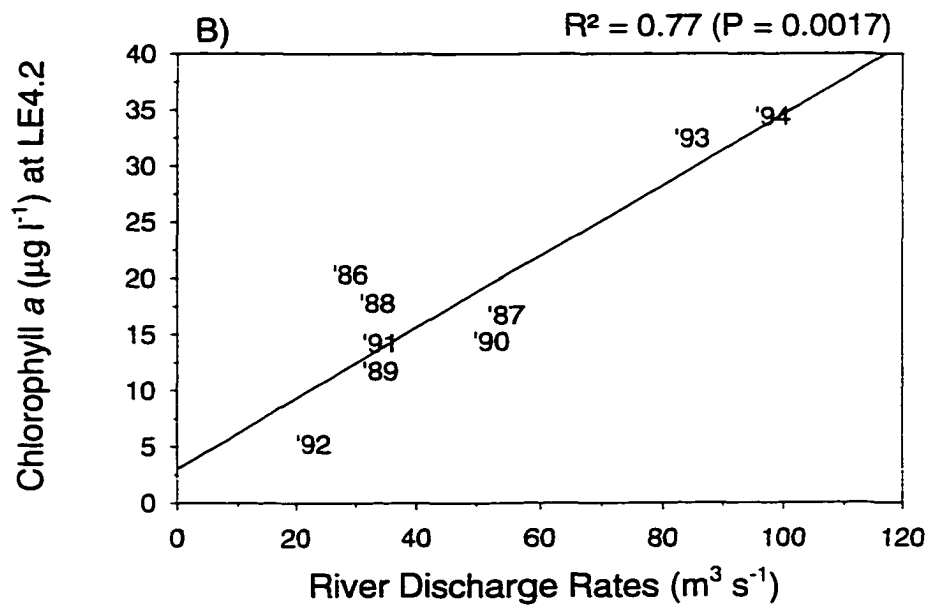
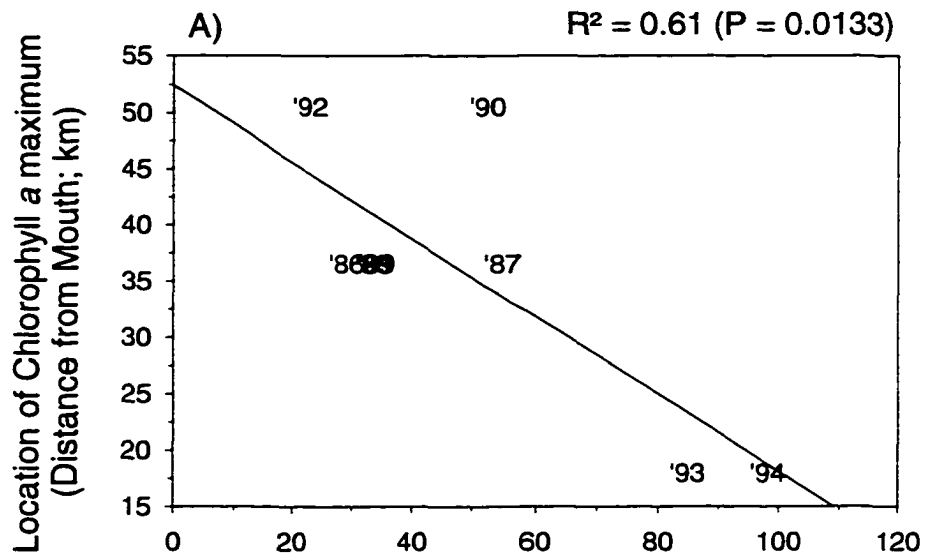
Stations	Parameters	1991 (Low Flow)				1990 (Mean Flow)				1994 (High Flow)			
		Q	K_d	PAR	T	Q	K_d	PAR	T	Q	K_d	PAR	T
TF4.2		-0.14 (0.17)	0.28 ^a (0.29 ^a)		0.26 ^a (0.32 ^b)	-0.30 ^a (0.11)			0.45 ^b (0.38 ^b)	-0.11 ()			0.47 ^b (0.71 ^b)
RET4.1		-0.27 ^a	-0.34 ^b	0.55 ^b	0.60 ^b	-0.49 ^b	-0.17		0.68 ^b	-0.15	-0.12	0.23	0.33 ^b
RET4.3		()	-0.20 ()		0.11 (0.29 ^a)	(0.21)	(0.15)	(0.16)	(0.87 ^b)	-0.34 ^b (0.28 ^a)	()	0.11	0.48 ^b (0.66 ^b)
LE4.1					-	0.15	0.14			0.74 ^b			
LE4.2		0.19			-0.15	0.32 ^b	0.15	0.13		0.66 ^b	0.69 ^b	0.31 ^a	
LE4.3						0.32 ^b	0.49 ^b	0.30 ^a	-0.18	0.49 ^b	0.63 ^b		
WE4.2		()	0.64 ^b (0.13)	0.29 ^a (0.20)	()	0.11 ()	(0.44 ^b)	0.28 ^a (0.15)	(0.26 ^a)	0.48 ^b (0.66 ^b)	0.23 (0.35 ^b)	()	()

^a : $P < 0.1$, ^b : $P < 0.05$

years (1991, 1990, and 1994, respectively). Chlorophyll *a* concentrations and distributions were generally correlated with river discharge (Table 2). The correlations were highest and more evident during years of mean (1990) and high flow (1994) than during low flow (1991). For all flow conditions, chlorophyll *a* was negatively correlated with river discharge rate in the upper, tidal freshwater and oligohaline regions of the estuary and positively correlated for mean and high discharge rates in the lower estuary. A 1-D hydrodynamic model (Dr. J. Shen, VIMS) was run to estimate residual velocity (m s^{-1}) in the tidal freshwater zone using mean river discharge rates over 9 years (1983-1992) for the months of August and January. Residual velocities in August and January were estimated to be 3.63 and 6.85 km d^{-1} respectively at the tidal freshwater station (TF4.2). Mean doubling times of phytoplankton in the Pamunkey River are reported to be 2.12 and 0.92 d^{-1} for August and December respectively (Kindler 1991). Using these estimates, phytoplankton would require 0.47 and 1.09 days to double their biomass during summer (August) and winter (December) and would be transported 1.71 and 7.47 km in the required time intervals. This suggests that the phytoplankton are flushed out of the upper, tidal freshwater regions during the winter or high flow periods, preventing phytoplankton biomass from accumulating.

In the mesohaline zone the positive correlation between chlorophyll *a* and river discharge rate is strongest during high flow years such as 1994 indicating riverine input enhances the phytoplankton growth in this zone. Figure 4 shows the relationship between river discharge and the location of peak chlorophyll concentration (A) and between river discharge and chlorophyll *a* during winter-spring at the mid-estuary station LE4.2 (B). The location of peak chlorophyll *a* concentration was significantly correlated ($r^2 = 0.61$;

Fig. 4. Correlation between river discharge rates and location of chlorophyll *a* peaks (A) and mean chlorophyll *a* at station LE4.2 (B) during winter-spring period January-April for 9 years 1986-1994.



$P = 0.0133$) with river discharge rates over the period 1986 to 1994 and spring chlorophyll *a* concentration was significantly correlated ($r^2 = 0.77$; $P = 0.0017$) with spring river discharge over the period 1986 to 1994. These results indicate that river discharge determines the location and magnitude as well as timing of winter-spring blooms.

Light limitation, temperature and potential grazing effects

The relationship between light attenuation (K_d) and chlorophyll *a* was positive in the mesohaline zone but negative at stations in the Pamunkey River. This pattern is generally similar to the relationship observed between chlorophyll *a* and river discharge. River discharge was strongly and positively correlated with K_d during the high flow year (1994) indicating K_d may be a good predictor of potential riverine nutrient inputs to the York River system ($R^2 = 0.47$ ($P = 0.014$) at station TF4.2, $R^2 = 0.71$ ($P < 0.001$) at station RET4.3, and $R^2 = 0.52$ ($P = 0.008$) at station LE4.2). The relationship between chlorophyll *a* and PAR at 1 m depth was examined for direct effects of light on phytoplankton biomass but a general pattern was not evident from the results (Table 2).

In order to determine the general pattern of light limitation, monthly means of data (1989-1994) were used to examine the general relationship between chlorophyll *a* and PAR at 1 m depth. Only at station RET4.1 was chlorophyll *a* concentration strongly correlated with PAR ($R^2 = 0.77$; $P = 0.0002$) indicating light limitation of phytoplankton production at this station.

To further investigate potential light limitation in the York River system, a light limitation index was derived based on DiToro et al. (1971) and computed as;

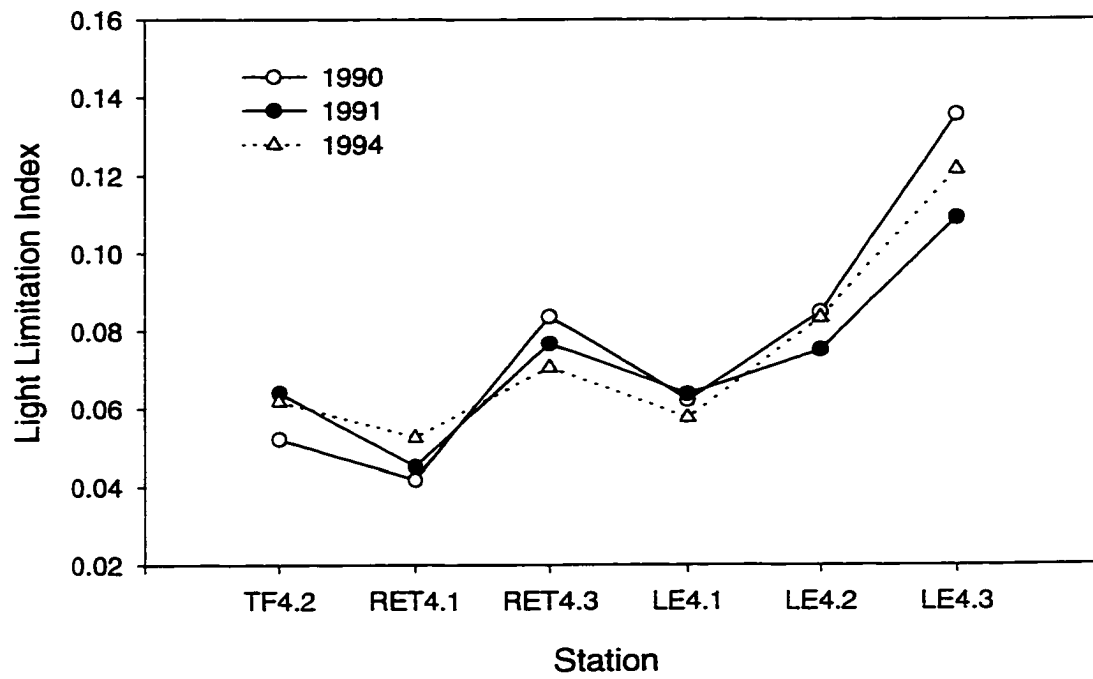
$$LtLim = \frac{ef}{kz} \cdot \left[e^{-\frac{I_m}{I_{opt}} e^{-kz}} - e^{-\frac{I_m}{I_{opt}}} \right]$$

where e = base of the natural logarithms, f = photoperiod as a fraction of a day, k = attenuation coefficient (m^{-1}), z = the depth (m), I_m = incident average light intensity ($E_{in} d^{-1}$), and I_{opt} = optimal light intensity ($E_{in} d^{-1}$). Thus, the lower the index, the greater the degree of light limitation. Figure 5 shows the light limitation index ($LtLim$) during years of low, mean and high flow indicating that transitional station RET4.1 is most light-limited in the York River system. Chlorophyll a and the light limitation index were also significantly correlated over the three years (1990, 1991 and 1994) at station RET4.1 ($R^2 = 0.28$; $P < 0.001$).

Chlorophyll a and primary production were significantly and positively correlated with temperature at stations in the upper river (Pamunkey) during years of low, mean and high flow but not in the lower estuary (Table 2).

Relationships between microzooplankton and mesozooplankton abundances and chlorophyll a were examined for the stations where data were available to investigate possible grazing effects on phytoplankton populations. At stations TF4.2, RET4.3, and WE4.2 there was no significant correlation between mesozooplankton abundances and chlorophyll a , or microzooplankton abundance. Microzooplankton abundance and chlorophyll a were both strongly ($R^2 = 0.55$) and significantly ($P < 0.0001$) correlated at stations TF4.2 and RET4.3 but not at station WE4.2. There was also no apparent lag time between microzooplankton and chlorophyll a . Thus, there are no evident grazing effects

Fig. 5. Light limitation index calculated from a mechanistic equation (DiToro et al. 1971) during low (1991), mean (1990) and high (1994) flow years.

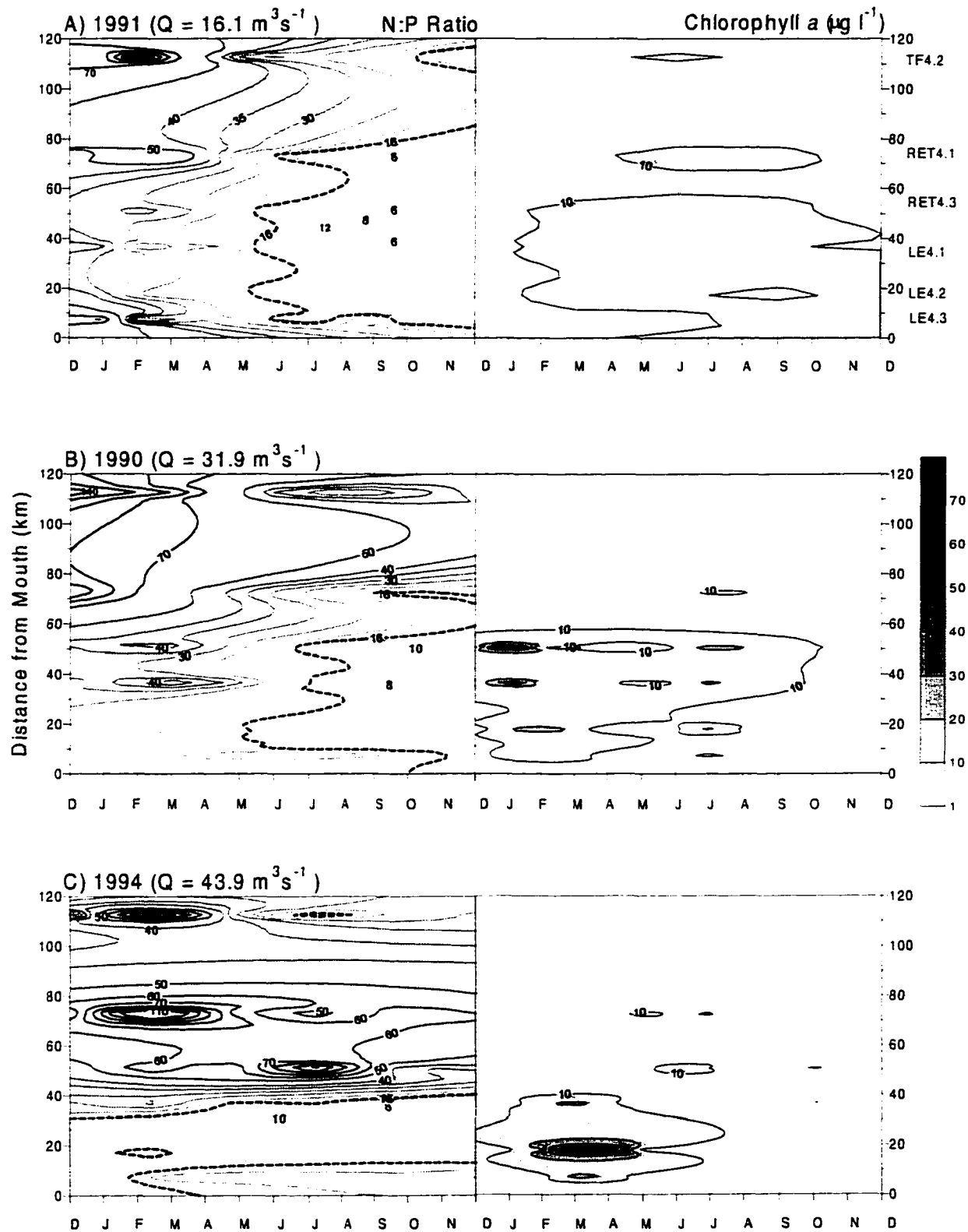


on the phytoplankton dynamics but microzooplankton abundance in tidal fresh and transition zones may be regulated by bottom-up controls.

Nutrient dynamics

Figure 6 shows the spatial and temporal distributions in the dissolved inorganic nitrogen (DIN):dissolved inorganic phosphorus (DIP) molar ratio and chlorophyll *a* concentration for the years representing low, mean and high river discharge rates. DIN:DIP molar ratio were used as an index for potential nutrient limitation based on Redfield ratio (16:1). Potential P limitation, from the high DIN:DIP ratio at the tidal freshwater station (TF4.2) was present during all seasons and its longitudinal extent was directly proportional to river discharge rate suggesting that riverine input of $\text{NO}_2 + \text{NO}_3$ regulated potential P limitation. Potential P limitation was highest during winter-spring due to N input from runoff whereas potential N limitation, low DIN:DIP ratio was apparent from the transitional zone stations downriver especially during the summer-fall period. During high flow years, potential N limitation was present at mid and lower reaches of the mesohaline zone throughout the year except for the period of peak river discharge rate (February; see Fig. 2). The early appearance of potential N limitation during the high flow year appears to coincide with the occurrence of large winter-spring blooms following peak river discharge. Higher N uptake during spring blooms might induce the earlier N limitation in the mesohaline zone. During the low flow year, there was no apparent bloom event throughout the river system. From these results, not only does the timing and magnitude of potential nutrient limitation relative to N and P appear

Fig. 6. Distributions of N:P molar ratio and chlorophyll *a* in the York River over annual cycles during the low (1991), mean (1990) and high flow years (1994). Left panels describe patterns of N:P molar ratio and right panels those of chlorophyll *a*; color scale applies only to right panels.

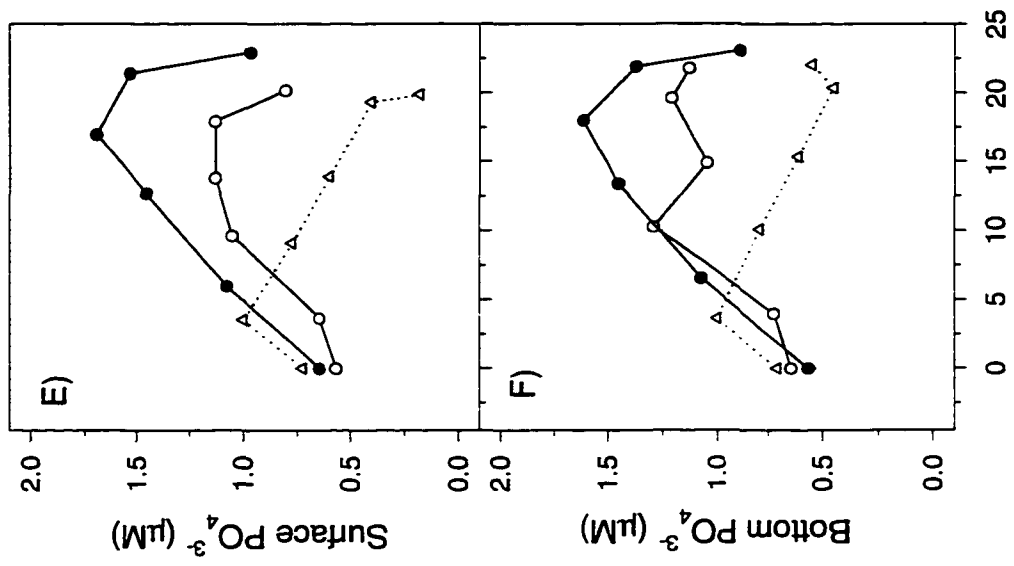
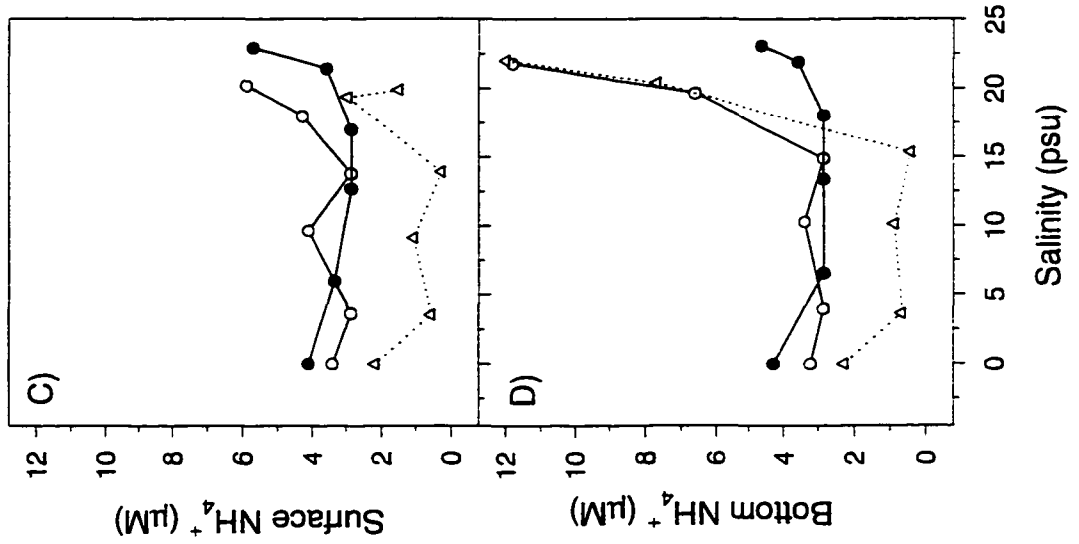
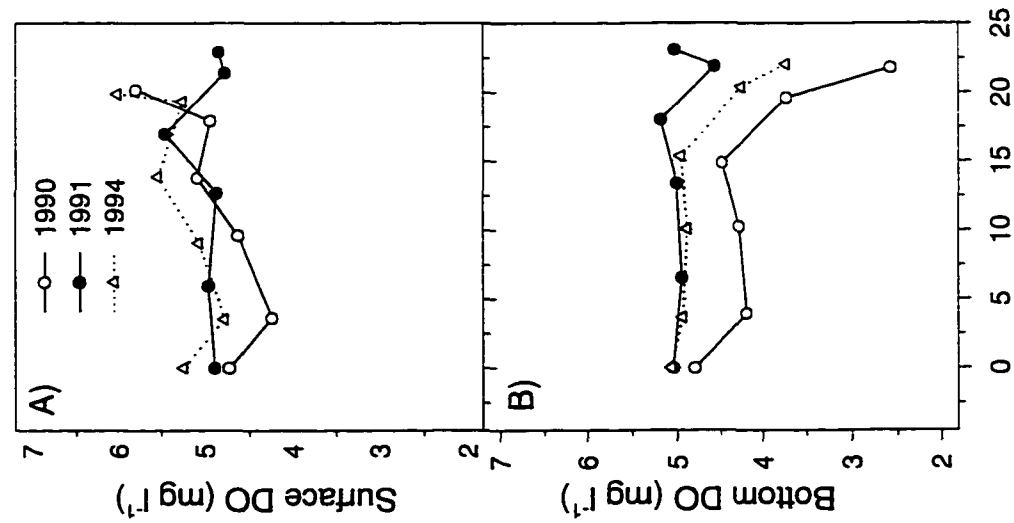


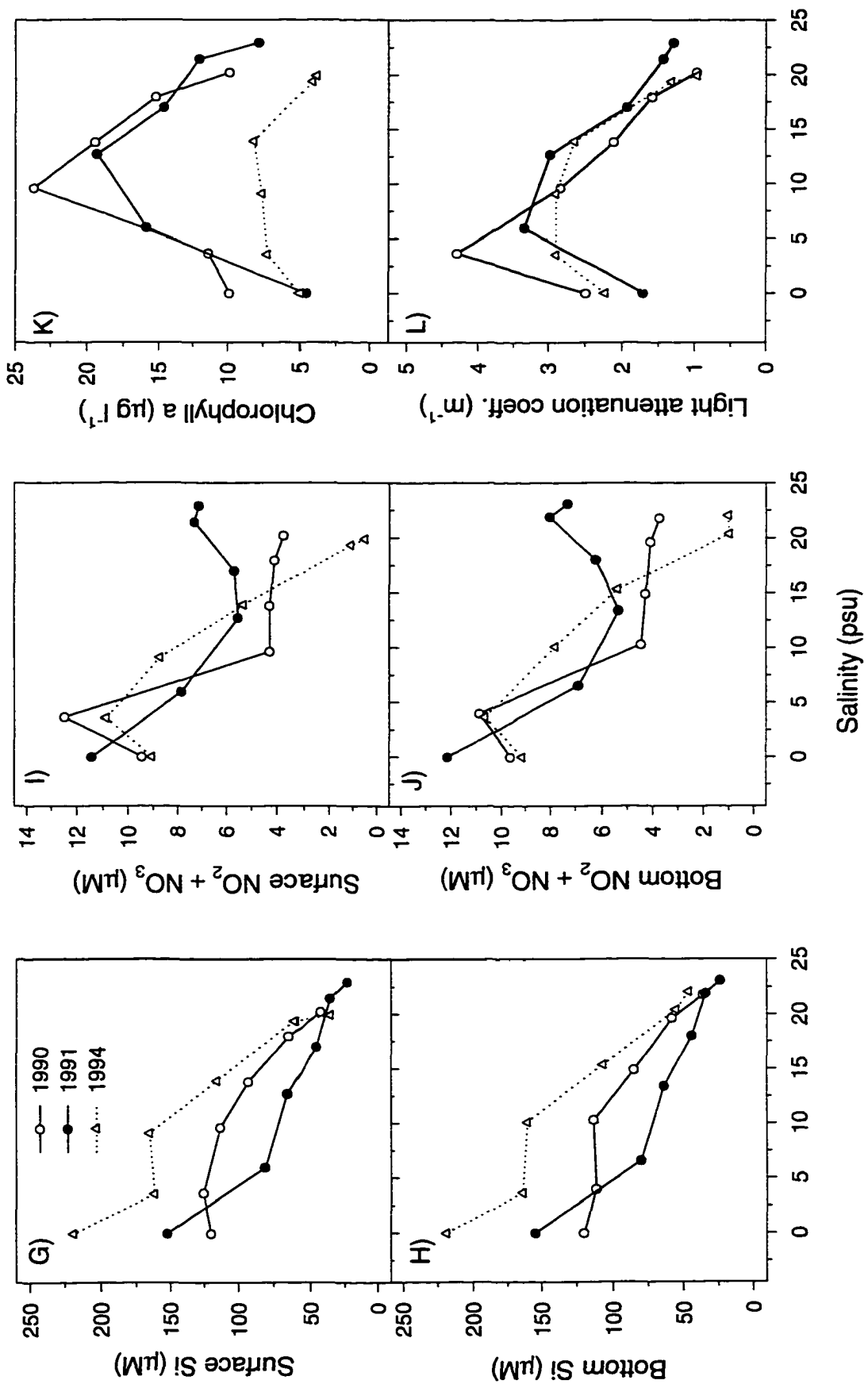
related to river discharge but chlorophyll distribution within the estuary reflects different river discharge regimes.

Salinity dilution plots were used to examine sources and sinks of DO, ammonium, orthophosphate, silicate, and nitrite+nitrate as well as chlorophyll *a* and light attenuation coefficient for the summer period July to August (Fig. 7) during years of low (1991), mean (1990) and high flow (1994) in the York River system. Summer DO concentrations in bottom water decreased sharply at approximately 15 psu while surface water DO concentrations remained relatively constant along the salinity gradient (Fig. 7A, 7B). In bottom water, ammonium concentrations increased at the same salinity as DO concentration decreased (Fig. 7D). Differences in ammonium (especially) and orthophosphate concentrations were detected between surface and bottom water at the lower reach of the mesohaline zone during the years of mean and high flow years (Fig. 7B - 7F) indicating that ammonium and orthophosphate were released from the benthic environment or due to heterotrophic activity in bottom waters. Interestingly, mesozooplankton abundances (1993-1994) were significantly correlated with ammonia ($R^2 = 0.42$; $P = 0.0006$) and orthophosphate concentrations ($R^2 = 0.24$; $P = 0.015$) at station WE4.2 (data not shown).

Summer ammonia and orthophosphate concentrations in the water column decreased as river discharge rates increased (Fig. 7C-7F) due in all likelihood to both phytoplankton uptake and flushing. Sources of ammonium appear to be bottom water or sediment in the lower reaches of the mesohaline zone. Phosphorus increases linearly downstream in both surface and bottom waters to the upper region of the mesohaline zone and then abruptly decreases in the lower estuary for low and mean river discharge

Fig. 7. Salinity dilution curves of DO, ammonium, orthophosphate, silicate, nitrite+nitrate, chlorophyll *a* and light attenuation coefficient in the water column of the York River system for low (1991), mean (1990) and high (1994) flow years during the summer-fall period (June through October).



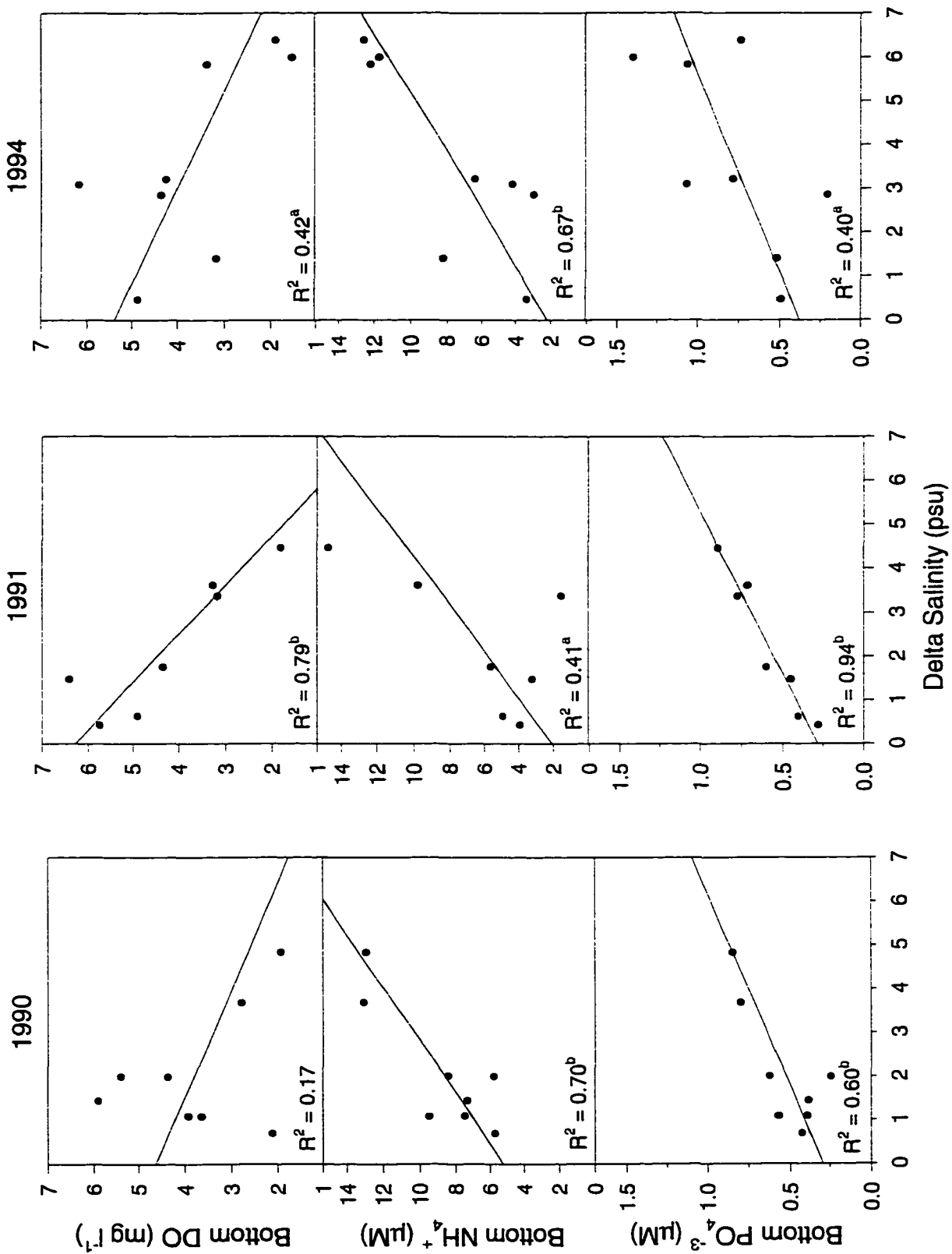


years (Fig. 7E, 7F). For the high discharge year, the pattern is reversed suggesting uptake or simple dilution. How these differences might be related to differences in river discharge is not apparent.

Silicate and nitrite+nitrate concentrations decreased downstream suggesting runoff is the major source for those nutrient pools in the York River estuary (Fig. 7G-7J). Silicate showed relatively conservative properties while nitrite+nitrate did not above 10 psu except during the high flow year. Rapid decrease of nitrite+nitrate concentrations at 10 - 15 psu appears to be due to phytoplankton uptake corresponding to peak chlorophyll *a* concentration (see Fig. 7K). Silicate concentration increased as river discharge rates increased whereas nitrite+nitrate concentrations were not clearly related to river discharge rates. No difference in silicate and nitrite+nitrate was detected between surface and bottom. Chlorophyll *a* peaks were observed at 10 - 15 psu (Fig. 7K) whereas maximum light attenuation coefficients were recorded in the range of 17 to 22 psu (Fig. 7L).

The final set of analyses done for the mesohaline stations was to investigate other mechanisms potentially affecting ammonium and phosphorus dynamics and in particular the role of tidal mixing and benthic regeneration. Figure 8 shows the relationship between surface and bottom water salinity differences and concentrations of dissolved oxygen, ammonium and phosphorus in bottom water for the lower York River station during the summer-fall period (June to October). It is clear that ammonium and phosphorus are regenerated (released from the sediments) in bottom waters as the water column becomes stratified. Low DO concentrations indicate high metabolic rates with the concomitant release of nutrients which on destratification are mixed with surface

Fig. 8. Regression of water quality parameters (DO, NH_4^+ and PO_4^{3-} in bottom water) vs. salinity difference between surface and bottom water during the summer-fall (June-October) of mean (1990), low (1991) and high (1994) flow years at the lower estuary station WE4.2 (^a: $P < 0.1$, ^b: $P < 0.05$).



waters. These results support previously reported studies in the lower estuary by Haas (1977), Webb and D'Elia (1980), and D'Elia, et al. (1981).

DISCUSSION

Nutrient limitation

Nutrient limitation is commonly defined as the constraint on phytoplankton growth rates and potential rate of net primary production (biomass accumulation) by the low concentration of a specific nutrient (Howarth 1988). Nutrient limitation of growth rates is based generally on small temporal and spatial scales (hours to days; liters to m³) whereas nutrient limitation of net primary production is based on larger scales (weeks to months; hectares to km³). Nutrient limitation has been assessed by many approaches including: comparing ambient nutrient concentrations to half-saturation constants (Fisher et al. 1992), molar DIN:DIP ratios (Redfield 1963; Fisher et al. 1992), molar total N:P ratios (Magnien et al. 1992), nutrient addition bioassays (D'Elia et al. 1986; Haas and Wetzel 1993) and ecosystem overviews (Boynton et al. 1982; Malone et al. 1988). Since nutrient and phytoplankton data analyzed in this study were based on ecosystem spatio-temporal scales (weeks, km³), nutrient limitations on net primary production at ecosystem scales were examined by molar ratios of ambient DIN and DIP concentrations in the surface water based on the ratio of 16:1 (Redfield et al. 1958). Absolute concentrations of nutrients in the study sites were mostly higher than half-saturation constants for uptake (DIN \approx 2 μ M, PO₄³⁻ \approx 0.2 μ M; Fisher et al. 1988) which are accepted as an index for

nutrient limitations of growth rates. Therefore, we used DIN:DIP ratios as indicators of potentials for N and P limitations rather than actual nutrient limitation.

Based on this rationale, potential P limitation was present in the tidal freshwater regions but shifted to N limitation in the lower estuarine regions during summer and fall (Fig. 6). This conforms to the generally accepted view that marine phytoplankton are more likely to be limited by N whereas freshwater phytoplankton are more likely to be limited by P (Hecky and Kilman 1988). Magnien et al. (1992) reported greater overall potential for phosphorus rather than nitrogen-limitation of phytoplankton in the upper mainstem of the Chesapeake Bay, the Patuxent Estuary, and the Potomac Estuary. They hypothesized that a greater loss of phosphorus than nitrogen through sedimentation and burial drives the patterns of nutrient limitation in these systems. The high loss of phosphorus was thought to be due to the significantly greater fraction of particulate phosphorus versus particulate nitrogen in the load input at the head of the estuaries. This mechanism could explain why tidal freshwater and/or transitional stations may experience potential P limitation in the York River system. It is known that some of the nutrient load deposited to bottom sediment is remobilized into the water column through mechanisms such as remineralization or desorption (Kemp and Boynton 1984; Boynton and Kemp 1985; Magnien et al. 1992). The ammonium concentrations varied with temperature-driven cycles of benthic regeneration and release whereas the orthophosphate concentrations are affected by the change in redox potential concomitant with benthic DO depletion (Kemp and Boynton 1992). Magnien et al. (1992) found that recycling was occurring at N:P ratios lower than those delivered as inputs, inducing a relatively large phosphorus source during summer and fall and a lowering of water

column N:P ratios during these periods. This process could be an important mechanism for the shift from potential P limitation to potential N limitation in transitional or mesohaline stations in the York River system. Salinity dilution diagrams for 1990 and 1991 showed that surface orthophosphate increased linearly downstream until it decreased rapidly at 15 - 20 psu (Fig. 7E). Surface ammonium ranged 0.3 – 5.9 μM was relatively constant over the river regions (Fig. 7C) while orthophosphate increased resulting in potential N limitation in the water column during the period in transitional regions. Potential N limitation may become less intense as surface orthophosphate decreases rapidly below ca. 15 psu in both surface and bottom waters. It is interesting that surface orthophosphate concentrations did not decrease (Fig. 7E) in the region of summer chlorophyll *a* maximums (10 psu; Fig. 7K). It is not clear if this is either an indication of P sources in addition to orthophosphate (e.g. Malone et al. 1996) or an indication of rapid recycling and the ‘buffering’ effect of adsorption-desorption reactions which partition phosphate between particulate and dissolved phases (e.g. Liss 1976).

These spatial shifts also agree with the proposed scenario that P limitation shifts to N limitation with movement downstream during fall and winter and in turn a shift to N limitation with movement upriver during summer for salinity gradients of 3.8-25 psu (Webb 1988). Webb (1988) proposed that a direct effect of winter runoff caused the shift over “salinity gradients”. The direct effect of winter runoff was obvious when we examined the spatial distribution of N:P ratios during years with different river discharge (Fig. 6). Seasonal patterns in nutrient limitation were also observed in nutrient enrichment studies carried out in the lower York River (Webb 1988), in the Patuxent River (D’Elia et al. 1986), and in the main stem of Chesapeake Bay (Fisher et al. 1992).

Persistent P limitation in tidal freshwater regions was found in nutrient bioassay studies by Haas and Wetzel (1993) who also reported that phytoplankton biomass in tidal freshwaters of the Rappahannock River is weakly limited by phosphorus and by light throughout the year. At a station located at the mouth of the Rappahannock River, phytoplankton experienced prolonged nitrogen limitation throughout the year except for a period of phosphorus limitation during March to May. Si limitation was not found in these bioassay studies as well as other enrichment studies in the York River (Dr. K. Webb, Personal Communication).

Based on the comparison of our analyses with the results from enrichment studies, molar N:P ratios of ambient nutrients appear to be a good indicator of nutrient limitation on phytoplankton biomass accumulation in these systems. Malone et al. (1996) discussed the scales on which phytoplankton production oscillates in response to nutrient supply and suggested that the extrapolation of results from small-scale nutrient-enrichment and uptake-turnover rate experiments to the larger ecosystem scale is disputable, as Hecky and Kilham (1988) suggested. Malone et al. (1996) concluded that seasonal blooms and annual phytoplankton production at the baywide scale are a consequence of phytoplankton response to riverine nitrogen input. The Chesapeake Bay is N limited rather than P limited on estuarine time and space scales. Results of this study (Fig. 6) also showed that winter-spring blooms in the mesohaline zone are the response of phytoplankton to nitrogen input through river discharge.

Accumulation of ungrazed phytoplankton results in high heterotrophic microbial production (Malone et al. 1986; Verity 1987) and seasonal oxygen depletion in bottom water (Malone 1992). The large winter-spring blooms following peaks of river discharge

might contribute to summer oxygen depletion in bottom water in the lower estuary which aggravates water quality in the York River system and suggests the importance of controlling N input from runoff in nutrient reduction strategies. Temporal and spatial variations of nutrient limitation also must be considered in the process of controlling point source nutrients since the extent to which phytoplankton biomass responds to the nutrient supply varies with physiological status of phytoplankton. Potential nutrient limitation of the phytoplankton in the York River system had temporal and spatial variations whose extent was determined by river discharge rate (see Fig. 6).

Seasonal variations in biomass and productivity

A comparative analysis of 63 estuaries (Boynton et al. 1982) showed that chlorophyll *a* concentrations were highest during warm seasons (May-Oct) and peak primary production always occurred during warm periods (June-Sept.) while minima generally occurred during the winter. Chlorophyll *a* concentrations, in all except one case, were higher than the annual mean at the time when maximum production rates occurred. Thus, chlorophyll *a* concentration is generally in phase with phytoplankton production. This pattern has been considered as evidence that temperature is a principal factor affecting nutrient recycling processes and plankton growth rates which are required to maintain high production rates (Eppley 1972; Nixon 1981). In tidal fresh water regions of the York River estuary, the patterns of phytoplankton biomass were also in phase with temperature and primary production (Table 2) probably due to temperature and light effects on maximum algal growth rate combined with low flushing rates in the head of the York River estuary. Similar patterns were observed in other river dominated

systems; e.g., the Rappahannock (Haas and Wetzel 1993) and James River (Filardo and Dunstan 1985) systems in the lower Chesapeake Bay, the mainstem Chesapeake Bay (Harding 1994), and San Francisco Bay (Cloern et al. 1983). Summer peaks of chlorophyll *a* in the York River were similar to those in the Rappahannock (Haas and Wetzel 1993) but much lower than those in the James River (Filardo and Dunstan 1985).

River discharge effects were also evident and act as a controlling factor for phytoplankton dynamics in the head of estuaries. Filardo and Dunstan (1985) reported that chlorophyll *a* and photosynthetic production of particulate organic carbon in very low salinity regions (0 - 0.78 psu) were inversely correlated with river discharge rates. Primary production in the upper bay of the Louisiana Estuary also was negatively correlated with river discharge rates (Randall and Day 1987). Results of this study also showed that phytoplankton populations are flushed out of tidal freshwater regions during the winter high flow periods and phytoplankton biomass accumulation is limited by high flushing rates in spite of high concentration of DIN and silicates in the tidal freshwater regions.

For the transition stations below the freshwater regions, controls on phytoplankton dynamics are more complex since the river-estuary transition regions experience a turbidity maximum where the location and degree of mixing are controlled by river discharge (Hansen and Rattray 1965). Phytoplankton in the turbidity maximum zone has been reported to be limited by light (Cloern et al. 1983; Wofsy 1983; Harding et al. 1986; Pennock and Sharp 1994). Salinity change (osmotic stress) has also been suggested as a mechanism resulting in mass mortality of freshwater phytoplankton species (Filardo and Dunstan 1985). In addition, Avnimelech et al. (1982) reported the

tendency of clay minerals to form flocs incorporating phytoplankton, and further reducing phytoplankton biomass in these regions. The results of our study also indicated the highest light limitation at the upper transitional station (RET4.1) in the York River estuary. The upper river-estuary transition station maintained low phytoplankton biomass throughout the annual cycle except for a characteristic small summer bloom (Fig. 3B) suggesting phytoplankton in this region are influenced by both river discharge and limited by light. On the other hand, chlorophyll *a* maxima have been observed in clearer waters upstream or seaward of the turbidity maximum during summer or fall and associated with removal of ammonium, nitrate, phosphate and silicate in estuaries (Anderson 1986; Harding et al. 1986; Fisher et al. 1988). Increased light penetration and sufficient nutrients are thought to be major causes for the accumulation of phytoplankton biomass in clearer waters upstream of the turbidity maximum zone (Harding et al. 1986; Fisher et al. 1988). In the James River, high chlorophyll *a* levels were reported to be derived largely from high concentrations of physiologically healthy freshwater diatoms due to selective trapping that resulted from the balance between diatom sinking rate and the net upward water velocity in very low salinity waters (0.5 psu) during periods of low river discharge in the summer and fall (Moon and Dunstan 1990). A chlorophyll *a* maximum was also observed at the lower transition station (RET4.3) in this study (Fig. 3C). Salinity dilution plots showed that chlorophyll *a* maxima developed in the salinity range of 10 - 15 psu, i.e., the upstream part of the turbidity maximum (Fig. 7K, 7L). The chlorophyll *a* maximum may be attributed to more available light and sufficient nutrients remineralized by heterotrophic activity in the water column and bottom sediments since there were no differences in surface and bottom ammonium, silicate and nitrite+nitrate

concentrations (Fig. 7). These results suggest that the water column in the oligohaline zone is relatively well-mixed with rapid recycling of nutrients or there may be another source for N to support phytoplankton growth during summer. Glibert et al. (1991) reported that urea accounted for 70 - 80 % of the total phytoplankton N uptake in the plume of the Chesapeake Bay estuary. They also suggested grazers as important organisms releasing dissolved organic N (DON) in late summer whereas nutrient-deficient phytoplankton seemed to release more DON in winter.

The highest turbidity occurred in mesohaline regions instead of oligohaline areas (Fig. 7L) and generally paralleled the light limitation function (Fig. 5) indicating that the turbidity maximum zone of the York River system may have been missed in the sampling scheme employed here. Turbidity maxima have been generally recorded in the oligohaline (1 - 10 psu) zone in the Chesapeake, Delaware and Hudson estuaries (Fisher et al. 1988).

In the lower region of the transition zone (RET4.3), the short winter bloom suggests that phytoplankton growth may not be limited by high flushing rates during the winter in contrast to the upper transition zone (RET4.1). Channel morphology changes dramatically between the upper transition station (RET4.1) with a narrow and deep channel and the lower transition station (RET4.3) with a broad and shallow channel. This change in channel morphology might relax the limitation by high flushing rates. An extraordinarily high chlorophyll *a* concentration ($70.8 \mu\text{g l}^{-1}$) recorded in January, 1990 at this station (data not shown) may be explained by patchy distribution of phytoplankton (e.g. Sellner et al. 1991) or selective trapping of large cells which can grow at fairly low light levels and high nutrient levels in this region.

In the mesohaline zone of the Chesapeake Bay, seasonal variations in phytoplankton biomass were correlated with riverine nitrate whereas seasonal variations in productivity were correlated with temperature and light (Malone et al. 1988). Phytoplankton biomass peaks occurred during spring when river discharge and riverine nutrient input were high, but phytoplankton productivity was highest during summer when river discharge and riverine nutrient input were low. Malone et al. (1988) concluded that the summer productivity peak in the mesohaline reach of the Chesapeake Bay is due to remineralization of nitrogen delivered to the system during the previous spring. Grazing was suggested as the major process controlling phytoplankton biomass in the surface water during summer which was characterized as high primary productivity and low biomass relative to spring (Sellner and Kachur 1987; White and Roman 1992). Malone et al. (1986) observed that most of the summer flux of POM into the benthos is derived from phytoplankton.

In the mesohaline zone of the York River system, on the other hand, variations in phytoplankton biomass were significantly correlated with riverine nitrate whereas variations in primary production were not correlated with either temperature or light (see Table 2). Seasonal variation of phytoplankton biomass was similar to that of productivity at the mouth of the York River estuary (Fig. 3). This result differs from reports on other estuaries (Boynton et al. 1982) and the mainstem of the Chesapeake Bay (Malone et al. 1988) suggesting riverine N input coupled with other physical factors controls phytoplankton production as well as phytoplankton biomass in the lower York River estuary. Malone et al. (1988) indicated that high grazing rates explain low phytoplankton biomass during summer phytoplankton productivity maximum. The similarity in

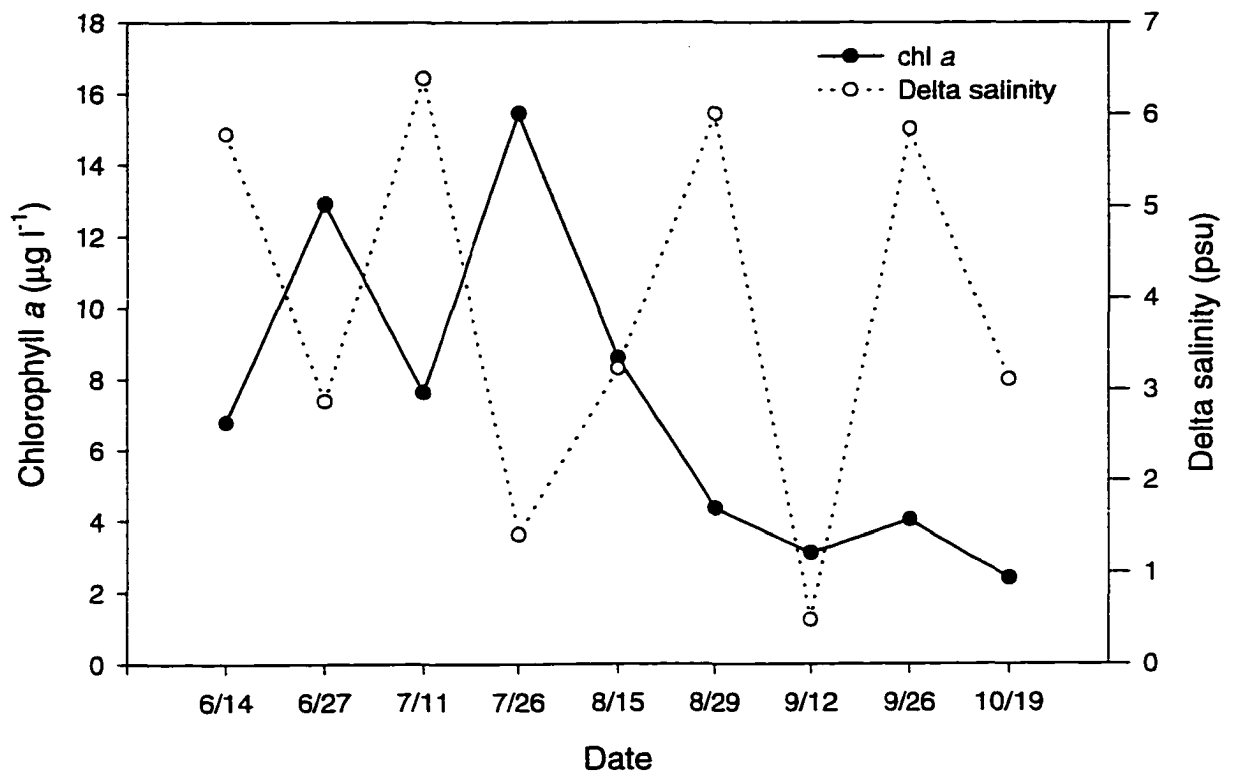
seasonal patterns between biomass and production in this study suggests there are limited grazing effects in the mesohaline zone of the York River estuary.

The effect of destratification and stratification of the water column was evident on summer chlorophyll *a* in the mesohaline zone when we examined the relationship between chlorophyll *a* and salinity differences between surface and bottom water during summer time (Fig. 9). Tidal mixing is thought to be a mechanism supplying ammonium and orthophosphate released from bottom water and/or benthic sediments to surface water during summer and fall based on observed differences in ammonium and orthophosphate concentrations between surface and bottom water (Fig. 7). Significant correlations of bottom ammonium and orthophosphate vs. surface-bottom salinity difference (Fig. 8) indicate an important role of water column mixing in recycling of ammonium and orthophosphate. Destratification of the water column also affected DO distributions in the mesohaline zone. Webb and D'Elia (1980) reported that spring-tidal destratification enhances the input of benthic-regenerated nutrients into the surface water and replenishes O₂ in the deep water from surface water in the lower York River.

Nutrient recycling is thought to be induced by high activity of benthic or bottom water heterotrophic metabolism stimulated by warm temperature and allochthonous organic matter derived from freshwater or ungrazed phytoplankton produced during the winter of previous year. Summer ammonium concentration in lower reaches (station LE4.3) of the mesohaline zone was correlated with spring chlorophyll *a* of previous years in middle reach (station LE4.2) of the mesohaline regions ($R^2 = 0.76$; $P = 0.0048$).

The concept of the river continuum (Minshall et al. 1985) plays a role in leading to a general understanding of organic carbon processing and metabolism in rivers

Fig. 9. Variations of chlorophyll *a* and salinity difference between surface and bottom water during summer and fall (June-October) in 1994 at the mouth (WE4.2) of the York River estuary.



(Howarth et al. 1996). The concept assumes that ecological processes downstream in a river are coupled to upstream processes, and to changes in channel morphology of the river moving downstream. The York River appears to conform to this concept since phytoplankton growth in the lower river relies on the nutrient, especially nitrite+nitrate, delivered from the upper river. Large portions of nutrients in the upper river are thought to be delivered to the lower river since phytoplankton growth in the upper river is limited by short residence time during high flow season due to the characteristic morphology of channel in the upper river. This mechanism is more clear when the effect of N input through river discharge on spring blooms in lower estuary was considered (Fig. 4). The unusually high summertime peak of chlorophyll *a* ($68.7 \mu\text{g l}^{-1}$) at station RET4.3 in 1989 and non-bloom during summer at station TF4.2 in 1989 (data not shown) may be explained by the effect of N input and short residence time and/or light limitation due to relatively high rates of river discharge during the summer of 1989 compared with other years (see Fig. 2). This unusual pattern implies that river discharge has a direct impact on phytoplankton dynamics in the entire York river system supporting the river continuum concept in the York River system.

CONCLUSIONS

We use a spatially and temporally extensive data set to analyze variations in factors potentially limiting phytoplankton biomass and production in the York River estuary. By affecting residence time, nutrient input, light regime, and tidal mixing, river

discharge rates regulate the magnitude, location and timing of phytoplankton blooms in the York River estuarine system indicating that ecological processes of the York River system are predictable based on the river continuum concept. Phytoplankton growth in tidal fresh water is limited since the residence time (dependent on the river discharge rate) can be less than the cell doubling time. Temperature-dependent metabolism is also an important mechanism in this zone. In the transition zone or turbidity maximum zone, phytoplankton are limited mainly by light and internal processes dependent on temperature and estuarine circulation. In mesohaline regions, riverine nitrite + nitrate input during the winter results in winter-spring blooms at locations experiencing potential nitrogen limitation. Tidal mixing also influences summer phytoplankton dynamics in the mesohaline zone by supplying regenerated nutrients via a predictable cycle of column stratification-destratification. In general, phytoplankton dynamics appear controlled to large extent by resource limitation (bottom-up control) rather than zooplankton grazing (top-down control).

LITERATURE CITED

- Aksnes, D. L. and Lie, U. 1990. A coupled physical-biological pelagic model of a shallow sill fjord. Estuarine, Coastal and Shelf Science 31:459-486.
- Alpine, A. E. and J. E. Cloern. 1992. Trophic interactions and direct physical effects control phytoplankton biomass and production in an estuary. Limnology and Oceanography 37(5): 946-955.
- Anderson, G. F. 1986. Silica, diatoms and a freshwater productivity maximum in Atlantic coastal plain estuaries, Chesapeake Bay. Estuarine, Coastal and Shelf Science 22:183-197.
- Armstrong, R. A. 1994. Grazing limitation and nutrient limitation in marine ecosystems: Steady state solutions of an ecosystem model with multiple food chains. Limnology and Oceanography 39(3):597-608.
- Avnimelech, Y., Troeger, B. W. and Reed, L. W. 1982. Mutual flocculation of algae and clay. Evidence and implication. Science 216:63-65.
- Bell, C. F., D. L. Belval, and J. P. Campbell. 1996. Trends in Nutrients and Suspended Solids at the Fall Line of Five Tributaries to the Chesapeake Bay in Virginia, July 1988 through June 1995. Water-Resources Investigations Report 96-4191. U.S. Geological Survey, Richmond, VA.
- Bender, M. E. 1986. The York River: A Brief Review of Its Physical, Chemical and Biological Characteristics. Virginia Institute of Marine Science, School of Marine Science, The College of William and Mary, Gloucester Point, VA 23062
- Boyer, J. P., R. R. Christian and D. W. Stanley. 1993. Patterns phytoplankton primary productivity in the Neuse River estuary, North Carolina, USA. Marine Ecology Progress Series 97:287-297.
- Boynton, W. R. and Kemp, W. M. 1985. Nutrient regeneration and oxygen consumption by sediments along an estuarine salinity gradient. Marine Ecology Progress Series 23:45-55.

- Boynton, W. R., W. M. Kemp and C. W. Keefe. 1982. A comparative analysis of nutrients and other factors influencing estuarine phytoplankton production, p. 69-90. In V. Kennedy (ed.), *Estuarine Comparisons*. Academic Press, New York.
- Caraco, N. F., J. J. Cole, P. A. Raymond, D. L. Strayer, M. L. Pace, S. E. G. Findlay, and D. T. Fisher. 1997. Zebra mussel invasion in a large, turbid river: Phytoplankton response to increased grazing. *Ecology* 78(2): 588-602.
- Carpenter, S. R., J. F. Kitchell, and J. R. Hodgson. 1985. Cascading trophic interactions and lake productivity. *BioScience* 35:634-639.
- Carpenter, S. R., and others. 1987. Regulation of lake primary productivity by food web structure. *Ecology* 68:1863-1876.
- Cloern, J. E. 1996. Phytoplankton bloom dynamics in coastal ecosystems: a review with some general lessons from sustained investigation of San Francisco Bay, California. *Reviews of Geophysics* 34(2):127-168.
- Cloern, J. E. 1991. Tidal stirring and phytoplankton bloom dynamics in an estuary. *Journal of Marine Research* 49:203-221.
- Cloern, J. E., Alpine, A. E., Cole, B. E., Wong, R. L. J., Arthur, J. F., Ball, M. D. 1983. River discharge controls phytoplankton dynamics in the Northern San Francisco Bay estuary. *Estuarine, Coastal and Shelf Science* 16:415-429.
- Corish, K., M. Berman and C. H. Hershner. 1995. An economic analysis of the York River basin. Center for Coastal Management and Policy, Department of Resource Management and Policy, Virginia Institute of Marine Science, College of William and Mary, Gloucester Point, Virginia.
- Day, J. W., Jr., C. A. S. Hall, W. M. Kemp, A. Yanez-Arancibia. 1989. Estuarine Ecology: 4. Estuarine phytoplankton, p. 147-187. John Wiley & Sons, Inc., New York.
- D'Elia, C.F., K. L. Webb and R. L. Wetzel. 1981. Time varying hydrodynamics and water quality in an estuary, p. 597-606. In B.J. Neilson and L.E. Cronin (eds.), *Estuaries and Nutrients*. The Humana Press, Clifton, New Jersey.
- D'Elia, C. F., J. G. Sanders, and W. R. Boynton. 1986. Nutrient enrichment studies in a coastal plain estuary: Phytoplankton growth in large-scale, continuous cultures. *Canadian Journal of Fisheries and Aquatic Science* 43:397-406.
- DiToro, D. M., O'Connor, D. J., Thomann, R. V. 1971. A dynamic model of phytoplankton populations in the Sacramento-San Joaquin Delta. *Advances in Chemistry Series* 106:131-180.

- Eppley, R. W. 1972. Temperature and phytoplankton growth in the sea. Fishery Bulletin 70:1063-1085.
- Filardo, M. J. and Dunstan, W. M. 1985. Hydrodynamic control of phytoplankton in low salinity waters of the James River estuary, Virginia, U.S.A. Estuarine, Coastal and Shelf Science 21:653-667.
- Fisher, T. R., Peele, E. R., Ammerman, J. W., Harding, Jr. L. W. 1992. Nutrient limitation of phytoplankton in Chesapeake Bay. Marine Ecology Progress Series 82:51-63.
- Fisher, T. R., L. W. Harding, Jr., D. W. Stanley, and Larry G. Ward. 1988. Phytoplankton, nutrients, and turbidity in the Chesapeake, Delaware, and Hudson estuaries. Estuarine, Coastal Shelf Science 27:61-93.
- Gallegos, C. L., T. E. Jordan, and D. L. Correll. 1992. Event-scale response of phytoplankton to watershed inputs in a subestuary: Timing, magnitude, and location of blooms. Limnology and Oceanography 37(4):813-828.
- Glibert, P. M., C. Garside, J. A. Fuhrman and M. R. Roman. 1991. Time-dependent coupling of inorganic and organic nitrogen uptake and regeneration in the plume of the Chesapeake Bay estuary and its regulation by large heterotrophs. Limnology and Oceanography 36:895-909
- Haas, L. W. 1975. Plankton Dynamics in a Temperate Estuary with Observations on a Variable Hydrographic Conditions. Doctoral Dissertation, School of Marine Science, College of William and Mary, Gloucester Point, Virginia.
- Haas, L.W. 1977. The effect of the spring-neap tidal cycle on the vertical salinity structure of the James, York and Rappahannock rivers, Virginia, USA. Estuarine, Coastal Marine Science 5:485-496.
- Haas, L. W. and R. L. Wetzel. 1993. Nutrient Limitation in the Chesapeake Bay: Nutrient Bioassays in the Virginia Bay System. Final Report to Virginia Coastal Resources Management Program, Virginia Institute of Marine Science, School of Marine Science, College of William and Mary, Gloucester Point, Virginia.
- Hansen, D. V. and Rattray, M., Jr. 1965. Gravitational circulation in straits and estuaries. Journal of Marine Research 23:104-122.
- Harding Jr., L. W. 1994. Long-term trends in the distribution of phytoplankton in Chesapeake Bay: roles of light, nutrients and streamflow. Marine Ecology Progress Series 104:267-291.
- Harding, Jr., L. W., B. W. Meeson, and T. R. Fisher, Jr. 1986. Phytoplankton production in two east coast estuaries: Photosynthesis-light functions and patterns of carbon

- assimilation in Chesapeake and Delaware Bays. Estuarine, Coastal and Shelf Science 23:773-806.
- Hecky, R. E. and P. Kilham. 1988. Nutrient limitation of phytoplankton in freshwater and marine environments: A review of recent evidence on the effects of enrichment. Limnology and Oceanography 33:796-822.
- Howarth, R. W. 1988. Nutrient limitation of net primary production in marine ecosystems. Annual Review of Ecology 19:89-110.
- Howarth, R. W., R. Schneider, and D. Swaney. 1996. Metabolism and organic carbon fluxes in the tidal freshwater Hudson River. Estuaries 19(4):848-865.
- Hyer, P. V. 1977. Water Quality Model of York River, Virginia. Special Scientific Report No. 146. Virginia Institute of Marine Science, Gloucester Point, Virginia.
- Kemp, W. M., and W. R. Boynton. 1984. Spatial and temporal coupling of nutrient inputs to estuarine primary production: the role of particulate transport and decomposition. Bulletin of Marine Science 35:522-535.
- Kemp, W. M., and W. B. Boynton. 1992. Benthic-pelagic interactions: Nutrient and oxygen dynamics, p. 149-221. In D. E. Smith, M. Leffler, and G. Mackiernan (eds.), Oxygen Dynamics in the Chesapeake Bay: A Synthesis of Research. Maryland Sea Grant College, College Park, Maryland.
- Kindler, D. D. 1991. Contrasts Between Tidal Freshwater and Estuarine Phytoplankton Growth on Intracellular and Recycled Nutrient Pools over a Summer-Winter Seasonal Transition. M.A. Thesis. School of Marine Science, The College of William and Mary. Gloucester Point, Virginia
- Kivi, K., S. Kaitala, H. Kuosa, J. Kuparinen, E. Leskinen, R. Lignell, B. Marcussen, and T. Tamminen. 1993. Nutrient limitation and grazing control of the Baltic plankton community during annual succession. Limnology and Oceanography 38(5):893-905.
- Liss, P. S. 1976. Conservative and non-conservative behavior of dissolved constituents during estuarine mixing; p. 93-130. In Burton, J. D. and Liss, P. S. (eds.), Estuarine Chemistry. Academic Press, New York.
- Madariaga, I. de, Gonzalez-Azpiri, L., Villate, F., and Orive, E. 1992. Plankton responses to hydrological changes induced by freshets in a shallow mesotidal estuary. Estuarine, Coastal and Shelf Science 35:425-434.
- Magnien, R. E., R. M. Summers, and K. G. Sellner. 1992. External nutrient sources, internal nutrient pools, and phytoplankton production in Chesapeake Bay. Estuaries 15:497-516.

- Malone, T. C. 1992. Effects of water column processes on dissolved oxygen, nutrients, phytoplankton, and zooplankton, p. 61-112. In D. E. Smith, M. Leffler, and G. Mackiernan (eds.), *Oxygen dynamics in the Chesapeake Bay: A synthesis of research*. Maryland Sea Grant College, College Park, Maryland.
- Malone, T. C. and M. B. Chervin. 1979. The production and fate of phytoplankton size fractions in the plume of Hudson River, New York Bight. *Limnology and Oceanography* 24(4):683-696.
- Malone, T. C., D. J. Conley, T. R. Risher, P. M. Glibert, S. W. Harding, and K. G. Sellner. 1996. Scales of Nutrient-Limited Phytoplankton Productivity in Chesapeake Bay. *Estuaries* 19:371-385.
- Malone, T. C., L.H. Crocker, S. E. Pike and B. W. Wendler. 1988. Influences of river flow on the dynamics of phytoplankton production in a partially stratified estuary. *Marine Ecology Progress Series* 48:235-249
- Malone, T. C., W. M. Kemp, H. W. Ducklow, W. R. Boynton, J. H. Tuttle, and R. B. Jonas. 1986. Lateral variation in the production and fate of phytoplankton in a partially stratified estuary. *Marine Ecology Progress Series* 32:149-160.
- Malone, T. C., P. J. Neale and D. Boardman. 1980. Influences of estuarine circulation on the distribution and biomass of phytoplankton size fractions, p. 249-262. In V. Kennedy (ed.), *Estuarine Perspectives*. Academic Press, New York.
- Minshall, G. W., K. W. Cummins, R. C. Peterson, C. E. Cushing, D. A. Bruns, J. R. Sedell, and R. L. Vannote. 1985. Development in stream ecosystem theory. *Canadian Journal of Fisheries and Aquatic Sciences* 42:1045-1055
- Moon, C. and Dunstan, W. M. 1990. Hydrodynamic trapping in the formation of the chlorophyll *a* peak in turbid, very low salinity waters of estuaries. *Journal of Plankton Research* 12:323-336.
- Nixon, S. W. 1981. Freshwater inputs and estuarine productivity, p.31-57. In R. Cross and D. Williams (eds.), *Proceedings of the National Symposium on Freshwater Inflow to Estuaries*. U.S. Fish and Wildlife Service, Office of Biological Services, FWS/OBS-81/04, Vol I, San Antonio, Texas.
- Pennock, J. R. 1985. Chlorophyll distributions in the Delaware Estuary: regulation by light-limitations. *Estuarine, Coastal and Shelf Science* 21:711-725.
- Pennock, J. R., and Sharp, J. H. 1994. Temporal alternation between light-and nutrient-limitation of phytoplankton in a coastal plain estuary. *Marine Ecology Progress Series* 111:275-288.

- Randall, J. M. and Day, Jr. J. W. 1987. Effects of river discharge and vertical circulation on aquatic primary production in a turbid Louisiana (USA) estuary. Netherlands Journal of Sea Research 21(3): 231-242.
- Ray, T. R., L. W. Haas, and M. E. Sieracki. 1989. Autotrophic picoplankton dynamics in a Chesapeake Bay sub-estuary. Marine Ecology Progress Series 52:273-285.
- Redfield, A. C. 1958. The biological control of chemical factors in the environment. American Science 46:205-222.
- Redfield, A. C., B. H. Ketchum, and F. A. Richards. 1963. The influence of organisms on the composition of sea-water, p. 26-77. In M. N. Hill (ed.), *The Sea*. John Wiley & Sons, New York.
- Sellner, K. B. and M. E. Kachur. 1987. Phytoplankton: Relationships between phytoplankton, nutrients, oxygen flux, and secondary producers, p. 12-37. In K. L. Heck (ed.), *Ecological Studies in the Middle Reach of Chesapeake Bay*. Springer-Verlag, New York.
- Sellner, K. G., R. V. Lacouture, S. J. Cibik, and A. Brindley. 1991. Importance of a winter dinoflagellate-microflagellate bloom in the Patuxent River estuary. Estuarine, Coastal and Shelf Science 32:27-42.
- Tilman, D. 1982. Resource competition and community structure. Princeton University Press, Princeton, New Jersey.
- Verity, P. G. 1987. Factors driving changes in the pelagic trophic structure of estuaries with implications for the Chesapeake Bay, p 35-56. In M. P. Lynch and E. C. Krome (eds.), *Perspectives on the Chesapeake Bay: Advances in Estuarine Science*. Publ. No. 127, Chesapeake Bay Research Consortium, Gloucester Point., Virginia.
- Virginia Water Control Board, 1987. Tributary Water Quality 1986, Characterization Report. Chesapeake Bay Water Quality Monitoring Program, Chesapeake Bay Office, Virginia Water Control Board, Richmond, Virginia.
- Webb, K. L. and C. F. D'Elia. 1980. Nutrient and oxygen redistribution during a spring neap tidal cycle in a temperate estuary. Science 207:983-985.
- Webb, K. L. 1988. Comment on "Nutrient limitation of phytoplankton growth in brackish coastal ponds" by Caraco, Tamse, Boutros, and Valiela (1987). Canadian Journal of Fisheries and Aquatic Science 45:380
- White, J. R. and M. R. Roman. 1992. Seasonal study of grazing by metazoan zooplankton in the mesohaline Chesapeake Bay. Marine Ecology Progress Series 86:251-261
- Wofsy, S. C. 1983. A simple model to predict extinction coefficients and phytoplankton biomass in eutrophic waters. Limnology and Oceanography 28(6):1144-1155.

SECTION II

Seasonal Variations of Size Fractionated Phytoplankton along the Salinity Gradient in the York River Estuary, Virginia[†]

[†]: To be submitted to *Journal of Plankton Research*

ABSTRACT

The dynamics of phytoplankton size structure were investigated in the freshwater, transitional and estuarine reaches of the York River over an annual cycle. The contribution of large cells (micro-plankton, $>20\ \mu\text{m}$) to total biomass increased downstream during winter whereas that of small cells (nano-plankton, $3 - 20\ \mu\text{m}$; pico-plankton, $<3\ \mu\text{m}$) increased downstream during summer. In the freshwater region, the contribution of micro-phytoplankton to phytoplankton biomass was significant during warm seasons (spring and summer) but not during colder seasons (winter), whereas the contribution of small-sized cells (especially picoplankton) increased during cold seasons. Temperature, light and high flushing rate appear to control phytoplankton community structure in the freshwater region. In the transitional region, nano-sized cells dominated the phytoplankton population throughout all seasons except during the spring bloom (April) when the biomass of micro-phytoplankton increased. Size structure in the transitional region is most likely regulated by light availability. In the mesohaline region, nano- and pico-sized cells dominated the phytoplankton population during the summer bloom whereas micro-sized cells dominated during winter bloom. Factors controlling phytoplankton community size structure in the mesohaline zone may be riverine nitrogen input, temperature and/or advective transport from upriver. We conclude from these studies that spatial and seasonal variations in size structure of phytoplankton observed on

the estuarine scale is determined both by the different preferences of micro-, nano-, and picoplankton for nutrients and by their different light requirements, suggesting that analyses of size structure phytoplankton dynamics are necessary to better understand phytoplankton dynamics and to better manage water quality in estuarine systems.

INTRODUCTION

It is important to understand phytoplankton dynamics since phytoplankton are the dominant primary producers and main sources of carbon and nutrients (e.g. nitrogen, phosphorus) in marine food webs (Haines 1976, Thayer et al. 1978, Kemp and Boynton 1981, Boynton et al. 1982, Coffin and Sharp 1987, Sundbaeck et al. 1990).

Phytoplankton affect water quality, especially dissolved oxygen by photosynthesis and respiration and can serve as substrates for microbial decomposition resulting in oxygen depletion when their ungrazed biomass has accumulated (Morris et al. 1978, 1982, Officer et al. 1984, Seliger et al. 1985, Malone et al. 1986, Jackson et al. 1987, Tuttle et al. 1987, Sundbaeck et al. 1990). Plankton are also light-absorbing particles which can limit their own growth, i.e., self-shading (Kirk 1994), and the depth of light penetration.

In eutrophic estuarine environments characterized by high nutrient input, primary production tends to be unstable, and zooplankton or other higher level organisms typically can not respond quickly to oscillations in standing stocks of primary producers (biomass), resulting in an accumulation of biomass. Accumulations of ungrazed biomass can modify the composition of the classic food chain that includes phytoplankton, copepods and fishes into a microbially-dominated food chain that includes DOC (from phytoplankton), bacteria, protozoa and copepods. This shift in food chain composition

may give rise to enhanced microbial decomposition and oxygen depletion (Sundbaeck et al, 1990, Jonas 1992).

It is necessary to fractionate phytoplankton assemblages into different size classes in order to elucidate phytoplankton dynamics since cell size influences the response of phytoplankton communities to environmental variation (Williams 1964, Smayda 1965, Eppley & Thomas 1969, Malone & Chervin 1979, Takahashi & Bienfang 1983, Fogg 1986, Oviatt et al. 1989, Glibert et al. 1992, Armstrong 1994, Hein et al. 1995), thereby impacting aquatic food web structure and fisheries (Brooks & Dodson 1965, Longhurst et al. 1967, Martin 1970, Parsons & Lebrasseur 1970, De Mendiola 1971, Walsh 1976, Lenz 1992, Painting et al. 1993). In estuarine food webs, cells less than 12 μm are grazed by copepod larvae, copepodites, tintinnids, oyster larvae, and other microzooplankton (Capriulo & Carpenter 1983, Turner et al. 1983, Fritz et al. 1984, Maurer et al. 1984), whereas netplankton ($>20 \mu\text{m}$) are grazed by adult copepods, fish larvae, scallops, Atlantic menhaden, and others (Mullen and Brooks 1967, Durbin and Durbin, 1975, Scura and Jerde 1977, Pierson 1983). Over long (or short) time scales anthropogenic inputs to estuarine systems may change both the quality (size structure) and quantity (biomass) of primary producers. These changes in size classes and fluctuating biomass resulting from environmental disturbance impact nutrient and DO distribution as well as heterotrophic consumers in the water column. Since cell size influences sinking (Michaels & Silver 1988) and transport rates, it will determine where ungrazed biomass accumulates and undergoes microbial processing by bacteria and protozoa which then play a role in depleting DO (Jonas 1992) and in recycling nutrients (Caron 1991) which can support primary production (Kemp and Boynton 1984).

In past studies, estuarine phytoplankton were usually categorized into two size fractions: netplankton (20-200 μm) and nanoplankton ($<20 \mu\text{m}$). However, in recent years picoplankton (0.2-2 μm), comprised of minute chroococcoid cyanobacteria and eukaryotic phytoplankton, have received attention in estuarine phytoplankton studies (Ray et al. 1989, Lacouture et al. 1990, Malone et al. 1991, Iriarte 1993). Their major contribution to primary production in oceanic environments has been well established (Joint & Pomroy 1983, Li et al. 1983, Glover et al. 1988, Jochem 1988), and the dominance of these minute plankton has been attributed to their efficient light-harvesting processes (Glover et al. 1985, Fogg 1986, Kirk 1986), efficient nutrient uptake-phycoerythrin synthesis-photosynthesis linkages (Raven 1986), and low sinking rates (Takahashi & Bienfang 1983). On the other hand, picoplankton experience some disadvantages of small size, including the inability to move into nutrient-rich or more sufficiently illuminated regimes, and a greater vulnerability to grazers (Fogg, 1986). Small size classes may be selectively grazed by zooplankton, as was experimentally demonstrated by Ryther and Sanders (1980). Perissinotto (1992) also reported that smaller cells (nanophytoplankton) were preferentially selected by zooplankton in the community of the Prince Edward Archipelago. In this study, phytoplankton were grouped into three size classes; micro-size ($> 20 \mu\text{m}$), nano-size ($3 - 20 \mu\text{m}$) and pico-size ($< 3 \mu\text{m}$).

The EPA Chesapeake Bay Program has monitored chlorophyll *a* concentrations as a water quality parameter once or twice per month since mid-1980 in the York River estuary. However, chlorophyll *a* content was not determined for the different size classes. Therefore, to better understand phytoplankton processes in the York River estuary, size

structure dynamics need to be established. Main goals of this study were to: (1) examine temporal and spatial variations in abundance of various size classes of phytoplankton in the York River estuary; (2) investigate mechanisms controlling size structure dynamics and provide information for the projected ecosystem model for this system.

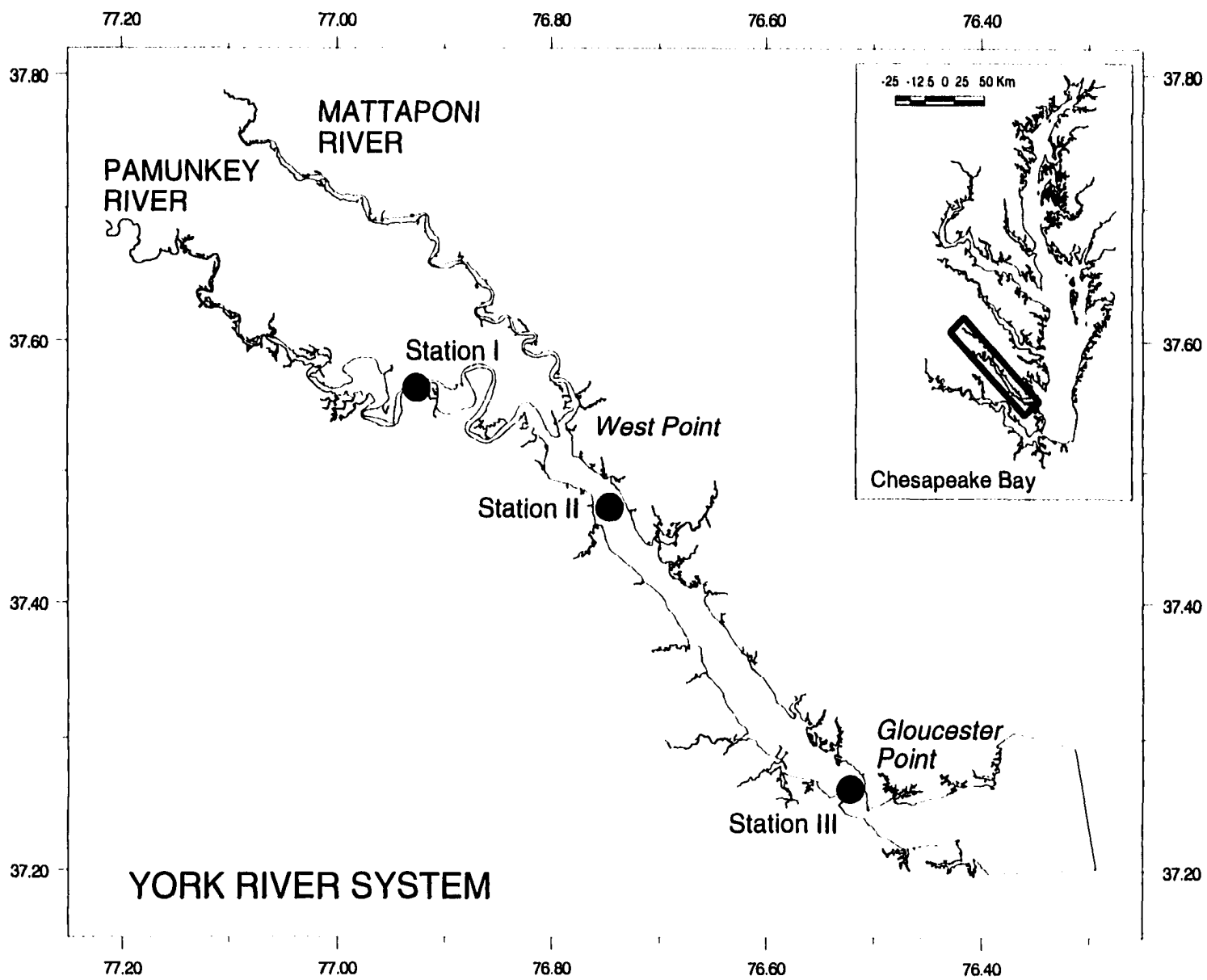
MATERIALS AND METHODS

Study site and sample collection.

The York River system, a subestuary of the Chesapeake Bay, is composed of three rivers: the York, Pamunkey, and Mattaponi (Fig. 1). The York River is formed by the confluence of the Pamunkey and Mattaponi rivers at West Point, 48 km from its mouth. Total average freshwater discharge to the river system is $70 \text{ m}^3 \text{ sec}^{-1}$ (Hyer 1977). The salinity distribution of the York River system is affected by the interactions of freshwater, salt water, tidal energy and wind. Salinity gradients between the surface and bottom layers are influenced by neap and spring tidal cycles with destratification of the water column occurring at high spring tides and stratification developing during the intervening periods (Haas 1975). During low flow conditions, salt water extends 21 to 31 km upriver from West Point (Bender 1986).

Three stations along the axis of the York and Pamunkey River (Fig. 1) were sampled over one annual cycle at high tide during the spring tidal cycle. Sample dates were August 8, 1996, August 15, August 21, September 26, November 11, January 23, 1997, February 20, March 10, April 7, and June 4. One sample (August 8, 1996) was

Fig. 1. Sampling stations in the tidal freshwater (Station I), transitional (Station II) and mesohaline (Station III) regions of the York River estuary.



collected at low tide during the neap tidal cycle. The stations represent the tidal fresh (Station I), river-estuary transition (Station II) and mesohaline zones (Station III) in the York River estuarine system. Samples were collected from 1 m depth below the surface and 1 m above the bottom using either a water pump or Nanssen bottle. Bottom concentrations of nutrients and chlorophyll *a* were not measured from November 1996 or February 1997 to June 1997 at Station I since this station was characterized as a well-mixed water column. Measurements of biological, chemical and physical properties showed little difference of the properties between surface and bottom water at the station. Surface concentrations were used to calculate molar N:P ratios or averages of the parameters in the bottom water over the sampling period at Station I.

Chlorophyll a measurement

Phytoplankton were fractionated by filtration through 20 μm Nytex[®] mesh (1-2 liters) and 3 μm PORETICS[®] polyester membrane filters (1 liter) with minimal vacuum (< 150 mm Hg). For chlorophyll *a* (chl *a*) determinations, ten ml of non-fractionated whole water, 20 ml of 20 μm filtrate, and 40 ml of 3 μm filtrate were filtered through Whatman[®] 25 mm GF/F[™] glass fiber filters (0.7 μm) under vacuum (< 120 mm Hg). Sample filtration was performed in duplicate and immediately following sampling to minimize the grazing effect. The filters were placed in dark test tubes pre-filled with 8 ml extraction solution (45% dimethyl sulfoxide (DMSO), 45% acetone, 10% deionized water, and 1% diethylamine (DEA) (Webb & Hayward unpubl.)) After storage for 12 hrs at room temperature, fluorescence was read on a Turner Designs[®] 10-AU Fluorometer. One or two drops of HCL (2N) were added and the extractant re-read for determination of

pheopigments following acidification. The ratio of fluorescence before and after acidification was used to examine grazing effects on phytoplankton population (e.g. Welschmeyer and Lorenzen 1985) in the York River estuary. Chlorophyll *a* concentrations were determined using the equation: chlorophyll *a* concentrations = chlorophyll *a* readings before acidification × [volume of extraction solution / volume of filtered sample]

Chlorophyll *a* in each size fraction was determined by consecutive subtraction of fractions < 3 μm and < 20 μm from whole water chlorophyll *a*.

Measurement of dissolved inorganic nutrient and physical properties

Water samples (50 ml) for nutrient analysis were filtered (0.45 μm Gelman Supor[®]) immediately following sampling to minimize uptake by phytoplankton and stored refrigerated until analysis. Ammonium was analyzed by the phenolhypochlorite method (Greenberg et al., 1992), and nitrite (NO₂⁻) + nitrate (NO₃⁻) were measured by Alpkem[®] autoanalyzer at the Ecosystem Process Lab, Virginia Institute of Marine Science (VIMS). Orthophosphate (PO₄⁻³) was measured by the molybdate method as discussed in Parsons et al. (1984). The detection limit of the autoanalyzer is 0.012 μM for nitrite + nitrate and 0.032 μM for orthophosphate. Dissolved silica (Dsi) was measured using a TECHNICON AAII[®] Continuous Flow Analyzer (Segmented) at VIMS Analytical Service Center. The basic procedure for the determination of soluble silicates is based on the reduction of a silicomolybdate in acidic solution to molybdenum blue by ascorbic acid (Technicon Industrial Systems 1973). Detection limit for the Dsi is 0.013 mg l⁻¹.

A YSI® Model 33 S-C-T Meter was used to measure temperature and salinity. A LICOR® PAR Radiometer was used for measuring solar and submarine irradiance at depths of 10, 35, 60, 85 and 110 cm. Light attenuation coefficients were determined using Beer's Law, $I_z = I_0 e^{-kz}$, where I_z is the intensity of light at z , the depth of interest, I_0 is the intensity at the surface, and k is the attenuation coefficient of water. Water depth was measured using either a sonar depth meter installed on the boat or a scale marked on the Nansen bottle's line.

Other data collections and statistical analysis

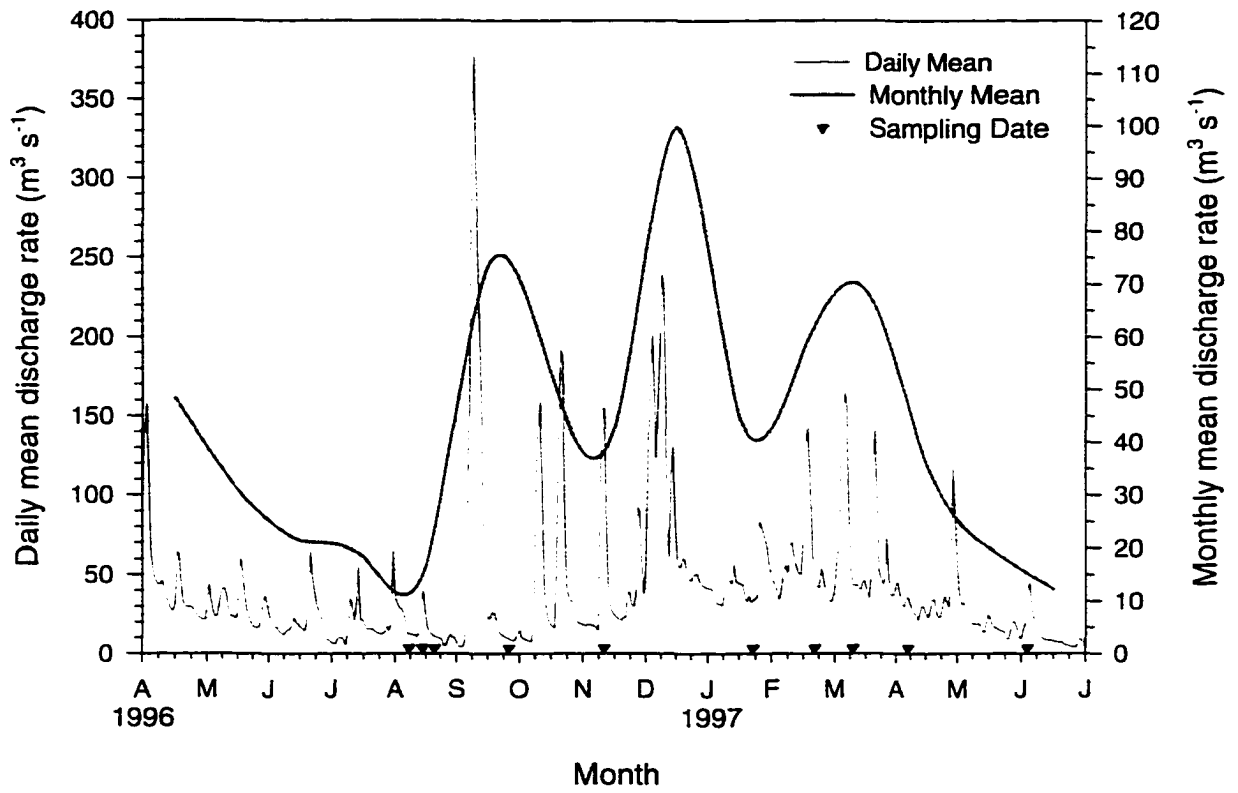
Daily mean solar irradiation data were collected at Virginia Institute of Marine Science, Gloucester Point, Virginia, also site of Station II (Fig. 1). Monthly means of solar irradiance were calculated from the data downloaded from VIMS data archives.

Daily discharge rates near the fall line on the Pamunkey River at Hanover were collected by U.S. Geological Survey, and monthly means were calculated from the data.

Extraordinarily high river discharge occurred for 3 days in early September 1996; this is probably due to a large storm event (Fig. 2). Samples were not collected until late September although the storm event significantly increased the monthly mean discharge rate. Because of the delay in our sampling following the storm, the river discharge rates for the 3 days affected by the storm event were not included in the calculation of monthly mean river discharge rates used for regression analysis. Linear simple and multiple regression analyses were employed to investigate correlations between phytoplankton size class abundance and physical and biological properties.

Fig. 2. Time series of river discharge rates from April 1996 to June 1997 at fall line of the Pamunkey River in the York River estuary.

River Discharge Rates of Pamunkey River



RESULTS

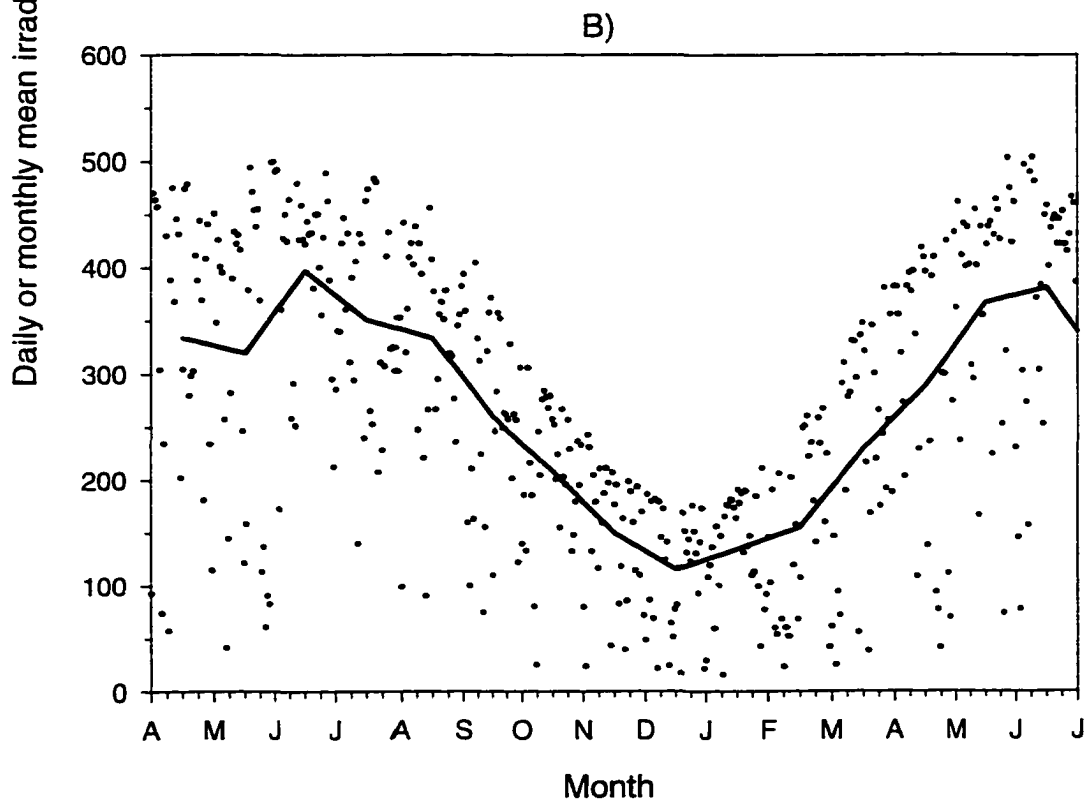
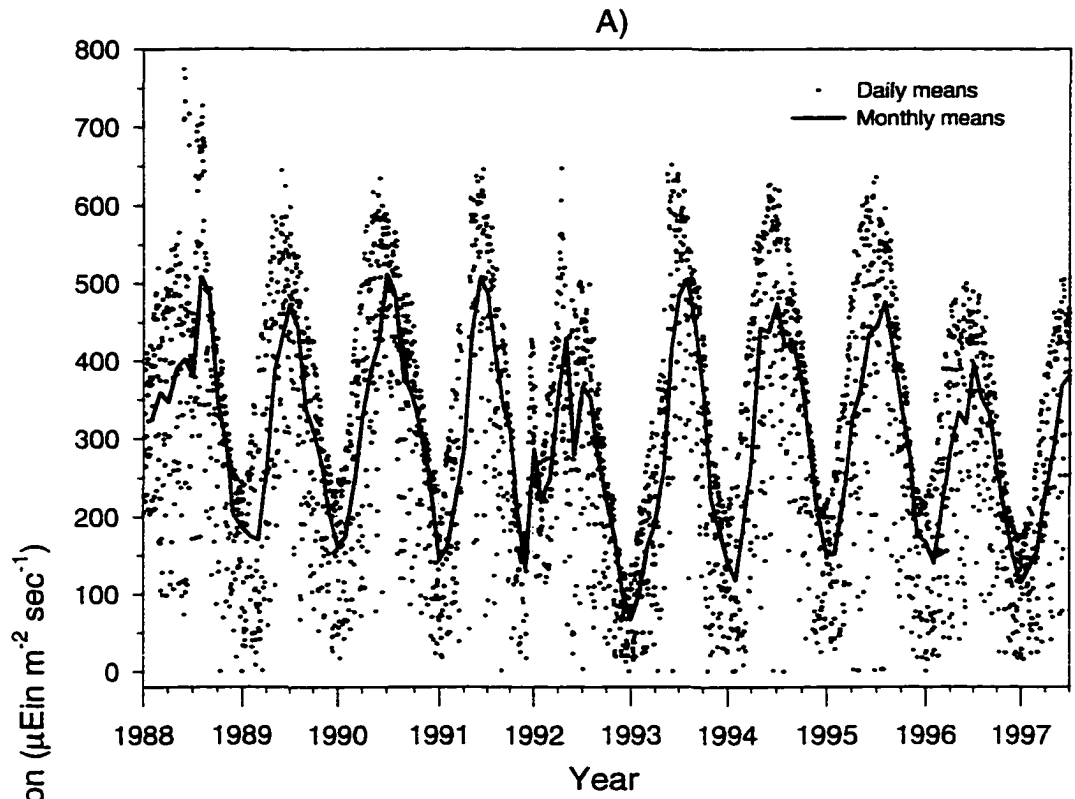
River discharge and solar irradiation

River discharge rates for the period from July 1996 to June 1997 (Fig. 2) displayed a seasonality similar to that in the long-term datasets (see Fig. 2 in Section I); rates were high during winter and spring, and low during summer and fall. Discharge rates were extraordinarily high during fall, especially September probably due to a storm (Fig. 2). The wettest month was December 1996 and the driest one was June 1997. River discharge rates near the fall line on the Pamunkey River (Hanover) averaged $45.3 \text{ m}^3 \text{ s}^{-1}$, a rate higher than the ten-year (1985-1994) mean of $28.6 \text{ m}^3 \text{ s}^{-1}$. Therefore, the period for this present study is considered as wet. Monthly mean discharge rates ranged from 12.2 (June) to $99.8 \text{ m}^3 \text{ s}^{-1}$ (December).

Solar irradiation data collected at Gloucester Point also revealed a seasonal trend with PAR highest during June and lowest during December for the period 1988 to 1997 (Fig. 3A). Peaks of irradiation in 1996 and 1997 were lower than during most years during 1988 to 1995. Average irradiance ($248.2 \mu\text{E m}^{-2} \text{ s}^{-1}$) was lower than during the period July 1996 to June 1997 and lower than average irradiance ($301.8 \mu\text{E m}^{-2} \text{ s}^{-1}$) measured over the period January 1988-July 1997. The monthly mean solar irradiation ranged from $115.3 \mu\text{E m}^{-2} \text{ s}^{-1}$ in December to $381.8 \mu\text{E m}^{-2} \text{ s}^{-1}$ in June (Fig. 3B).

Other physical properties; water depth, temperature, salinity and light attenuation coefficients

Fig. 3. Surface daily and monthly PAR ($\mu\text{E m}^{-2} \text{s}^{-1}$) at Gloucester Point, Virginia from January 1988 to June 1997 (A) and April 1996 to June 1997 (B).



Water depths of Stations I, II and III were 7.06 ± 0.35 , 7.11 ± 0.29 and 16.06 ± 0.47 m respectively. High flushing rates in the tidal freshwater region (Station I) of the York River estuary are thought to be due to a characteristic bottom morphology with a deep and narrow channel. Surface water temperatures at Station I ranged from 3.3 to 28.0 °C over the sampling period (Table 1). There were no temperature differences between surface and bottom layers at Station I, indicating that the water column was well-mixed. At Station II, surface water temperature ranged from 5.2 to 28.5 °C whereas bottom temperature ranged from 5.2 to 27.0 °C. Temperature differences between surface and bottom water were greater during summer, especially August, than during winter. At Station III, surface water temperatures ranged from 4.5 to 26.5 °C whereas bottom temperature ranged from 4.5 to 26.0 °C. Temperature differences between surface and bottom waters at Station III were smaller than at Station II. Water temperatures at all stations were highest during August and lowest during January.

Station I had 0 ‰ salinity (Table 1) throughout the sampling period except in June 1997 (0.8 ‰) following a severe drought (see Fig. 2) indicating that the water column is well-mixed. At Station II, surface water salinity ranged from 1.8 to 13.0 ‰ whereas bottom salinity ranged from 4.0 to 14.0 ‰. The water column at Station II was somewhat stratified, especially during August, February and March. Surface salinities at Station III ranged from 12.0 (February) to 17.5 ‰ (August 21) whereas bottom salinities ranged from 16.0 (March) to 22.2 ‰ (November). Average salinities at Stations II and III for the sampling period were 7.76 ± 1.0 and 15.83 ± 0.53 ‰ for surface water and 9.16 ± 0.88 and 18.41 ± 0.64 ‰ for bottom water.

Table 1. Temperature ($^{\circ}\text{C}$), salinity (‰) and light attenuation coefficient (K_d , m^{-1}) collected at the stations (I, II and III) in the York River estuarine system.

Date	Depth	Stations:	-----Temperature-----			-----Salinity-----			----- K_d -----		
			I	II	III	I	II	III	I	II	III
Aug 8, 1996	Surface		28.0	28.5	26.5	0.0	8.0	17.0	2.62	2.61	2.61
	Bottom		28.0	27.0	26.0	0.0	9.0	18.0			
Aug 15	Surface		26.0	26.0	25.0	0.0	10.0	17.0	3.08	2.81	1.43
	Bottom		26.0	24.5	24.0	0.0	11.0	20.0			
Aug 21	Surface		26.8	27.2	27.0	0.0	8.2	17.5	2.79	3.33	1.27
	Bottom		26.8	26.2	26.9	0.0	10.2	18.8			
Sep 26	Surface		22.0	22.0	22.5	0.0	9.0	15.0	3.73	3.60	1.30
	Bottom		22.0	21.2	22.0	0.0	10.9	16.5			
Nov 11	Surface		13.2	12.5	13.0	0.0	9.0	17.0	3.69	3.64	1.10
	Bottom		13.2	13.0	15.0	0.0	10.0	22.2			
Jan 23, 1997	Surface		3.3	5.2	4.5	0.0	6.3	15.0	3.24	2.92	1.17
	Bottom		3.2	5.2	4.5	0.0	7.3	18.2			
Feb 20	Surface		6.8	6.8	6.2	0.0	1.8	12.0	2.57	4.25	1.70
	Bottom		6.8	6.0	5.2	0.0	4.0	19.0			
Mar 10	Surface		10.5	10.0	9.0	0.0	3.8	15.0	4.42	6.68	2.01
	Bottom		10.5	10.0	9.0	0.0	6.2	16.0			
Apr 7	Surface		16.0	15.0	13.8	0.0	8.5	15.8	2.75	3.51	1.52
	Bottom		16.0	15.0	*	0.0	9.0	*			
Jun 4	Surface		21.0	20.0	19.0	0.8	13.0	17.0	3.9	3.2	1.1
	Bottom		21.0	20.0	18.0	0.8	14.0	17.0			

* : No measurement taken.

Average light attenuation coefficients (K_d) during the sampling period were 3.28 ± 0.2 , 3.66 ± 0.37 and $1.52 \pm 0.15 \text{ m}^{-1}$ for Stations I, II and III respectively. Attenuation coefficients (Table 1) ranged from 2.57 (February) to 4.42 m^{-1} (March) at Station I, from 2.61 (August 8) to 6.68 m^{-1} (March) at Station II and from 1.1 (November, June) to 2.61 m^{-1} (August 8) at Station III. Although there was no clear seasonal effect, K_d was clearly affected by river discharge since it peaked at all stations during March (Fig. 4G, 4H, 4I) corresponding to a sharp decrease in salinity due to high river discharge rates (see Fig. 2). It was reported in Section I of this dissertation that river discharge was significantly positively correlated with K_d .

Dissolved inorganic nutrients in the water column

Figure 5 shows the seasonal variations in concentrations of inorganic nutrients at the study sites. Ammonium concentrations did not vary seasonally at Station I (Fig. 5A). They were high during winter and low during summer at Station II (Fig. 5B) whereas they were low during winter and high during summer-fall at Station III (Fig. 5C). Surface-bottom differences were found at Station II (Fig. 5B) but were not as obvious at Station III (Fig. 5C). Bottom ammonium concentrations at Station III were generally higher than surface concentration throughout the sampling period, especially during summer and fall (Fig. 5C). Table 2 shows that the average ammonium concentration was higher in bottom water than in surface water at Station III and higher in surface than in bottom waters at Station II. Average bottom ammonium concentrations were highest in the mesohaline zone (Station III), whereas average surface ammonium concentrations were highest in the river-estuary transition zone (Station II).

Fig. 4. Temperature, salinity and light attenuation coefficient distributions at each station in the York River system.

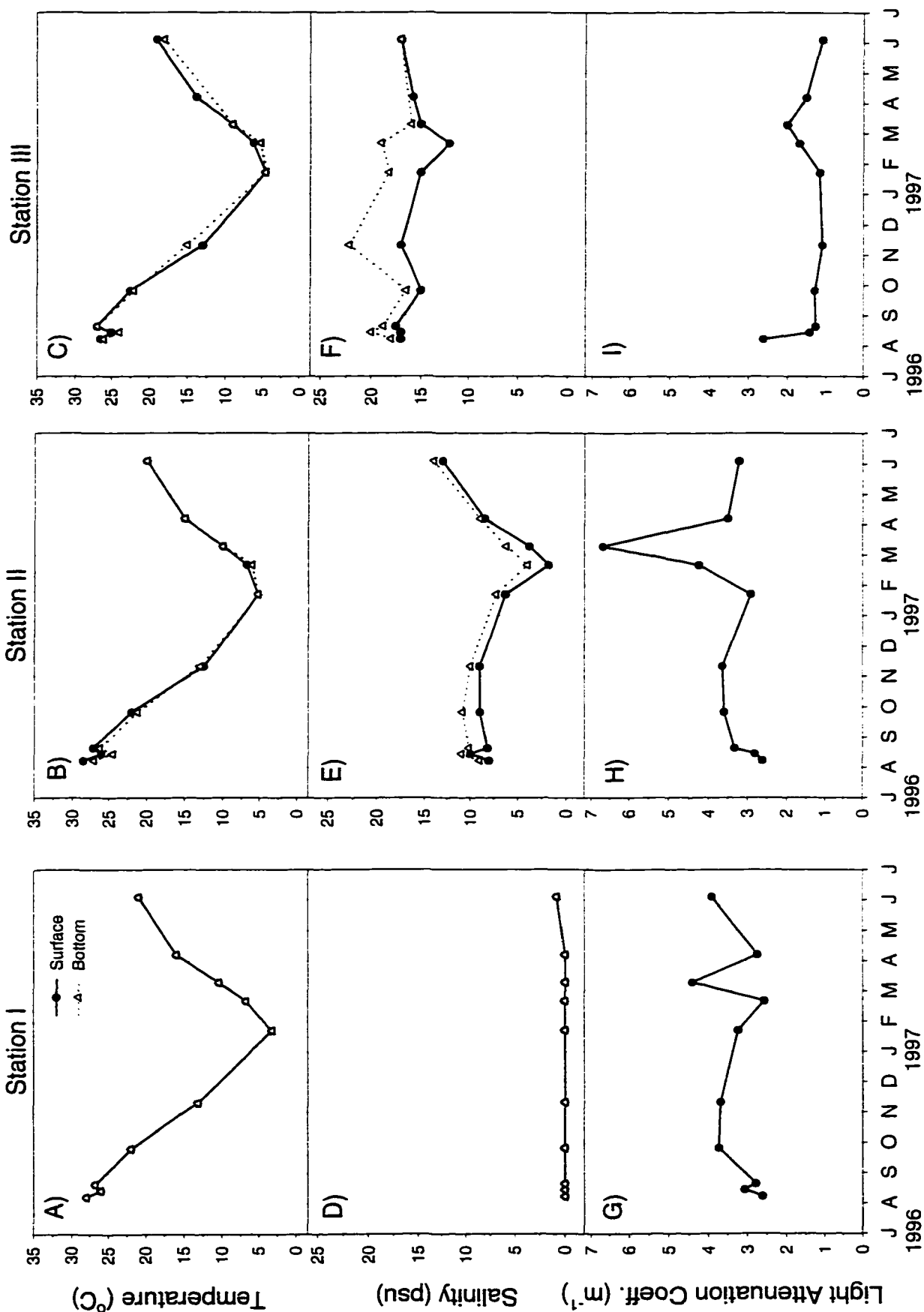


Fig. 5. Seasonal distributions of ambient ammonium (NH_4^+), nitrite+nitrate ($\text{NO}_2^- + \text{NO}_3^-$), orthophosphate (PO_4^{3-}) and dissolved silicate (Dsi) at three stations along the axis of the York River system.

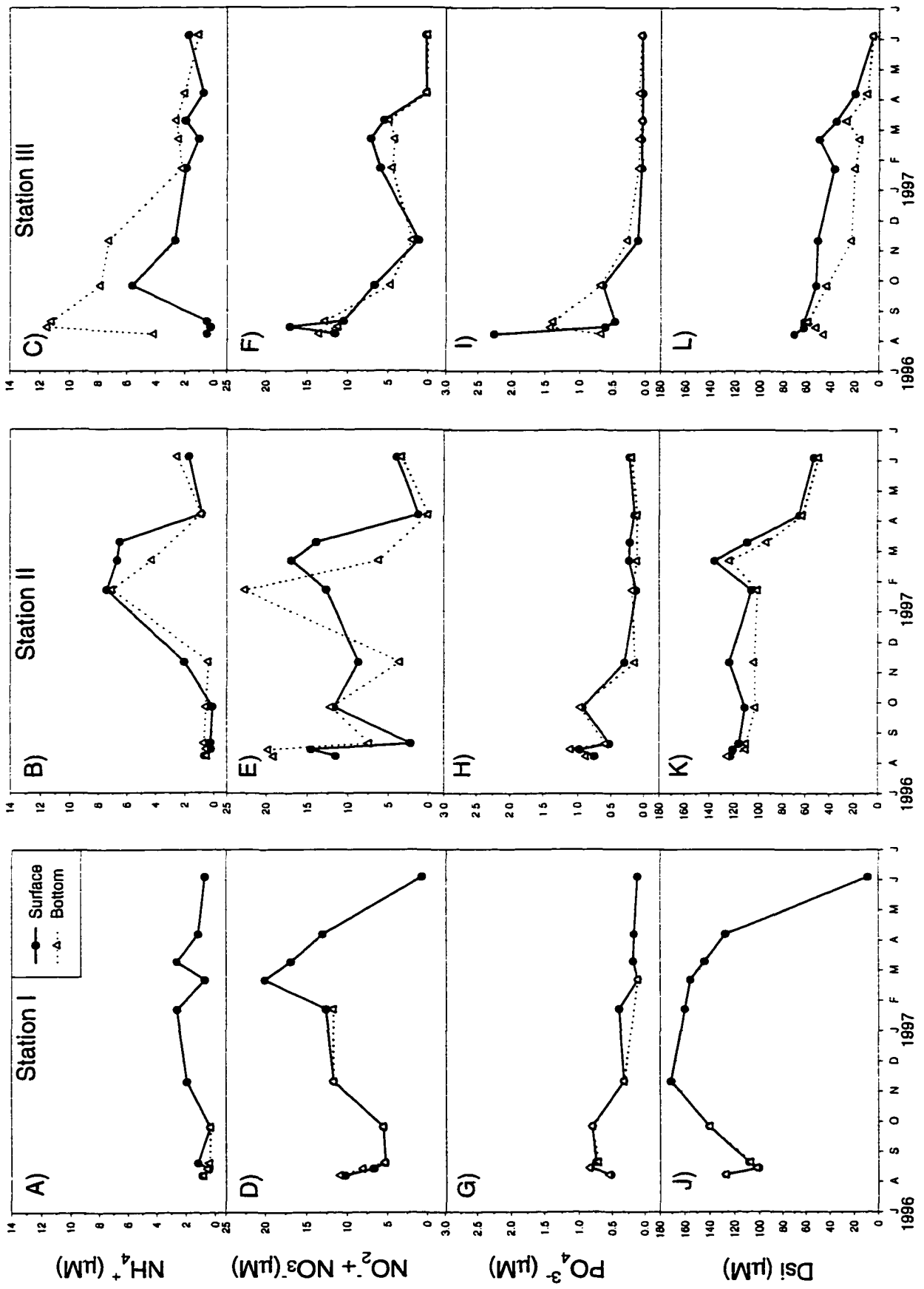


Table 2. Average ambient concentrations and standard errors of ammonium (NH_4^+ , μM), nitrite + nitrate ($\text{NO}_2^- + \text{NO}_3^-$, μM), dissolved inorganic nitrogen (DIN, μM), orthophosphate (PO_4^{3-} , μM), and dissolved silicate (Dsi, μM) in the York River estuary.

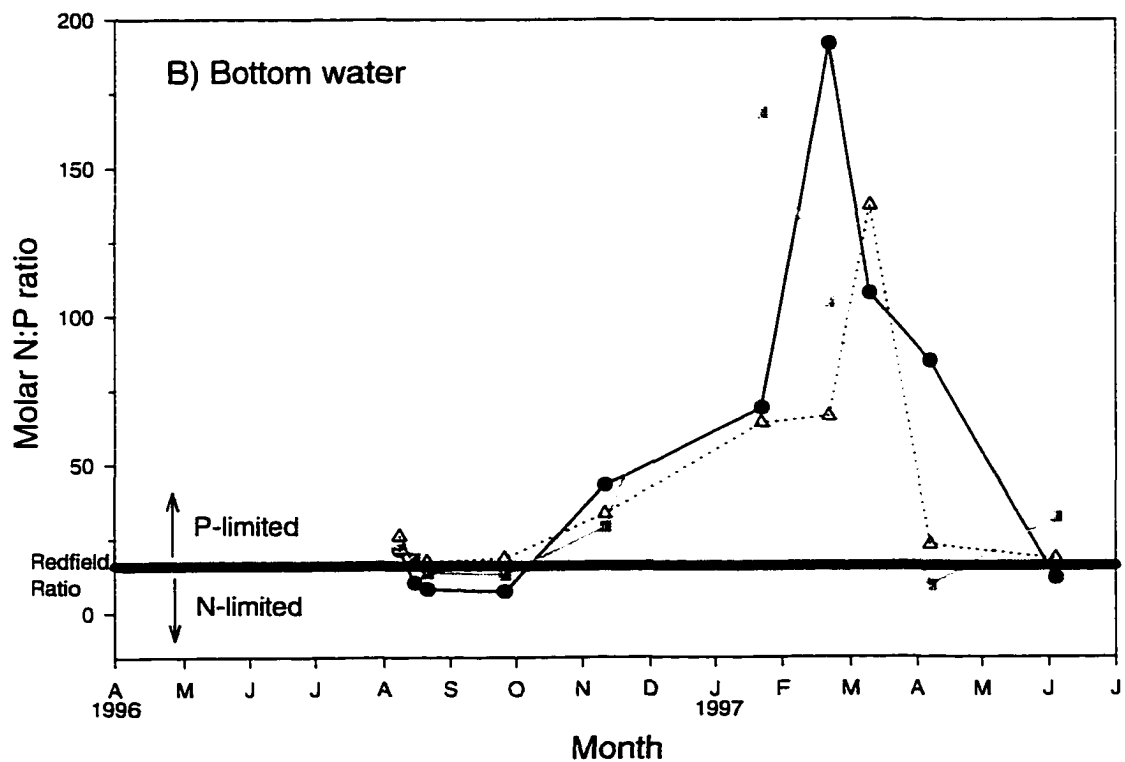
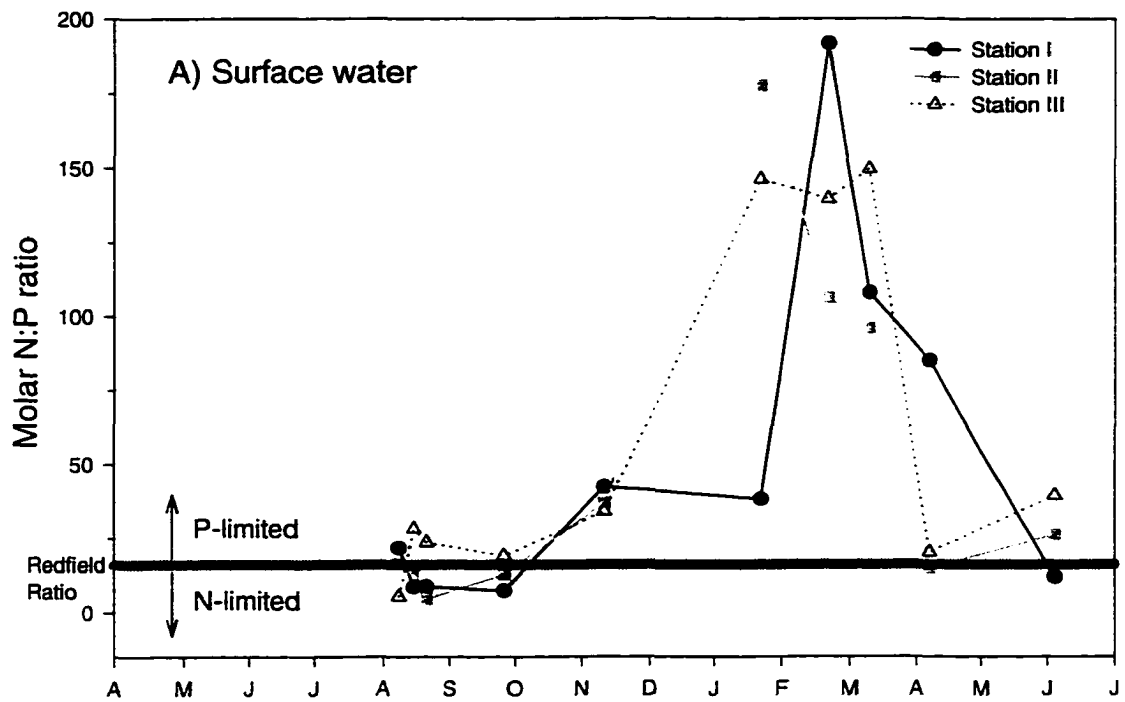
Stations	Depth	Nutrients:	NH_4^+ (μM)	$\text{NO}_2^- + \text{NO}_3^-$ (μM)	DIN (μM)	PO_4^{3-} (μM)	Dsi (μM)
Station I	Surface		1.27 ± 0.27	10.2 ± 1.85	11.6 ± 1.99	0.42 ± 0.09	124.3 ± 14.6
	Bottom		1.21 ± 0.29	10.4 ± 1.79	11.6 ± 1.99	0.39 ± 0.09	124.3 ± 14.6
Station II	Surface		2.63 ± 0.95	9.74 ± 1.73	12.37 ± 2.37	0.43 ± 0.10	106.2 ± 8.33
	Bottom		1.92 ± 0.77	10.4 ± 2.76	12.4 ± 3.08	0.47 ± 0.14	97.9 ± 7.79
Station III	Surface		1.70 ± 0.51	6.61 ± 1.71	8.31 ± 1.62	0.44 ± 0.22	44.4 ± 6.48
	Bottom		5.23 ± 1.24	5.80 ± 1.58	11.0 ± 2.55	0.49 ± 0.17	29.8 ± 5.90

At Station I nitrite + nitrate levels were highest during periods of high river discharge, especially February (Fig. 5D). Surface nitrite + nitrate concentrations peaked in February at Station II (Fig. 5E) and increased at Station III (Fig. 5F). Similar seasonal patterns were detected for silicate in surface waters (Fig. 5J, 5K, 5L). Surface nitrite + nitrate concentrations were not different than bottom concentrations at Stations II and III whereas surface silicate concentrations were consistently higher than bottom concentrations. Low silicate concentrations in both surface and bottom waters occurred at all stations concurrent with low river discharge rates. Average nitrite + nitrate and silicate concentrations over the sampling period were highest in the tidal freshwater zone (Station I), and decreased moving downstream (Table 2).

There were no clear seasonal variations in orthophosphate concentrations at Station I (Fig. 5G). At Station II, orthophosphate concentrations were high during summer-fall but low during winter (Fig. 5H). Significant differences between surface and bottom water were not observed at Station II. On the other hand, bottom concentrations were generally higher than surface concentrations during August at Station III (Fig. 5I). Average orthophosphate concentrations increased downstream in bottom water but not in surface water (Table 2). At Station III, average orthophosphate concentrations were higher in bottom than in surface waters. Field data for nutrients (ammonium, nitrite + nitrate, dissolved inorganic nitrogen, orthophosphate, and silicate) collected at the study sites are presented in Appendices I and II.

Figure 6 shows molar N:P ratios for the 3 study sites. Significant differences were not observed between surface and bottom waters at any station. There was an apparent seasonal pattern. The N:P ratio is lower than Redfield during the warm season suggesting

Fig. 6. Temporal variations of molar N:P ratios of ambient inorganic dissolved nutrients at study sites in the York River estuary.



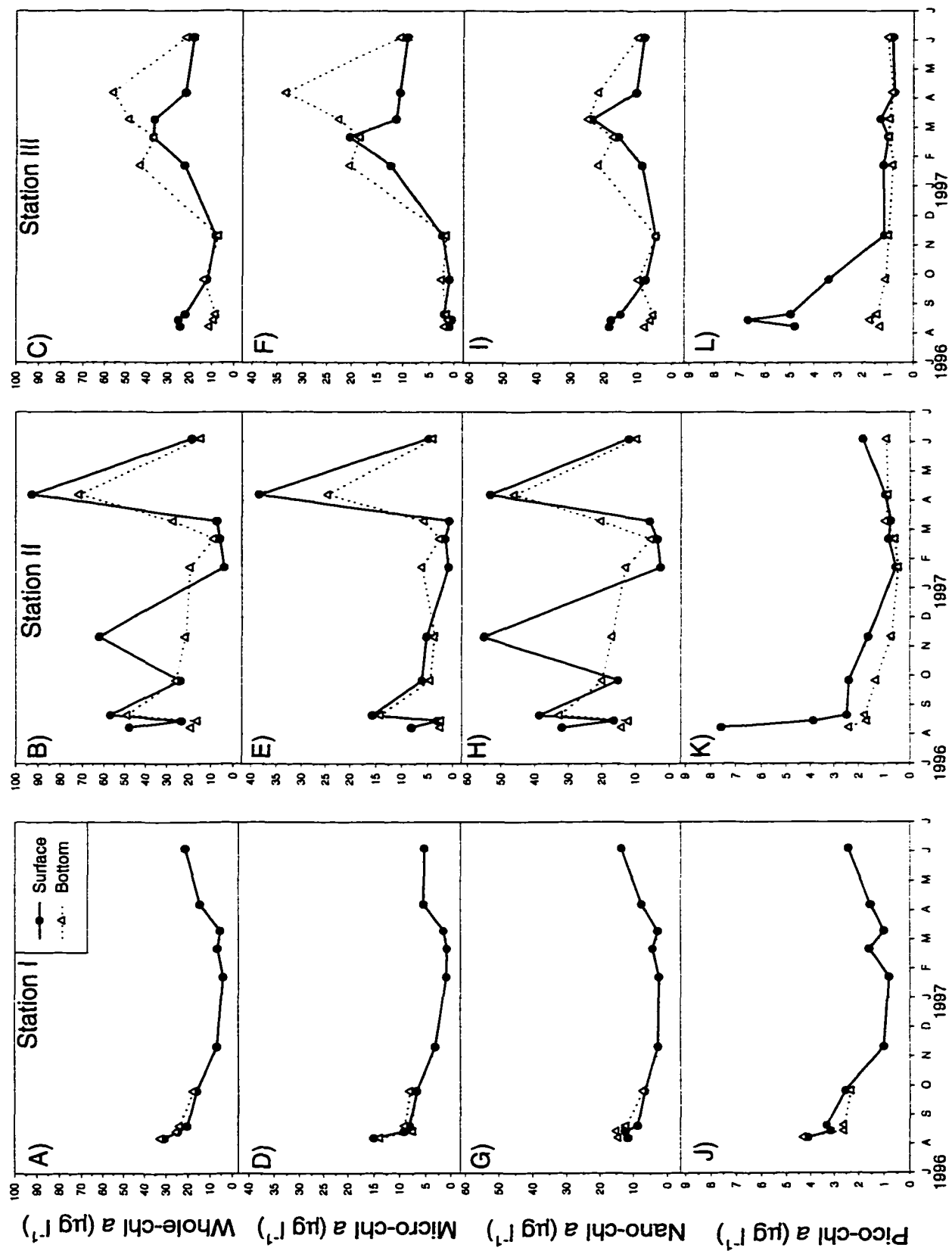
N limitation of phytoplankton growth and higher during the cold season suggesting P limitation due to high riverine N input during winter-spring. A shift from P to N limitation moving downstream during the warm season was not observed in this study as documented in the first section of this dissertation.

Temporal and spatial variations of chlorophyll a

At Station I total chlorophyll *a* concentrations in surface water were at a minimum during winter, increased in March and peaked during summer (Fig. 7A). The concentrations began to increase after March (Fig. 7A). This same seasonal chlorophyll *a* signal applied to all phytoplankton size classes (see Fig. 7D, 7G, 7J) and was also observed in the EPA long-term dataset analyzed in Section I. There was little difference in chlorophyll *a* concentrations between surface and bottom waters, probably due to mixing at Station I.

At Station II, surface chlorophyll *a* concentrations were generally higher than at other stations except for the cold season (January, February and March (Fig. 7B)). High chlorophyll *a* concentrations were observed during November when other stations experienced their minimum. The spring bloom occurred during April, with chlorophyll *a* higher than observed at any other station (close to $100 \mu\text{g l}^{-1}$ (Fig. 7B)). Microphytoplankton biomass significantly increased during the spring bloom (Fig. 7E). The seasonal pattern of nanophytoplankton stocks (Fig. 7H) was nearly the same as that for total chlorophyll *a* (Fig. 7B), indicating that phytoplankton biomass is generally dominated by nanophytoplankton except during the spring bloom. Picophytoplankton were abundant during summer but their biomass decreased as temperatures declined (Fig.

Fig. 7. Seasonal distributions of size fractionated chlorophyll *a* (whole, micro, nano and pico) at three stations along the axis of the York River system.

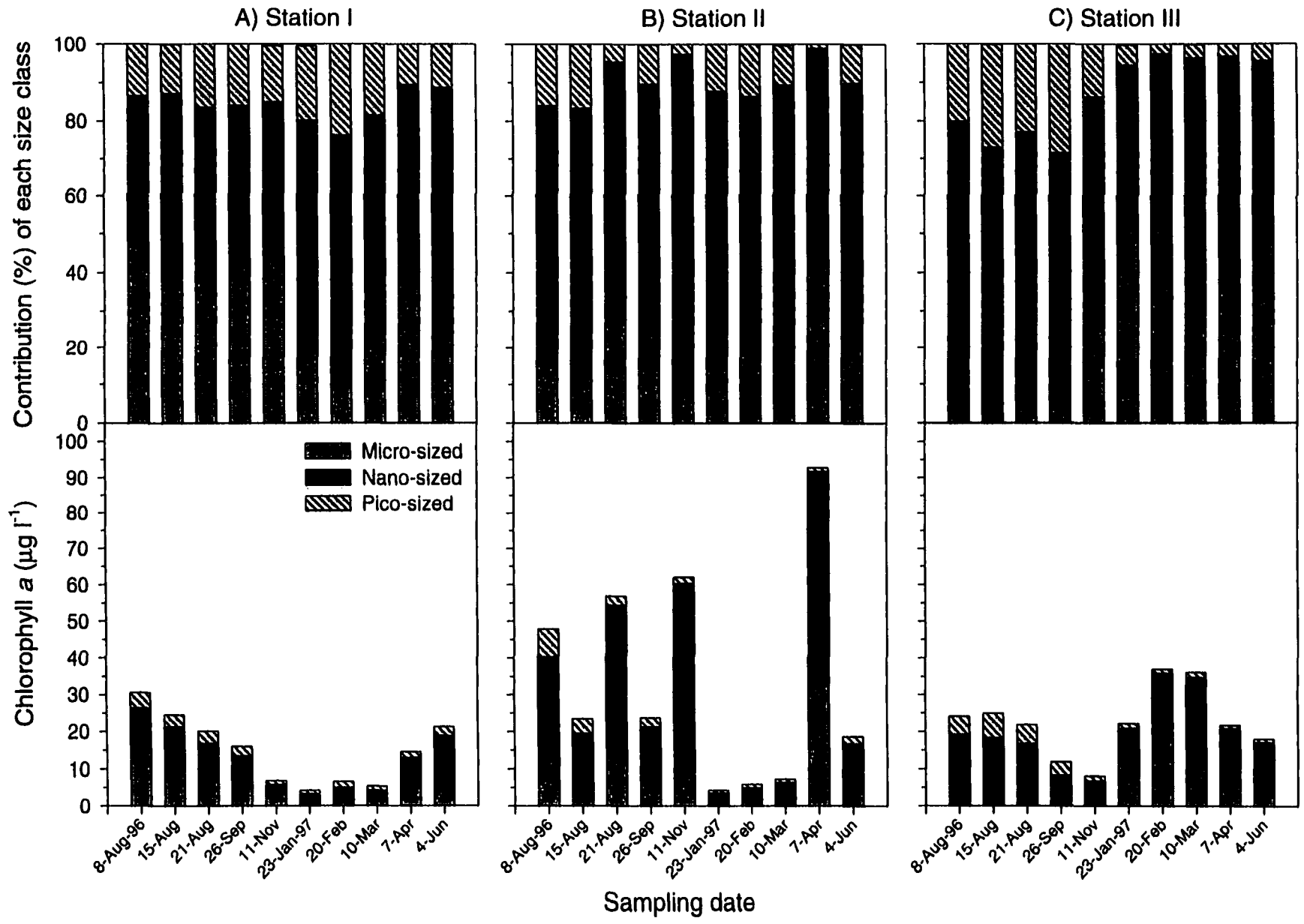


7K). All size classes had minimum biomass during the cold season. In bottom water, seasonal patterns of phytoplankton biomass were similar to those in surface water although they were consistently lower except during the cold season.

Station III showed a clear seasonality with a small scale summer bloom and larger-scale winter-spring blooms (Fig. 7C). The winter bloom developed at a time when other stations experienced their minimum abundance. Microplankton biomass was highest during winter and lowest during summer in surface water (Fig. 7F). Nanoplankton had a bimodal pattern with high abundances during summer and winter-spring (Fig. 7D). In contrast to microplankton, picoplankton had the highest abundances during summer and the lowest abundances during winter (Fig. 7L). Surface chlorophyll *a* (whole) concentrations were higher than bottom concentrations during summer, especially August, but the opposite was shown during winter-spring (Fig. 7C). The peak of chlorophyll *a* (whole) in bottom water coincided with peak bottom microplankton biomass in April (Fig. 7F), and a significant surface-bottom difference was observed during this period. These results showed that microplankton were the most significant component of phytoplankton in the bottom water of the mesohaline zone. The biomass of all three size classes was relatively low during summer in bottom water with stratification observed for nanoplankton and picoplankton.

In the surface water of Station I the contribution of large cells (microphytoplankton) to total chlorophyll *a* was significant during the warm season whereas the contribution of small cells (nano, picophytoplankton) increased rapidly during the cold period (Fig. 8A). At Station II nanophytoplankton dominated the phytoplankton community throughout the sampling period (Fig. 8B). The contribution of

Fig. 8. Percent contributions of three size classes (micro, nano and pico) to the total chlorophyll *a* in the surface water of the study sites of the York River estuary; upper panels describe contributions of size classes based on chlorophyll *a* concentrations shown in the lower panels.



large cells increased rapidly during the spring bloom. At Station III small cells (nano, picophytoplankton) dominated the mesohaline phytoplankton community during the warm season whereas large cells dominated the community during the winter bloom (Fig. 8C). Shifts in size structure at Station III initiated in fall just as river discharge rates began to rise, suggest a cause and effect relationship.

At Station I contributions of various size classes to phytoplankton abundance in bottom water were similar to those of size classes in surface water (Fig. 9A). At Station II, the microphytoplankton contribution appeared to increase over the sampling period although nano-sized cells remained dominant in the bottom phytoplankton community (Fig. 9B). At Station III, small cells (nano-, pico-sized), especially pico-sized cells, decreased whereas the contribution of micro-sized cells increased over the sampling period (Fig. 9C) compared to each size class in surface water (see Fig. 8C).

In the surface water of our study sites average chlorophyll *a* concentrations of whole, micro-size and nano-size classes were highest at Station II, whereas chlorophyll *a* from the pico-size class was highest at Station III (Table 3). In the bottom water whole and nano-size classes were most abundant at Station II whereas pico-size and micro-size classes dominated at Stations III and I respectively. Surface averages were higher than bottom averages except for the nano-size class at Station I and the whole and micro-size class at Station III. These results indicate the important role of the micro-size class in the accumulation of phytoplankton biomass in the lower estuary of the York River system. Field data for chlorophyll *a* concentrations of each size class are presented in Appendix III.

Fig. 9. Percent contributions of three size classes (micro, nano and pico) to the total chlorophyll *a* in the bottom water of the study sites of the York River estuary; upper panels describe contributions of size classes based on chlorophyll *a* concentrations shown in the lower panels.

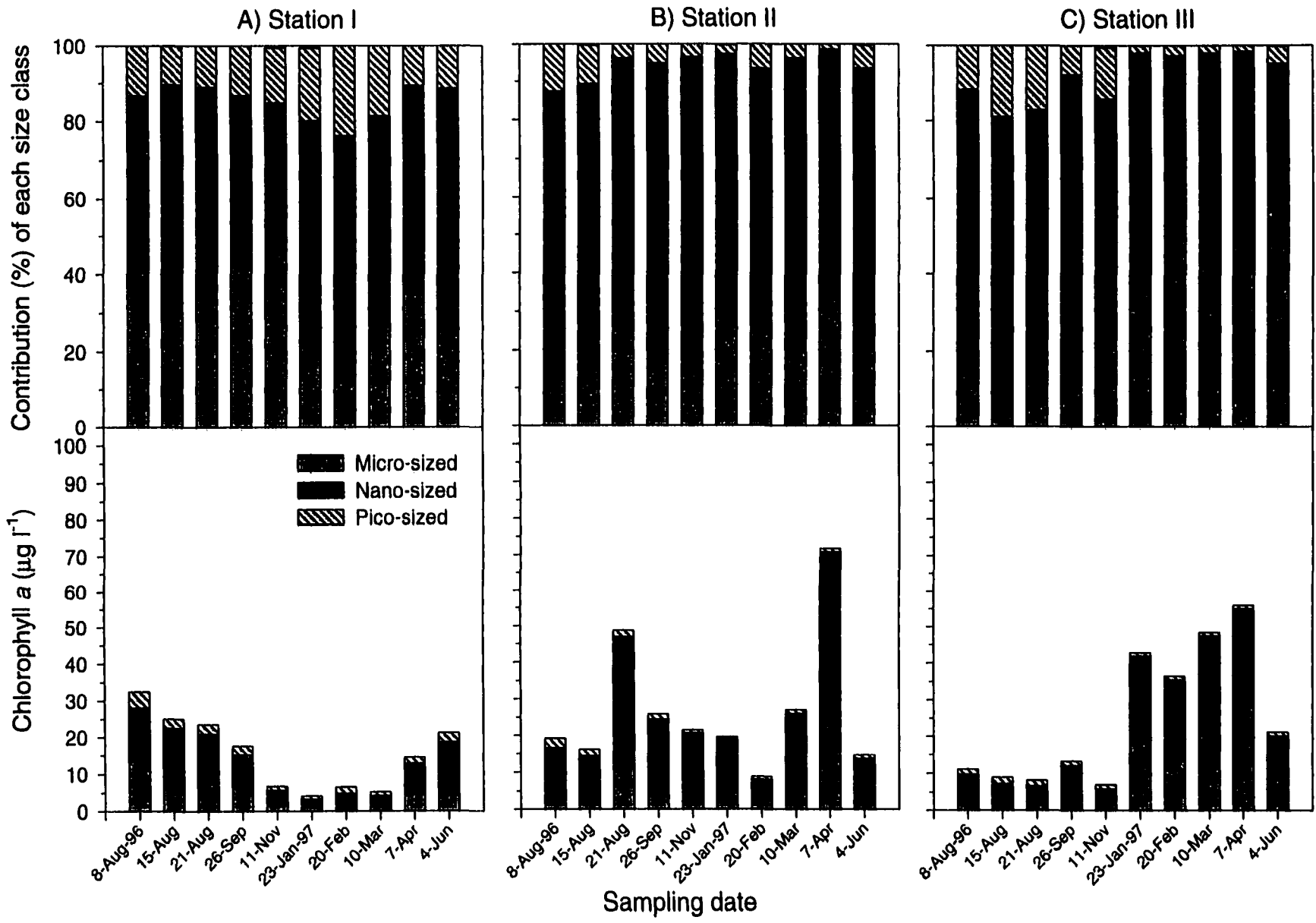


Table 3. Average chlorophyll *a* concentrations and standard errors ($\mu\text{g l}^{-1}$) of whole, micro-size, nano-size, and pico-size class collected during sampling period in the York River estuary.

Stations	Size class: Depth	Whole ($\mu\text{g l}^{-1}$)	Micro ($\mu\text{g l}^{-1}$)	Nano ($\mu\text{g l}^{-1}$)	Pico ($\mu\text{g l}^{-1}$)
Station I	Surface	15.0 ± 2.90	5.60 ± 1.40	7.25 ± 1.32	2.15 ± 0.36
	Bottom	15.7 ± 3.10	5.53 ± 1.32	8.20 ± 1.62	2.02 ± 0.33
Station II	Surface	34.28 ± 9.32	8.48 ± 3.61	23.5 ± 6.33	2.29 ± 0.67
	Bottom	27.8 ± 5.97	7.06 ± 2.23	19.1 ± 3.82	1.16 ± 0.20
Station III	Surface	22.6 ± 2.88	7.00 ± 2.13	13.0 ± 1.90	2.60 ± 0.69
	Bottom	25.3 ± 5.93	11.3 ± 3.66	12.9 ± 2.45	1.08 ± 0.09

Figure 10 shows the seasonal variations in chlorophyll:pheopigment ratios (chl:pheo; ratios of fluorometer readings before and after acidification) at three stations. For all stations and most classes chl:pheo ratios peaked during November indicating a decrease in percent of detrital particle. At Station II all size classes except micro-size in February had low chl:pheo ratios during winter-spring in surface water (Fig. 10B, 10H, 10K) indicating a high abundance of detrital particles.

Average chl:pheo ratios in unfractionated water were lowest in Station I surface water, and highest in Station I bottom water (Table 4). This may indicate riverine inputs of detrital particles to the tidal freshwater zone and fluxes of detrital particles from the surface to the bottom and/or oceanic inputs through estuarine circulation into the mesohaline zone of the York River estuary. When we examined size fractionated chl:pheo ratios, the average ratio of the micro-size class was lowest at Station III whereas average ratios of nano- and pico-size classes were lowest at Station I. In the bottom water at Station III, average ratios decreased as cells size increased (Table 4) suggesting a possible role of large cells or aggregates in supporting benthic heterotrophy. Compared to other size classes, average chl:pheo for pico-sized cells in bottom water was close to that in surface water of Station III. This indicated that there was little depth variation of detrital particles in the small size class. During the entire sampling period pico-sized cells generally had lower chl:pheo ratios than did other size classes at all three stations, indicating that they included more detrital particles than did other size classes.

Linear simple and multiple regression analysis

Fig. 10. Seasonal patterns of acidification ratios i.e., chlorophyll:pheopigment ratios (chl:pheo; ratio of fluorometer readings before and after acidification) at three stations along the axis of the York River system.

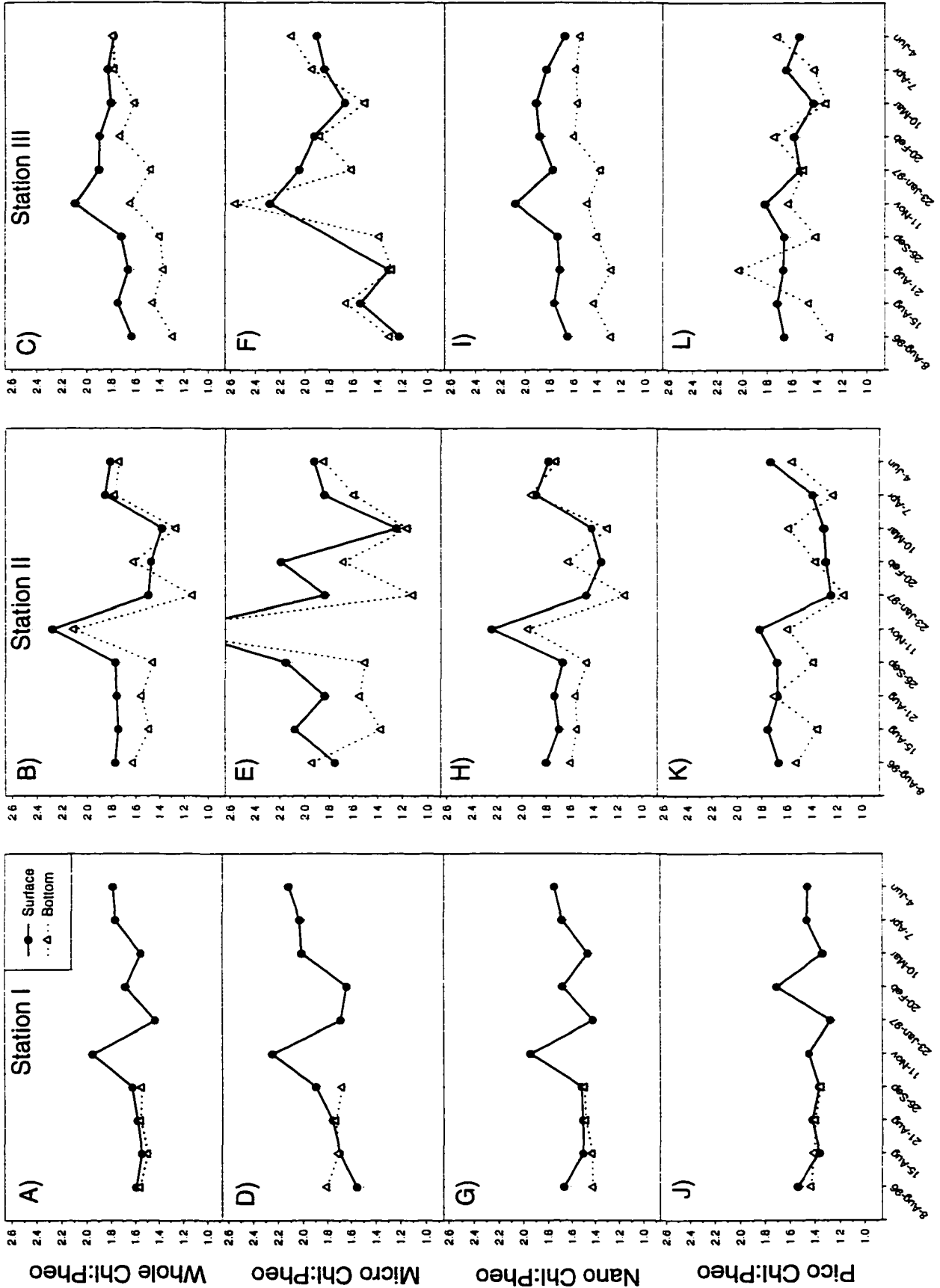


Table 4. Average chlorophyll:pheopigment ratios (ratios of chlorophyll *a* readings before and after acidification) and standard errors of whole, micro-size, nano-size, and pico-size classes collected during sampling period in the York River estuary.

Stations	Size class: Depth	Whole	Micro	Nano	Pico
Station I	Surface	1.65 ± 0.05	1.86 ± 0.07	1.61 ± 0.05	1.44 ± 0.04
	Bottom	1.63 ± 0.05	1.86 ± 0.07	1.58 ± 0.06	1.43 ± 0.04
Station II	Surface	1.73 ± 0.08	1.99 ± 0.14	1.70 ± 1.08	1.56 ± 0.07
	Bottom	1.58 ± 0.09	1.70 ± 0.19	1.57 ± 0.08	1.44 ± 0.06
Station III	Surface	1.81 ± 0.04	1.75 ± 0.12	1.80 ± 0.04	1.63 ± 0.03
	Bottom	1.55 ± 0.06	1.42 ± 0.13	1.45 ± 0.04	1.56 ± 0.07

Table 5 shows results (r^2) of linear regression analyses of relationships between the biomass of various phytoplankton size classes and various physical and biological properties of the York River estuary including river discharge rates, chl:pheo, PAR and temperature. At Station I, river discharge rates (Q, m^3s^{-1}) were significantly negatively correlated with phytoplankton biomass in unfractionated water. This relationship was similar for the nano-size class at the 0.05 significance level and for micro- and pico-size classes at the 0.1 significance level. Chl:pheo ratios were not correlated with any size class abundance at Station I (Table 5). PAR and temperature were significantly positively correlated with abundance of all size classes except the nano-size class for PAR at the 0.05 significance level. Nano-size class biomass was correlated with temperature at the 0.1 significance level. Temperature was significantly and negatively correlated with percent contributions of pico-size ($\alpha = 0.05$) and nano-size classes ($\alpha = 0.1$); however, temperature was positively correlated with percent contribution of the micro-size class to the phytoplankton community. Multiple regression analysis showed that river discharge rates, PAR, and temperature were responsible for 92 % (whole), 87 % (micro-size class), 80 % (nano-size class) and 89 % (pico-size class) of the variation in size class structure at Station I.

At the river-estuary transition Station (Station II), river discharge was not correlated with phytoplankton abundance (Table 5); however, chl:pheo ratios were significantly positively correlated with whole and nano-size class abundances. PAR and temperature were significantly correlated only with pico-size class abundances. Based on multiple regression analysis, PAR and temperature were responsible for 75% of the variation in pico-size class biomass.

Table 5. Results (r^2) of linear regression analysis on surface chlorophyll a ($\mu\text{g l}^{-1}$) or percent contribution by each size class (%) vs. river discharge rates (Q , $\text{m}^3 \text{s}^{-1}$), chlorophyll:pheophytin ratio (chl:pheo), PAR at 1 m water depth (PAR, $\mu\text{Ein m}^{-2} \text{s}^{-1}$) and temperature (T , $^\circ\text{C}$) during the sampling period. r^2 less than 0.1 omitted and denoted by '-'. r^2 in parenthesis represents correlation of percent contributions vs. parameters, and negative value represents negative relationship.

Parameters: Size Class	Station I				Station II				Station III			
	Q	Chl:Pheo	PAR	T	Q	Chl:Pheo	PAR	T	Q [†]	Chl:Pheo	PAR	T
Whole	-0.52**	-	0.54**	0.86**	0.12	0.46**	-	0.12	-	-0.19	-	0.12
Micro	-0.36*	-0.15	0.58**	0.81**	-	-	-	-	0.58**	0.19	-	-0.69**
	(-)	(-)	(0.14)	(0.49**)	(-)	(-)	(-)	(-)	(0.55**)	(0.49**)	(-)	(-0.70**)
Nano	-0.59**	-	0.35*	0.68**	0.10	0.74**	-	0.10	-	-	0.14	-
	(-)	(-)	(0.10)	(-0.33')	(-)	(0.17)	(-)	(-)	(-0.33)	(-)	(-)	(0.58**)
Pico	-0.37*	-	0.58**	0.84**	0.26	0.28	0.73**	0.61**	-0.48**	0.16	-	0.66**
	(0.36')	(-)	(-0.11)	(-0.41**)	(-)	(-)	(0.16)	(-)	(-0.71**)	(0.36')	(-)	(0.66**)

Whole, Micro, Nano, and Pico: total, micro-sized, nano-sized, and pico-sized chlorophyll a .

[†]: One month-lag time considered.

*: $P < 0.1$, **: $P < 0.05$.

At the mesohaline Station (Station III), river discharge rates were significantly correlated with micro-size class abundance ($r^2 = 0.58$, $P < 0.05$), whereas temperature was significantly correlated with pico-size class abundance ($r^2 = 0.66$, $P < 0.05$). River discharge rates were significantly correlated with percent contribution of microphytoplankton, whereas temperature was significantly correlated with percent contributions of nanophytoplankton and picophytoplankton. Negative relationships between temperature and micro-size class biomass may be due to autocorrelation between temperature and river discharge rate. Similarly negative relationships between river discharge rates and pico-sized chlorophyll *a* may be due to autocorrelation between temperature and river discharge or due to slow growth rates of small cells at high supply rates of nutrients, compared to large cells (microphytoplankton). Based on multiple regression analysis, 69 % of the variation in pico-size class biomass was explained by river discharge and temperature. Chl:pheo ratios were correlated with the contribution of microplankton to total biomass but not with microplankton biomass. PAR at 1 m depth was not correlated with any size class in the mesohaline zone.

Table 6 shows results (r^2) of linear regression analyses of relationships between size class biomass (chlorophyll *a*) or percentage contribution of individual size classes to total biomass and physical and biological parameters in bottom water. At Station I, results of correlations of size class biomass or percent contributions of size classes vs. physical/biological parameters were similar to those in surface water (see Table 5). At Station II, there was no significant relationship between size class biomass and chl:pheo ratios whereas growth of pico-sized cells appeared to be regulated by light and temperature. Station III showed a strong positive relationships between river discharge

Table 6. Results (r^2) of linear regression analysis on the bottom chlorophyll *a* ($\mu\text{g l}^{-1}$) or percent contribution by each size class (%) vs. river discharge rates (Q , $\text{m}^3 \text{s}^{-1}$), chlorophyll:pheophytin ratio (Chl:Pheo), PAR at 1 m water depth (PAR, $\mu\text{Ein m}^{-2} \text{s}^{-1}$) and temperature (T , $^\circ\text{C}$) during the sampling period. r^2 less than 0.1 omitted and denoted by '-'. r^2 in parenthesis represents correlation of % contributions vs. parameters, and negative value represents negative relationship.

Parameters: Size Class	Station I				Station II				Station III			
	Q	Chl:Pheo	PAR	T	Q	Chl:Pheo	PAR	T	Q'	Chl:Pheo	PAR	T
Whole	-0.49**	-	0.57**	0.89**	-	-	-	-	0.95**	0.29	-0.12	-0.74**
Micro	-0.29 (-)	- (-)	0.55** (0.14)	0.84** (0.33')	- (-)	- (-0.10)	- (-0.16)	- (-0.25)	0.97** (0.85**)	- (-)	- (-)	-0.79** (-0.70**)
Nano	-0.63** (-)	- (-)	0.48** (-)	0.78** (-)	- (-)	0.10 (-)	- (-)	- (-)	0.83** (-0.82**)	0.28 (-0.54**)	0.19 (-)	-0.67** (0.60**)
Pico	-0.33' (0.38')	- (0.11)	0.56** (-0.19)	0.73** (-0.66**)	0.24 (-0.18)	0.16 (-)	0.62** (0.57**)	0.79** (0.31')	-0.48** (-0.69**)	- (-)	- (-)	0.64** (0.64**)

Whole, Micro, Nano, and Pico: total, micro-sized, nano-sized, and pico-sized chlorophyll *a*.

' : One month-lag time considered.

* : $P < 0.1$, ** : $P < 0.05$.

rates and biomass of unfractionated phytoplankton ($r^2 = 0.95$), microphytoplankton ($r^2 = 0.97$) and nanophytoplankton ($r^2 = 0.83$). River discharge rates were positively correlated with the contribution of microplankton to total biomass but negatively correlated with percent contribution of nanoplankton. Temperature was significantly correlated with picoplankton biomass.

DISCUSSION

It has been reported that nanoplankton (<20 μm) are dominant and more productive than netplankton (>20 μm) in oceanic waters whereas netplankton are more abundant in continental shelf and coastal upwelling waters (Malone 1980, Tremblay and Legendre 1994). In most estuaries nanoplankton are abundant although netplankton contribute more to total biomass. In estuarine waters nanoplankton have been recognized as more important contributors to primary production particularly during summer (McCarthy et al. 1974, Van Valkenberg & Flemmer 1974, Durbin et al. 1975, Haas 1975, Sellner 1983). The predominance of nanoplankton in nature has been postulated to result from their intrinsically higher rates of growth (e.g. Eppley and Sloan 1966), nutrient uptake (e.g. Munk and Riley 1952, Eppley and Thomas 1969, Friebele et al. 1978), and photosynthesis (Taguchi 1976, Malone 1980a, Malone and Neale 1981).

The tidal freshwater station (Station I) was thought to be enriched with riverine N and DSi input from riverine runoff throughout the year; however, the concentration of nitrite + nitrate was lower than that in the mesohaline zone during summer (see Fig. 5D,

5F) most likely due to high uptake by large phytoplankton which reportedly dominate when the supply of nitrate (“new” nitrogen) is high (Eppley & Peterson 1979, Malone 1980a,b, Probyn 1985). Based upon the observed positive significant correlation between temperature and biomass for all size classes of phytoplankton, we assume that warm summer temperatures stimulated nutrient uptake and, therefore, maximum algal growth rates in the tidal freshwater region of the river (Table 5). Such effects of temperature on the uptake of N and maximum algal growth rate have also been observed by Eppley (1972) and Carpenter & Dunham (1985). A significant correlation between light intensity and phytoplankton biomass also suggests that elevated light availability may have contributed to the increase in biomass during summer when the water column was less turbid (Fig. 3, Fig. 4G). High flushing rates during winter also appear to limit phytoplankton growth and biomass in the tidal freshwater region, since total community biomass as well as that of three of its size classes were generally inversely correlated with river discharge rate (Table 5). Limitation of phytoplankton growth by high flushing rates is also documented in Section I. We observed that the contribution of pico-sized phytoplankton to total biomass was negatively correlated with total chlorophyll *a* ($r^2 = 0.41$, $P < 0.05$). Chisholm (1992) similarly observed that the percentage of small cells in the phytoplankton community increased as total chlorophyll *a* decreased. Results of multiple regression analysis show that the phytoplankton community as a whole and its subclasses, including microphytoplankton, nanophytoplankton and picophytoplankton in the tidal freshwater portion of the York river estuary are regulated by river discharge rates, temperature and light.

Controls on phytoplankton dynamics at the transitional station (II) are more complex. The river-estuary transition region is the site of the turbidity maximum whose location and degree of mixing are controlled by the river discharge rate (Hansen & Rattray 1965). Based on light attenuation coefficients at three stations, we have determined that the turbidity maximum develops during February and March (Fig. 4G, 4H, 4I). The chlorophyll *a* minima observed during winter corresponded with peak light attenuation coefficients which probably resulted from high river discharge rates (see Fig. 4H, 7B). The effect of river flow rate on water column turbidity is supported by the inverse relationship between salinity and light attenuation (Fig. 4E, 4H). Thus, phytoplankton growth in this river-estuary transitional zone was likely limited by light during the cold season when river discharge rates were high. Low chl:phéo ratios during the cold season (Fig. 10B) appear to result from the increase of detrital particles either due to autolysis of phytoplankton under light-limited condition or due to grazing. Pheopigments, which are released as egested fecal material by grazers, have been used as an indicator of herbivorous grazing (e.g. Welschmeyer and Lorenzen 1985, Shuman and Lorenzen 1975). Suspended pheopigments can also be produced within phytoplankton cells during senescence of phytoplankton caused by poor growth environments or prolonged exposure to the dark (Yentsch 1967, Daley and Brown 1973). Thus, it is difficult to distinguish the relative importance of grazing vs. light limitation in regulating phytoplankton biomass in the river-estuary transition zone. Biomass of whole and nano-sized classes of phytoplankton was significantly correlated with chl:phéo ratios (Table 5) suggesting that they may be controlled by either light limitation or zooplankton grazing. However, it was documented in Section I that phytoplankton dynamics in the York River

are regulated primarily by resource limitation (bottom-up control) rather than zooplankton grazing (top-down control) in the York River estuary.

Picoplankton biomass was significantly correlated with both PAR and temperature. The extraordinarily large spring bloom (close to $100 \mu\text{g l}^{-1}$) observed during April 1997 was most likely caused by a combination of increased temperature and light availability (Fig. 4B, 5B). High nitrite + nitrate supply by river flow also may have supported the observed growth of large phytoplankton (micro-sized class) (Fig. 8B).

In estuaries chlorophyll *a* maxima have been observed in clearer waters both upstream and seaward of the turbidity maximum during summer or fall and have been associated with removal of ammonium, nitrate, phosphate and silicate (Anderson 1986, Harding et al. 1986, Fisher et al. 1988). In this study the chlorophyll *a* maximum was observed during August at the transition station (Fig. 7B, 8B), an occurrence which may be attributed to either more available light or nutrients remineralized from bottom water or sediment. Dominance of small cells such as nanoplankton during chlorophyll maxima suggests that phytoplankton in the transition regions rely on recycled nutrients (ammonium) rather than new nutrients (nitrite + nitrate) for their growth. This scenario is supported by low ammonium concentrations (probably due to rapid uptake by phytoplankton) but relatively high nitrite + nitrate concentrations observed during summer-fall (Fig. 5B, 5E).

Chl:phco ratios for microplankton were consistently lower in bottom than in surface water (Fig. 10E) compared with other size classes. Increased contributions of microplankton but decreased contributions of picoplankton were also observed in bottom water when surface chlorophyll *a* was at a minimum (Fig. 8B, 9B). These results suggest

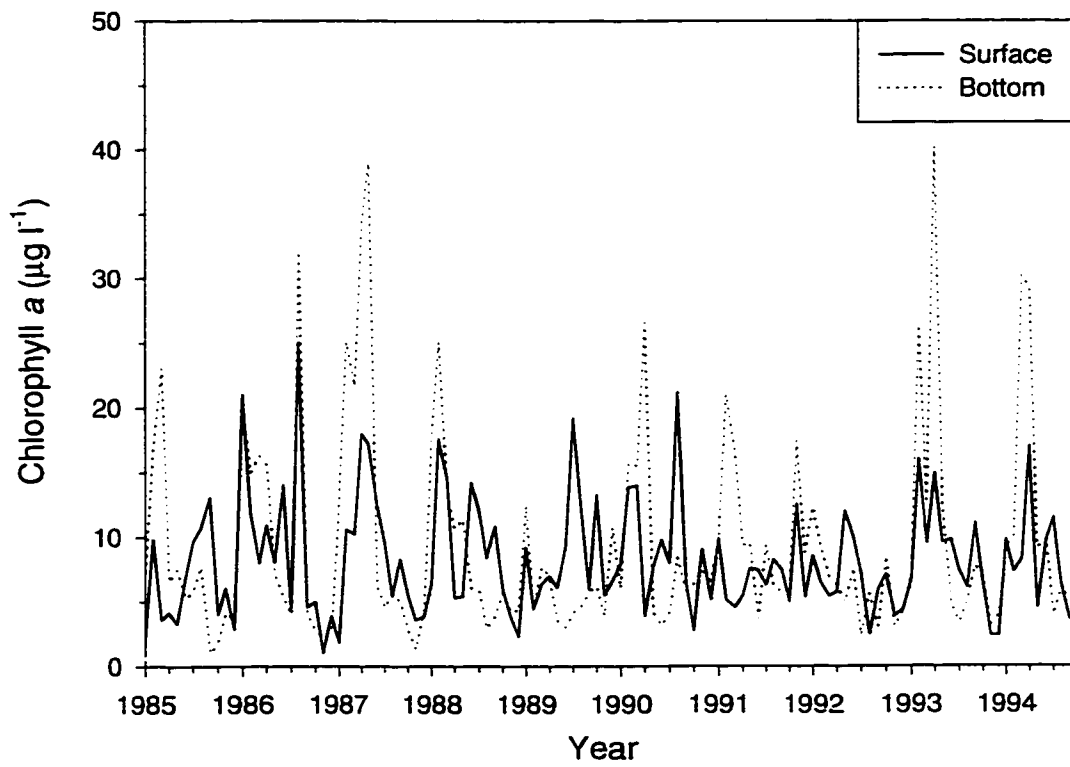
that dead cells moved from the lower estuary by tidal net upstream transport may be the major contributors to accumulation of phytoplankton biomass in the bottom waters of this station.

As discussed in the first section of this dissertation, during spring-summer nitrogen may limit phytoplankton growth in the mesohaline zone. During summer the biomass of small cells (pico- and nano-size classes) was most closely correlated with temperature (Table 5). High summer temperatures increase remineralization of organic nitrogen and phosphate in sediments (see Section I, this dissertation), thereby releasing ammonium and orthophosphate which can stimulate growth of small phytoplankton. The higher concentrations of ammonium and orthophosphate observed in bottom compared to surface waters in the mesohaline zone further support this contention (Fig. 5C, 5I). Regenerated ammonium was considered as the primary nutrient source for picoplankton and nanoplankton production in the southern Benguela upwelling system during winter (Probyn 1985). In this study, nitrite + nitrate concentrations were relatively high in surface water during summer, especially August (Fig. 5C) but ammonium concentrations were low (Fig. 5F). These results suggest that small phytoplankton prefer ammonium to nitrite + nitrate. Recycled nutrients accumulate in bottom water, especially during stratification cycles, which occur primarily during neap tides in the lower York river (Webb and D'Elia 1980), as discussed in chapter one of this dissertation.

In the mesohaline zone, phytoplankton biomass was higher in bottom than in surface water, but only during winter-spring.(Fig 9C). This trend was also apparent when we examined EPA long-term data (Fig. 11) for WE4.2 station located at the mouth of the

Fig. 11. Temporal distributions of chlorophyll *a* in the surface and bottom water at station WE4.2 (near the mouth of the York River estuary) from 1985 to 1994; station WE4.2 is one of the stations which have been monitored by EPA Chesapeake Bay Monitoring Program in the York River.

Station WE4.2



York River estuary. In addition, the contribution of large cells to total biomass increased while chl:pheo ratios for the large cell fraction of phytoplankton decreased throughout the sampling periods from summer through winter and spring (Fig. 8F; Table 4). These results indicate that either sinking of large-sized detrital particles from surface water or net upstream transports of the detrital particles in bottom water may be the mechanism responsible for the large accumulation of biomass in bottom water during winter in the mesohaline zone. Small cells have been shown to have negligible sinking rates compared to large cells (Takahashi & Bienfang 1983). Consequently, differences in quality (size structure) of phytoplankton in surface water may affect seasonal variations in total phytoplankton quantity (biomass) as well as size structure (quality) in bottom water. Considering the low biomass of picoplankton during winter-spring blooms, microplankton rather than aggregates of picoplankton (c.f. Gomes 1992) are likely to be the dominant contributors to organic carbon fluxes from surface to bottom water.

Strong correlations between large phytoplankton biomass and river discharge rates (Tables 8, 9) suggest that in surface water river discharge rates determine the location and magnitude of winter-spring blooms which, in turn, sink and contribute to high biomass in bottom water. The analysis of long-term EPA data in the first section of this dissertation similarly showed that river discharge determines both the location and magnitude of winter-spring blooms in the surface water of the lower estuary in the York River system. Based on results of regression analyses of data (Table 5) and as reported by others (Eppley & Peterson 1979, Malone 1980a,b, Probyn 1985), large phytoplankton cells (micro-sized) dominate in areas with high supply rates of new nitrogen as observed during winter-spring when river discharge rates are highest. However, it is difficult to

distinguish the relative importance of *in-situ* production supported by riverine N input vs. advective transport of microphytoplankton from the upper river as a principal source for winter-spring blooms of microphytoplankton. The accumulated biomass in bottom water during winter and subsequent remineralization by benthic microorganisms are likely to contribute to anoxic conditions during summer. These results demonstrate that analyses of size structure phytoplankton dynamics are necessary to understand the response of the total phytoplankton population to environmental change in estuarine systems.

With respect to spatial variations, we observed that small cells tend to be more abundant as one moves down the estuary (Malone 1980b). Iriarte (1993) found that biomass in the $>1 \mu\text{m}$ fraction was highest midway down the estuary and decreased both in landward and seaward directions. In contrast, biomass in the small sized ($0.2\text{-}1 \mu\text{m}$) fraction was highest at the seaward end of the estuary. A similar trend was observed for small size classes ($0.2\text{-}3 \mu\text{m}$) in Lacouture et al.'s study (1990). Observations made in this dissertation are similar to those of Lacouture et al. (1990); i.e. with contributions of small cells (nano-, pico-sized) to total biomass increasing downstream during summer and dominance of large cells increasing downstream during winter (Fig. 8).

In contrast to the lower estuary, rates of ammonium regeneration in the tidal freshwater zone are thought to be relatively low during summer due to the short residence time of detrital particles. This scenario is supported by the low ambient concentrations of ammonium and relatively high concentrations of nitrite + nitrate observed in bottom water of the tidal freshwater station (Fig. 5A, 5B) during summer. The high availability of "new" nutrients (nitrite + nitrate) may stimulate the growth of large cells relative to

small cells (e.g. Eppley & Peterson 1979, Malone 1980a,b, Probyn 1985). More turbid water in the tidal freshwater zone may also favor large cells which have a lower light optimum than small cells (c.f. Laws 1975). Downstream ammonium concentrations increase and light attenuation decreases supporting growth of small cells probably due to their efficient light-harvesting processes (Glover et al. 1985, Fogg 1986, Kirk 1986), efficient nutrient uptake-phycoerythrin synthesis-photosynthesis linkages (Raven 1986), and low sinking rates (Takahashi & Bienfang 1983), compared to large cells. During winter, on the other hand, all size classes are limited by the high flushing rates in the tidal freshwater zone. Increased dominance of small cells during this period reflects the general view that the contribution of small cells to phytoplankton standing stock increases as total chlorophyll a decreases (e.g. Chisholm 1992). During winter, nitrite + nitrate are dominant in N pools in the lower estuary, supporting the growth of large rather than small cells in the lower estuary.

In conclusion, phytoplankton growth in the tidal freshwater zone may be limited by high flushing rates and regulated by light and temperature. The large contribution of microplankton to total phytoplankton biomass is thought to be due to the availability of sufficient nitrite + nitrate compared with other regions in the York River estuary. In the river-estuary transition zone, phytoplankton production is most likely limited by light availability since this region experiences a turbidity maximum during winter.

Nanoplankton which dominate the phytoplankton community in the river-estuary transition zone throughout the year are most likely regulated by light. Growth of large cells in this zone is dependent on nitrite + nitrate input but only when light is not limiting.

In the mesohaline zone total phytoplankton biomass follows a bimodal seasonal distribution with both summer and winter blooms. During summer small cells (picoplankton and nanoplankton) dominate, while during winter large cells (microplankton) dominate. This seasonal shift in size structure is thought to be due to the different preferences of phytoplankton size classes for “new” (nitrite + nitrate) vs. “old” (ammonium) nutrients in the water column. We conclude from these studies that spatial and seasonal variations in size structure of phytoplankton observed on the estuarine scale is determined both by the different preferences of micro-, nano-, and picoplankton for nutrients and by their different light requirements. These results further indicate that phytoplankton size structure in the York river estuary may be regulated primarily by resource limitation (bottom-up control) rather than zooplankton grazing (top-down control). Consequently, the present study supports the conclusions established from the EPA long-term data analyses on phytoplankton and nutrient dynamics and further demonstrates that analyses of size structure phytoplankton dynamics are necessary to better understand phytoplankton dynamics including the response of the total phytoplankton population to environmental change in estuarine systems.

LITERATURE CITED

- Anderson, G. F. (1986) Silica, diatoms and a freshwater productivity maximum in Atlantic coastal plain estuaries, Chesapeake Bay. *Estuar. Coast. Shelf Sci.* 22:183-197.
- Armstrong, R. A. (1994) Grazing limitation and nutrient limitation in marine ecosystems: Steady state solutions of an ecosystem model with multiple food chains. *Limnol. Oceanogr.* 39(3):597-608.
- Bender, M. E. (1986) The York River: A Brief Review of Its Physical, Chemical and Biological Characteristics. Virginia Institute of Marine Science, School of Marine Science, The College of William and Mary, Gloucester Point, VA 23062
- Boynton, W. R., W. M. Kemp and C. W. Keefe. (1982) A comparative analysis of nutrients and other factors influencing estuarine phytoplankton production. pp69-90. In: V. Kennedy, ed. *Estuarine Comparisons*. Academic Press.
- Brooks, J. L. and Dodson, S. I. (1965) Predation, body size and composition of plankton. *Science* 150:28-35.
- Caron, D. A. (1991) Evolving role of protozoa in aquatic nutrient cycles. In: P. C. Ried, C. M. Turley, and P. H. Burkill. (eds.) *Protozoa and their role in marine processes*. NATO ASI, Springer-Verlag Berlin Heidelberg. G 25:387-415 (5.3)
- Carpenter, E. J. and Dunham S. (1985) Nitrogenous nutrient uptake, primary production, and species composition of phytoplankton in the Carmans River estuary, Long Island, New York. *Limnol. Oceanogr.* 30, 513-526.
- Capriulo, G. and E. Carpenter. (1983) Abundance, species composition and feeding impact of tintinnid micro-zooplankton in central Long Island Sound. *Mar. Ecol. Prog. Ser.* 10:277-288.
- Chisholm, S. W. (1992) Phytoplankton size. In P. G. Falkowski and A. D. Woodhead (eds.), *Primary Productivity and Biogeochemical cycles in the Sea*, Plenum Press, New York, pp. 213-237.
- Coffin, B. Richard, Sharp, H. Jonathan, (1987) Microbial trophodynamics in the Delaware Estuary. *Estuar. Coast. Shelf Sci.* 41:253-266.

- Daley, R. J. and S. R. Brown. (1973) Experimental characterization of lacustrine chlorophyll diagenesis. I. Physiological and environmental effects. *Arch. Hydrobiol.* 72: 277-304.
- De Mendiola, B. R. (1971) Some observation on the feeding of the Peruvian anchoveta *Engraulis ringens* in two regions of the Peruvian coast. In: Costlow, J. D. (ed.), *Fertility of the Sea*, Vol.2, pp417-440.
- Durbin, A. and E. Durbin. (1975) Grazing rates of the Atlantic menhaden *brevoortia tyrannus* as a function of particle size and concentration. *Mar. Biol.* 33:265-277.
- Durbin, E. G., Krawiec, R. W., and Smayda, T. J. (1975) Seasonal studies on the relative importance of different size and concentration. *Mar. Biol.* 33:265-277.
- Eppley, R. W., and P. R. Sloan. (1966) Growth rates of marine phytoplankton: Correlation with light absorption by cell chlorophyll *a*. *Physiol. Plant.* 19:47-59.
- Eppley, R. W. and Thomas, W. H. (1969) Comparisons of half-saturation constants for growth and nitrate uptake of marine phytoplankton. *J. Phycol.* 5:375-379.
- Eppley, R. W. (1972) Temperature and phytoplankton growth in the sea. *Fish. Bull.* 70:1063-1085.
- Eppley, R. W., and Peterson, B. J. (1979) Particulate organic matter flux and planktonic new production in the deep ocean, *Nature*, 282:677
- Fisher, T. R., L. W. Harding, Jr., D. W. Stanley, and Larry G. Ward. (1988) Phytoplankton, nutrients, and turbidity in the Chesapeake, Delaware, and Hudson estuaries. *Estuar. Cost. Shelf Sci.* 27:61-93.
- Fogg, G. E. (1986) Light and ultraphytoplankton. *Nature* 319:96.
- Friebele E. S., Correll, D. L. and Faust M. A. (1978) Relationship between phytoplankton cell size and the rate of orthophosphate uptake: *in situ* observations of an estuarine population. *Mar. Bio.* 45:39-52.
- Fritz, L. R. Lutz, M. Foote, C. Van Dourer, and J. Ewart. (1984) Selective feeding and grazing rates of oyster (*Crassostrea virginica*) larvae on natural phytoplankton assemblages. *Estuaries*. 7(4):513-518.
- Glibert, P. M., C. A. Miller, C. Garside, M. R. Roman, and G. B. McManus. (1992) NH_4^+ regeneration and grazing: interdependent processes in size-fractionated $^{15}\text{NH}_4^+$ experiments. *Mar. Ecol. Prog. Ser.* 82:65-74.

- Glover, H. E., B. B. Prezelin, L. Campbell, and M. Wyman. (1988) Pico- and ultraplankton Sargasso Sea communities: variability and comparative distributions of *Synechococcus* spp. and algae. *Mar. Ecol. Prog. Ser.* 49:127-139.
- Glover, H. E., D. A. Phinney, C. S. Yentsch. (1985) Photosynthetic Characteristics of Picoplankton Compared with Those of Larger Phytoplankton Populations, in Various Water Masses in the Gulf of Maine. *Biol. Oceanogr.* 3(3):223-248.
- Gomes, H. D. R., Goes, J. I. And Parulekar, A. H. (1992) Size-fractionated biomass, photosynthesis and dark CO₂ fixation in a tropical oceanic environment. *J. Plankton Res.* 14, 1307-1329.
- Haas, L. W. (1975). Plankton dynamics in a temperate estuary with observations on a variable hydrographic conditions. Doctoral dissertation, School of Marine Science, College of William and Mary, Gloucester Point, Virginia.
- Haines, E. B. (1976) Relation between the stable carbon isotope composition of fiddler crabs, plants and soils in a salt marsh. *Limnol. Oceanogr.* 21:880-883.
- Hansen, D. V. and Rattray, M., Jr. (1965) Gravitational circulation in straits and estuaries. *Journal of Marine Research* 23:104-122.
- Harding, Jr., L. W., B. W. Meeson, and T. R. Fisher, Jr. (1986) Phytoplankton production in two east coast estuaries: Photosynthesis-light functions and patterns of carbon assimilation in Chesapeake and Delaware Bays. *Estuar. Coast. Shelf Sci.* 23:773-806.
- Hein, M., M. F. Pedersen, and K. Sand-Jensen. (1995) Size-dependent nitrogen uptake in micro- and macroalgae. *Mar. Ecol. Prog. Ser.* 118:247-253.
- Hyer, P. V. (1977) Water quality model of York River, Virginia. Special Scientific Report No. 146. Virginia Institute of Marine Science.
- Iriarte, A. (1993) Size-fractionated chlorophyll a biomass and picophytoplankton cell density along a longitudinal axis of a temperate estuary (Southampton Water). *J. Plankton Res.* 15(5):485-500.
- Jackson, R. H., P. J. le B. Williams and I. R. Joint. (1987) Freshwater phytoplankton in the low salinity region of the River Tamar estuary. *Estuar. Coast. Shelf. Sci.* 25:299-311.
- Jochem, F. (1988) On the distribution and importance of picocyanobacteria in a boreal inshore area (Kiel Bight, Western Baltic). *J. Plankton Res.* 10:1009-1022.

- Joint, I. R. and A. J. Pomroy. (1983) Production of picoplankton and small nanoplankton in the Celtic Sea. *Mar. Biol.* 77:19-27.
- Jonas, R. (1992) Microbial Processes, Organic Matter and Oxygen Demand in the water column. pp113-148. In: D. E. Smith, M. Leffler, and G. Mackiernan, ed. *Oxygen Dynamics in the Chesapeake Bay*. Maryland Sea Grant College.
- Kemp, W. M., and W. R. Boynton. 1984. Spatial and temporal coupling of nutrient inputs to estuarine primary production: the role of particulate transport and decomposition. *Bull. Mar. Sci.* 35:522-535.
- Kemp, W. M. and W. R. Boynton. (1981) External and internal factors regulating metabolic roles of an estuarine benthic community. *Oecologia* 51:19-27.
- Kirk, J. T. O. (1994) *Light and Photosynthesis in Aquatic Ecosystems*. pp75-77. Cambridge University Press, Cambridge, England.
- Kirk, J. T. O. (1986) Optical properties of picoplankton suspensions. *Can. Bull. Fish. Aquat. Sci.* 214:501-520.
- Lacouture, R. V., B. B. Wagoner, E. Nealley, and K. G. Seller. (1990) Dynamics of the microbial food web in the Patuxent River: Autotrophic Picoplankton. In: Mihursky, J. A. and Chaney, A. (eds.), pp297-307. *New perspectives in the Chesapeake System: A Research and Management Partnership*. Chesapeake Research Consortium Publication No. 137.
- Laws, E. A. (1975) The importance of respiration losses in controlling the size distribution of marine phytoplankton. *Ecology*, 56, 419-426.
- Lenz, J. (1992) Microbial loop, microbial food web and classical food chain: Their significance in pelagic marine ecosystems. *Arch. Hydrobiol. Beih.* 37:265-279.
- Li, W. K. W., D. V. Subba Rao, W. G. Harrison, J. C. Smith, J. J. Culler, B. Irwin, and T. Platt. (1983) Autotrophic picoplankton in the tropical ocean. *Science* 219:292-295.
- Longhurst, A. R., Lorenzen, C. J., and Thomas, W. H. (1967) The role of pelagic crabs in the grazing of phytoplankton off Baja California. *Ecology* 48:190-220.
- Malone, T. C. (1980a). Algal Size. In: *The Physiological Ecology of Phytoplankton* (Ed) I. Morris. pp433-463.
- Malone, T. C. (1980b). Size-fractionated primary productivity of marine phytoplankton. In P. G. Falkowski (ed.), *Primary productivity in the sea*. Plenum, New York/London, vol. 31, 161-178.

- Malone, T. C. and P. J. Neale. (1981) Parameters of Light-Dependent Photosynthesis for Phytoplankton Size Fractions in Temperate Estuarine and Coastal Environments. *Mar. Biol.* 61:289-297.
- Malone, T. C. and M. B. Chervin. (1979) The production and fate of phytoplankton size fractions in the plume of Hudson River, New York Bight. *Limnol. Oceanogr.* 24(4):683-696.
- Malone, T. C., Ducklow, H. W., Peele, E. R., and Pike, S. E. (1991) Picoplankton carbon flux in Chesapeake Bay. *Mar. Ecol. Prog. Ser.* 78:11-22.
- Malone, T. C., W. M. Kemp, H. W. Ducklow, W. R. Boynton, J. H. Tuttle, and R. B. Jonas. (1986) Lateral variation in the production and fate of phytoplankton in a partially stratified estuary. *Mar. Ecol. Prog. Ser.* 32:149-160.
- Martin, J. H. (1970) Phytoplankton-zooplankton relationships in Narragansett Bay. IV. The seasonal importance of grazing. *Limnol. Oceanogr.* 15:413-418.
- Maurer, D., E. His, and R. Robert. (1984) Observations on the summer phytoplankton in the Bay of Arcachon. Its potential role in the feeding of *Crassostrea gigas* larvae. Special Report. Committee on Biological Oceanography. Int. Couns. Explor. Seas. Copenhagen. October 1984. p12.
- McCarthy, J. J., Taylor, W. R., Loftus, M. E. (1974). Significance of nanoplankton in the Chesapeake Bay Estuary and problems associated with the measurement of nanoplankton productivity. *Mar. Biol.* 24:7-16.
- Michaels, A. E. and M. W. Silver. (1988) Primary production, sinking fluxes and the microbial food web. *Deep-Sea Res.* 35:473-490.
- Morris, A. W., Mantoura, R. F. C., Bale, A. J., and Howland, R. J. M. (1978) Very low salinity regions of estuaries; important sites for chemical and biological reactions. *Nature* 274:678-680.
- Morris, A. W., Bale, A. J. and Howland, R. J. M. (1982) Chemical variability in the Tamar Estuary South-west England. *Estuar. Coast. Shelf Sci.* 14:649-661.
- Mullin, M. and E. Brooks. (1967) Laboratory culture, growth rate, and feeding behavior of a planktonic marine copepod. *Limnol. Oceanogr.* 12:657-666.
- Munk, W. H., and G. A. Riley. (1952) Absorption of nutrients by aquatic plants. *J. Mar. Res.* 11:215-240.

- Officer, C. B., R. B. Biggs, J. L. Taft, L. E. Cronin, M. A. Tyler, and W. R. Boynton. (1984) Chesapeake Bay anoxia: origin, development, significance. *Science* 223:22-27.
- Oviatt, C., P. Lane, F. French III and P. Donaghay. (1989) Phytoplankton species and abundance in response to eutrophication in coastal marine mesocosms. *J. Plankton Res.* 11(6):1223-1244.
- Painting, S. J., C. L. Moloney, and M. I. Lucas. (1993) Simulation and field measurements of phytoplankton-bacteria-zooplankton interactions in the southern Benguela upwelling region. *Mar. Ecol. Prog. Ser.* 100:55-69.
- Parsons, T. R. and LeBrasseur, R. J. (1970) The availability of food to different trophic levels in the marine food chain. In: Steele J. H. (ed.), *Marine Food Chains*, pp325-343. University of California Press, Berkeley.
- Parsons, T. R., Y. Maita, and C. M. Lalli. (1984) A manual of chemical and biological methods for seawater analysis. pp. 22-25. Pergamon Press, New York.
- Perissinotto, R. (1992) Mesozooplankton size-selectivity and grazing impact on the phytoplankton community of the Prince Edward Archipelago (Southern Ocean). *Mar. Ecol. Prog. Ser.* 79:243-258.
- Pierson, W. M. (1983) Utilization of eight algal species by the bay scallop, *Argopecten irradians concentricus* (Say). *J. Exp. Mar. Ecol.* 68:1-11.
- Probyn, T. A. (1985) Nitrogen uptake by size-fractionated phytoplankton populations in the southern Benguela upwelling system. *Mar. Ecol. Prog. Ser.*, 22, 249-258.
- Raven, J. A. (1986) Physiological consequences of extremely small size of autotrophic organisms in the sea. In: Platt, T., and Li, W. K. W. (eds.) *Photosynthetic picoplankton*. *Can. Bull. Fish. Aquat. Sci.* 214:1-70.
- Ray, T. R., L. W. Haas, and M. E. Sieracki. (1989) Autotrophic picoplankton dynamics in a Chesapeake Bay sub-estuary. *Mar. Ecol. Prog. Ser.* 52:273-285.
- Ryther, J. H., and J. G. Sanders. (1980) Experimental evidence of zooplankton control of the species composition and size distribution of marine phytoplankton. *Mar. Ecol. Prog. Ser.* 3:279-283.
- Scura, E. and C. Jerde. (1977) Various species of phytoplankton as food for larval northern anchovy, *Engraulis mordax* and relative nutritional value of the dinoflagellates *Gymnodinium splendens* on *Gonyaulax polyedra*. *Fishery Bull.* 75:577-583.

- Seliger, H. H., J. A. Boggs, and W. H. Biggley. (1985) Catastrophic anoxia in the Chesapeake Bay in 1984. *Science* 228:70-73.
- Seller, K. G. (1983) Plankton productivity and biomass in a tributary of the phytoplankton productivity, biomass and species composition in carbon export. *Estuar. Coast. Shelf Sci.* 17:197-206.
- Shuman, F. R. and C. M. Lorenzen (1975) Quantitative degradation of chlorophyll by a marine herbivore. *Limnol. Oceanogr.*, 20, 580-586.
- Smayda, T. J. (1965) II. On the relationship between ^{14}C assimilation and the diatom standing crop. *Bull. Inter-Am. Trop. Tuna Comm.* 9:467-531.
- Sundbaeck, K., B. Joensseon, P. Nilsson, and I. Lindstroem. (1990) Impact of accumulating drifting macroalgae on a shallow-water sediment system: An experimental study. *Mar. Ecol. Prog. Ser.* 58(3):261-274.
- Takahashi, M. and P. K. Bienfang. (1983) Size structure of phytoplankton biomass and photosynthesis in subtropical Hawaiian waters. *Mar. Biol.* 76:203-211.
- Taguchi, S. (1976) Relationship between photosynthesis and cell size of marine diatoms. *J. Phycol.* 12:185-189.
- Technicon Industrial Systems. (1973) Technicon AutoAnalyzer II Industrial method No. 186-72W, Silicates in water and seawater.
- Thayer, G. W., P. L. Parker, M. W. LaCroix and B. Fry. (1978) The stable carbon isotope ratio of some components of and eelgrass, *Zostera marina*, bed. *Oecologia* 35:1-12.
- Tremblay, J. E. and Legendre, L. 1994. A model for the size-fractionated biomass and production of marine phytoplankton. *Limnol. Oceanogr.* 39(8):2004-2014.
- Turner, J. T., S. Bruno, R. Larson, R. Staker, and G. Sharma. (1983) Seasonality of plankton assemblages in a temperate estuary. *Marine Ecol.* 4:81-99.
- Tuttle, J. H., R. B. Jonas, and T. C. Malone. (1987) Origin, development and significance of Chesapeake Bay anoxia, pp. 442-472. In: S. K. Majumdar, L. W. Hall, Jr., and H. M. Austin (eds), *Contaminant problems and management of living Chesapeake Bay resources*. Pennsylvania Academy of Sciences Press, Philadelphia.
- Van Valkenberg, S. D., Flemer, D. A. (1974) The distribution and productivity of nanoplankton in a temperate estuarine area. *Estuar. Coast. Mar. Sci.* 2:311-322.

Walsh, J. J. (1976) Herbivory as a factor in patterns of nutrient utilization in the sea. *Limnol. Oceanogr.* 21:1-13.

Webb, K. L. and C. F. D'Elia. (1980) Nutrient and oxygen redistribution during a spring neap tidal cycle in a temperate estuary. *Science* 207:983-985.

Welschmeyer, N. A. and C. J. Lorenzen. (1985) Chlorophyll budgets: Zooplankton grazing and phytoplankton growth in a temperate fjord and the Central Pacific Gyres. *Limnol. Oceanogr.* 30(1):1-21.

Williams, R. B. (1964) Division rates of salt marsh diatoms in relation to salinity and cell size. *Ecology* 45:877-880.

Yentsch, C. S. (1967) The measurement of chloroplastic pigments-thirty years of progress?, p. 225-270. In: H. C. Golterman and R. S. Clymo (eds.), *Chemical environment in the aquatic habitat*. North-Holland.

Appendix I. Ammonium (NH_4^+) and nitrite plus nitrate concentrations ($\text{NO}_2^- + \text{NO}_3^-$) at Stations I, II and III in the York River estuary.

Date	Depth	NH_4^+ (μM)			$\text{NO}_2^- + \text{NO}_3^-$ (μM)		
		Stations: I	II	III	I	II	III
Aug 8, 1996	Surface	0.90	0.65	0.48	10.3	11.5	11.6
	Bottom	0.79	0.48	4.14	10.9	19.1	13.6
Aug 15	Surface	0.42	0.21	0.25	6.71	14.6	17.1
	Bottom	0.53	0.53	11.5	8.07	19.7	11.2
Aug 21	Surface	1.19	0.21	0.50	5.28	2.21	10.5
	Bottom	0.39	0.68	11.2	5.35	7.35	12.8
Sep 26	Surface	0.34	0.09	5.64	5.54	11.7	6.68
	Bottom	0.32	0.53	7.85	5.52	12.1	4.70
Nov 11	Surface	1.96	2.06	2.69	11.7	8.74	1.16
	Bottom	1.96	0.39	7.28	*	3.56	1.98
Jan 23, 1997	Surface	2.65	7.41	1.93	12.6	12.7	6.00
	Bottom	2.65	7.02	2.21	11.8	22.7	4.46
Feb 20	Surface	0.73	6.68	1.05	20.1	16.9	7.14
	Bottom	*	4.28	2.44	*	6.16	4.16
Mar 10	Surface	2.65	6.48	1.96	16.9	13.9	5.48
	Bottom	*	*	2.60	*	*	4.86
Apr 7	Surface	1.18	0.83	0.71	13.0	1.24	0.20
	Bottom	*	0.88	2.03	*	0.00	0.16
Jun 4	Surface	0.71	1.73	1.74	0.64	3.94	0.22
	Bottom	*	2.53	1.03	*	3.34	0.050

* : No measurement taken.

Appendix II. Dissolved inorganic nitrogen (DIN), orthophosphate (PO_4^{3-}) and dissolved silicate (Dsi) concentrations (mg l^{-1}) at the study sites in the York River estuary.

Date	Depth	DIN (μM)			PO_4^{3-} (μM)			Dsi (μM)		
		Stations: I	II	III	I	II	III	I	II	III
Aug 8, 1996	Surface	11.2	12.2	12.1	0.52	0.74	2.26	127	123	70.8
	Bottom	11.7	19.5	17.7	0.55	0.87	0.68	127	125	45.7
Aug 15	Surface	7.13	14.8	17.3	0.82	0.97	0.61	101	120	62.4
	Bottom	8.60	20.2	22.8	0.84	1.10	1.42	102	110	52.0
Aug 21	Surface	6.47	2.42	11.0	0.74	0.52	0.47	109	116	62.1
	Bottom	5.74	8.03	24.0	0.71	0.58	1.39	107	110	58.7
Sep 26	Surface	5.88	11.8	12.3	0.80	0.92	0.65	140	111	52.0
	Bottom	5.84	12.6	12.6	0.80	0.96	0.68	140	102	42.9
Nov 11	Surface	13.7	10.8	3.85	0.32	0.29	0.11	171	124	50.6
	Bottom	13.7	3.95	9.26	*	0.14	0.28	*	104	22.6
Jan 23, 1997	Surface	15.3	20.1	7.93	0.40	0.11	0.05	160	106	36.9
	Bottom	14.4	29.7	6.67	0.21	0.18	0.10	*	101	19.8
Feb 20	Surface	20.8	23.5	8.19	0.11	0.22	0.059	156	135	49.3
	Bottom	*	10.4	6.60	*	0.10	0.10	*	123	16.0
Mar 10	Surface	19.5	20.4	7.44	0.18	0.21	0.050	144	109	35.2
	Bottom	*	*	7.46	*	*	0.054	*	93.4	26.3
Apr 7	Surface	14.2	2.07	0.91	0.17	0.14	0.045	127	65.4	19.6
	Bottom	*	0.88	2.19	*	0.09	0.095	*	62.1	9.57
Jun 4	Surface	1.35	5.67	1.96	0.11	0.22	0.050	8.79	52.7	4.77
	Bottom	*	5.87	1.08	*	0.18	0.059	*	48.7	4.88

* : No measurement taken.

Appendix III. Chlorophyll *a* ($\mu\text{g l}^{-1}$) of size classes including whole fractions (whole), micro-size (micro), nano-size (nano) and pico-size (pico) classes at the sampling stations in the York River estuary (*= no measurements taken).

Date	Depth	Whole ($\mu\text{g l}^{-1}$)			Micro ($\mu\text{g l}^{-1}$)			Nano ($\mu\text{g l}^{-1}$)			Pico ($\mu\text{g l}^{-1}$)		
		I	II	III	I	II	III	I	II	III	I	II	III
Aug 8, 1996	Surface	30.6	47.9	24.1	15.0	8.2	0.9	11.5	32.1	18.4	4.1	7.6	4.8
	Bottom	32.5	19.1	11.1	13.8	2.6	1.9	14.4	14.1	7.9	4.3	2.4	1.3
Aug 15	Surface	24.5	23.4	25.0	9.1	3.1	0.4	12.3	16.4	17.9	3.1	3.9	6.7
	Bottom	25.1	16.2	8.9	7.5	2.4	1.1	15.0	12.0	6.1	2.6	1.7	1.7
Aug 21	Surface	20.1	57.0	21.8	8.1	15.7	1.9	8.7	38.8	14.9	3.3	2.5	5.0
	Bottom	23.5	48.7	8.1	8.9	14.2	1.4	12.0	32.8	5.3	2.6	1.8	1.4
Sep 26	Surface	16.0	23.7	11.8	6.8	6.2	0.8	6.7	15.1	7.6	2.5	2.4	3.4
	Bottom	17.6	25.8	13.2	8.1	4.5	2.4	7.2	20.0	9.7	2.3	1.3	1.1
Nov 11	Surface	6.9	62.0	8.1	3.1	5.2	2.3	2.7	55.2	4.6	1.0	1.6	1.1
	Bottom	*	21.4	7.0	*	3.7	1.5	*	17.0	4.5	*	0.7	1.0
Jan 23, 1997	Surface	4.2	4.1	22.2	0.9	0.9	12.3	2.5	2.7	8.7	0.8	0.5	1.2
	Bottom	*	19.6	42.8	*	6.2	20.3	*	12.9	21.8	*	0.4	0.8
Feb 20	Surface	6.6	5.9	36.9	0.8	1.5	20.3	4.3	3.6	15.7	1.6	0.8	1.0
	Bottom	*	8.7	36.5	*	2.7	18.3	*	5.5	17.3	*	0.6	0.9
Mar 10	Surface	5.3	7.3	36.2	1.5	0.7	11.3	2.8	5.8	23.6	1.0	0.7	1.3
	Bottom	*	27.0	48.4	*	5.7	22.5	*	20.4	25.0	*	0.9	0.9
Apr 7	Surface	14.5	92.8	21.6	5.4	38.4	10.6	7.6	53.4	10.3	1.5	1.0	0.7
	Bottom	*	71.6	55.9	*	24.6	33.4	*	46.1	21.8	*	0.9	0.8
Jun 4	Surface	21.2	18.7	17.9	5.3	4.9	9.1	13.5	11.9	8.1	2.4	1.9	0.8
	Bottom	*	14.7	21.2	*	4.0	10.4	*	9.8	9.8	*	0.9	1.0

SECTION III

Ecosystem Modeling Analysis of Size-Structured Phytoplankton Dynamics in the York River Estuary, Virginia[†]

[†]: To be submitted to *Estuarine, Coastal and Shelf Science*

ABSTRACT

An ecosystem model was developed to investigate mechanisms controlling the size-structured phytoplankton dynamics in the mesohaline zone of the York River estuary. The model included 12 state variables in a unit volume (m^3) describing the distribution of carbon and nutrients (nitrogen, phosphorus) in the surface mixed layer. The state variables consisted of autotrophs including pico-, nano-, and micro-phytoplankton; heterotrophs including bacteria, flagellates + ciliates, microzooplankton, and mesozooplankton; the nutrients nitrite + nitrate, ammonium, and orthophosphate as well as dissolved organic carbon (DOC), and particulate organic carbon (POC). Groupings of autotrophs and heterotrophs were based on cell size and ecological hierarchy; mixotrophy was not considered. Forcing functions included incident radiation, temperature, wind stress, mean flow and tide which includes advective transport and turbulent mixing. The ecosystem model was developed in Fortran90 using differential equations that were solved using the 4th order Runge-Kutta technique. Model results supported the general view that phytoplankton dynamics are controlled by abiotic mechanisms (i.e. bottom-up control) rather than biotic, trophic interactions in the York River estuary. Larger, mesozooplankton appear to be controlled by top-down mechanisms. Model sensitivity tests showed that small cells (pico-, nano-sized) are more likely regulated by temperature and light whereas large cells (micro-sized) are regulated by physical processes such as advection and tidal mixing. Microphytoplankton blooms

during winter-spring resulted from a combination of longitudinal advection and vertical diffusion of phytoplankton cells rather than *in-situ* production.

INTRODUCTION

Phytoplankton dynamics in aquatic environments may be regulated by abiotic mechanisms; nutrient fluxes related to physical-chemical variability, i.e., bottom-up control and biotic; trophic interactions, i.e., top-down control. (Carpenter et al. 1987; Day et al. 1989; Alpine and Cloern 1992; Kivi et al. 1993; Armstrong 1994; Caraco et al. 1997). There has been continuing controversy and debate over the relative importance of bottom-up vs. top-down controls and established concepts of resource competition (Tilman 1982) and trophic cascade (Carpenter et al. 1985) for many years. In estuaries, these controlling mechanisms interact with phytoplankton in complicated ways, mainly due to freshwater and tidal energy inputs into the system (Alpine and Cloern 1992; Pennock and Sharp 1994; Cloern 1996). Temporal variations in river discharge to an estuary can affect phytoplankton production, biomass accumulation and size structure or taxon composition through several processes: 1. altering inputs of nutrients from the surrounding watershed; 2. altering light availability by way of estuarine gravitational circulation, stratification, and changing the turbidity maximum zone along the estuary; 3. altering rates of dilution or advection of phytoplankton; and, 4. altering the amount of detrital or suspended organic matter supporting heterotrophs in an estuarine system (e.g. Malone and Chervin 1979; Malone et al. 1980; Cloern et al. 1983; Pennock 1985; Malone et al. 1988; Gallegos et al. 1992; Madariaga et al. 1992; Boyer et al. 1993). While seasonal and interannual fluctuations in river discharge produce low-frequency

oscillations in the phytoplankton population, variations in tides (tidal mixing) result in high-frequency oscillations (Haas 1975; Ray et al. 1989; Aksnes and Lie 1990; Cloern 1991).

In previous sections of this dissertation, phytoplankton and nutrient dynamics were investigated by analyzing EPA long-term monitoring data and summarizing the results of an annual sampling program in the York River estuary, Virginia. The studies presented general spatio-temporal characteristics of phytoplankton biomass and size structure. Several conclusions on the potential controlling factors were indicated from the results but it was difficult to identify the major controlling factors for phytoplankton due to the complexity of interactions between phytoplankton and other plankton, and between phytoplankton and the variable physical-chemical environment.

For several decades, simulation models have been used to explore plankton dynamics in aquatic systems due to their ability to integrate and synthesize a tremendous array of information. Models have been used to describe interactions between various components of the plankton community and their physical-chemical environments which would be difficult otherwise due to the complexity of the interactions. In this regard, the objectives of this study were to 1. develop an ecosystem model focusing on size-structured plankton dynamics which would integrate the EPA long-term data base and the annual sampling data, and 2. investigate major mechanisms controlling size-fractionated phytoplankton and nutrient dynamics in mesohaline zone of the York River estuary, Virginia. The hypotheses established in Section I and II of this dissertation were further examined by the ecosystem modeling analyses.

MATERIALS AND METHODS

Area of model application

The York River estuarine system, a subestuary of the Chesapeake Bay, is composed of three rivers, i.e. the York, Pamunkey, and Mattaponi (Fig. 1). The York River is formed by the confluence of the Pamunkey and Mattaponi rivers at West Point (48 km from its mouth). Total average freshwater discharge to the river system is $70 \text{ m}^3 \text{ sec}^{-1}$ (Hyer 1977). Salinity distribution in the York River system is affected by the interaction of freshwater, salt water, tidal energy and wind. Salinity gradients between the surface and bottom layers are influenced by neap and spring tidal cycles with destratification of the water column occurring at high spring tides and stratification developing during the intervening periods (Haas 1975). The area of model application is located in the mesohaline zone, 13 km from mouth of the York River estuary (Fig. 1). Average water depth is 16.7 m and salinity ranged from 12.0 to 17.5 in surface water and from 16.0 to 22.2 in bottom water during the period of August 1996 to June 1997.

Model Description

1. General Conceptual Structure of the Model

The conceptual ecosystem model includes 12 state variables for describing the distribution of carbon and nutrients in the surface mixed-layer of the mesohaline zone in the York River estuary (Fig. 2). The state variables consist of autotrophs including pico- ($<3 \mu\text{m}$), nano- (>3 and $<20 \mu\text{m}$), and micro-phytoplankton ($>20 \mu\text{m}$); heterotrophs including bacteria, flagellates+ciliates, microzooplankton (>70 and $<202 \mu\text{m}$), and

Fig. 1. Study site is located in the mesohaline zone of the York River estuarine system. Water samples were collected at the site (Station III) over an annual cycle.

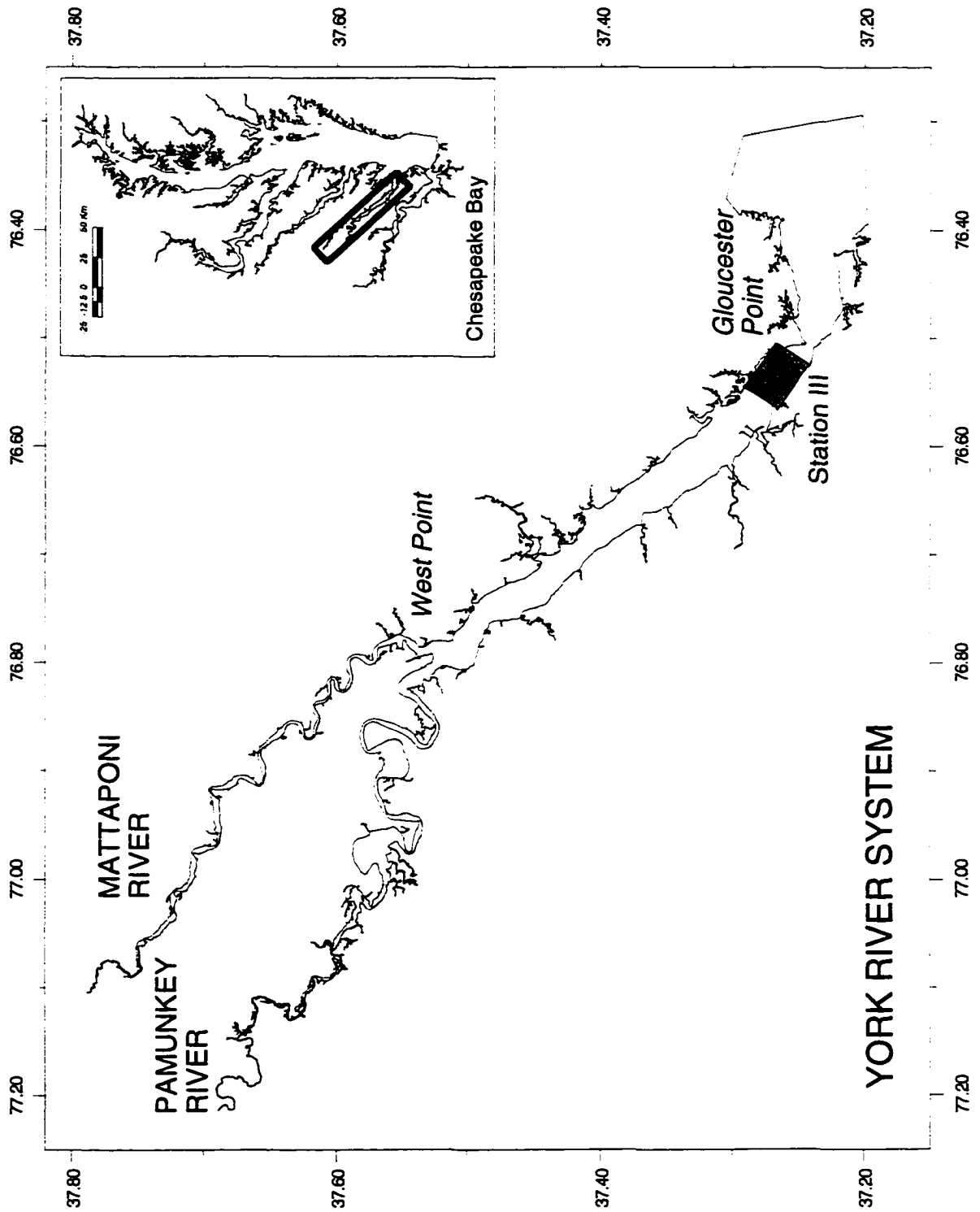
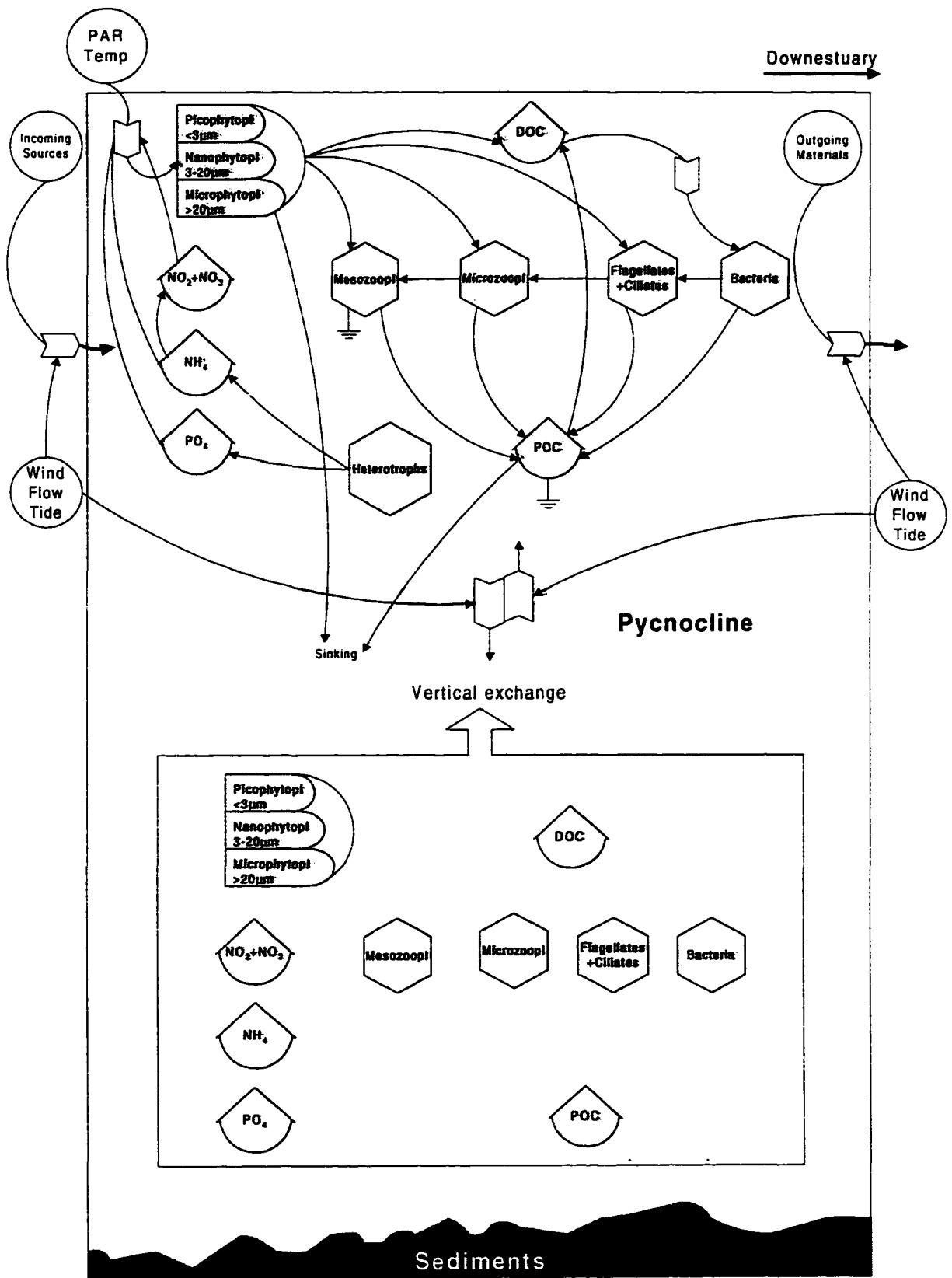


Fig. 2. Diagram describing biological and chemical processes coupled with forcing functions in the model of the York River system. Odum's symbols (1983) were used for this diagram.



mesozooplankton ($>202 \mu\text{m}$); the nutrients $\text{NO}_2^- + \text{NO}_3^-$, NH_4^+ , and PO_4^{-3} , and non-living organic materials, DOC, and POC. Groupings of autotrophs and heterotrophs are based on cell size and ecological hierarchy; mixotrophy was not considered in the model.

Forcing functions include incident radiation, temperature, tide, wind stress, and mean flow. Incident radiation and temperature were estimated using empirical equations for Gloucester Point, VA (Wetzel and Meyers, 1994). Salinity and wind stress data were collected by the Virginia Institute of Marine Science at Gloucester Point, VA. Daily river discharge rates at the fall line were collected by US Geological. The surface boundary condition is specified by a zero flux condition for all state variables at the atmosphere-water interface. Vertical transport by advection and diffusion, sinking for organisms, and fluxes for nutrients were incorporated into the model as the bottom boundary condition, in which the flux of organisms and nutrients was specified by vertical exchange or sinking rate times biomass and nutrient flux from bottom water respectively. Chlorophyll *a* and nutrients collected from bottom water over an annual cycle and presented in Section II of this dissertation were used as input data for the bottom boundary condition. The model was developed in Fortran90 (Microsoft® Fortran Power Station) and differential equations were solved using the 4th order Runge-Kutta technique.

Table I gives the variable names, symbols and units for the forcing functions, state variables and boundary conditions used in the model.

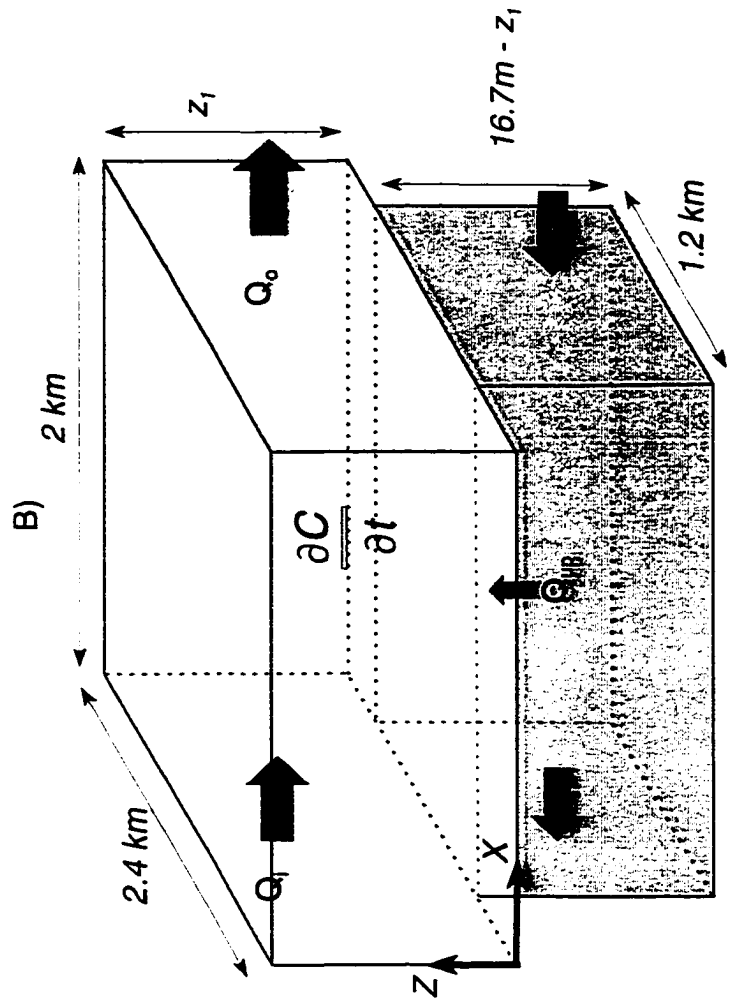
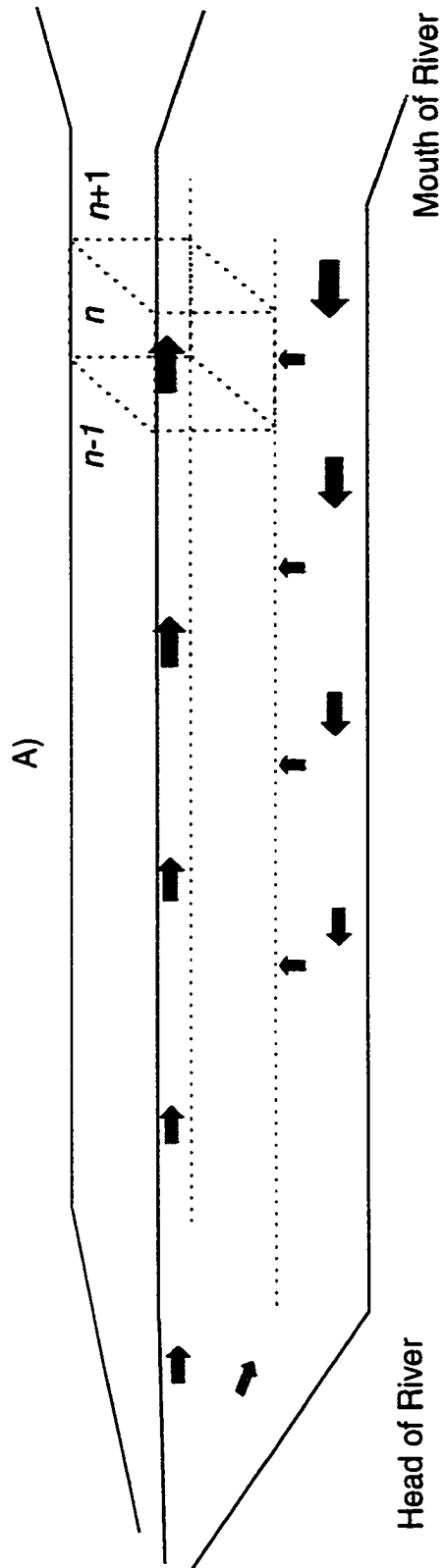
2. Mathematical Structure for Hydrodynamic Processes

The tidally averaged-model was simulated for plankton dynamics in the surface mixed-layer of the mesohaline zone in the York River system (Fig. 3). The surface

Table 1. Forcing functions, state variables and boundary conditions ($t = \text{time}$) used in the ecosystem simulation model.

Variable	Symbol	Unit
<i>Forcing (or driving) variables:</i>		
Incident radiation	$I(t)$	Ein d^{-1}
Temperature	$T(t)$	$^{\circ}\text{C}$
Salinity	$S(t)$	psu
Wind	$U_{10}(t)$	cm s^{-1}
Flow	$Q(t)$	$\text{m}^3 \text{s}^{-1}$
<i>State Variables (components)</i>		
Picophytoplankton	$PP(t)$	mg Chl m^{-3}
Nanophytoplankton	$NP(t)$	mg Chl m^{-3}
Microphytoplankton	$MP(t)$	mg Chl m^{-3}
Heterotrophic Bacteria	$HB(t)$	g C m^{-3}
Heterotrophic Flagellates+Ciliates	$HFC(t)$	g C m^{-3}
Microzooplankton	$Z1(t)$	g C m^{-3}
Mesozooplankton	$Z2(t)$	g C m^{-3}
Particulate Organic Carbon	$POC(t)$	g C m^{-3}
Dissolved Organic Carbon	$DOC(t)$	g C m^{-3}
Ammonium	$NI(t)$	μM
Nitite+Nitrate	$N2(t)$	μM
Orthophosphate	$P(t)$	μM
<i>Boundary Specifications:</i>		
Fluxes of state variables = 0 at interface of atmosphere-surface water, Fluxes = Sinking, vertical exchange at interface of surface mixed-layer and bottom layer, and flows = inflow (Q_{in}) and outflow (Q_{out}) of surface layer	Symbols of all state variables with time function	Same as the unit described above

Fig. 3. Schematic representation of net transport in an estuarine system (A) and geometric structure of the ecosystem model developed in this study (B). The surface mixed-layer depth, z_1 was determined by an empirical equation for the York River (Hayward et al. 1986).



mixed-layer depth, z_l was determined by an empirical equation derived for the York River estuary by Hayward (1986) as Equation 1.

$$z_l = \exp(3.0666 - 0.06064 \delta S^{0.6528}), \quad (1)$$

where, δS is the salinity difference between the surface and bottom waters. δS (Equation 2) was calculated as the top half of a sine wave (e.g. Eldridge and Sieracki 1993):

$$\delta S = a \sin\left(\frac{2\pi t}{\lambda}\right) \quad (2)$$

where, a is an amplitude of 5 ppt and λ is a wavelength of 28 days.

Table 2 presents the differential equations for the state variables and the symbols employed are given in Table 3. As described in Table 2, every state variable is affected by advective transport and turbulent mixing. Longitudinal transport in the surface mixed-layer is determined by the residual velocities ($m s^{-1}$) of incoming (Q_i) and outgoing river flows (Q_o) through the layer as shown in the second terms on the left hand side of the equations. The river flow (Q_i) entering section n (Fig. 3) is estimated by a function of surface salinity (SS_{n-1} , psu) and bottom salinity (BS_{n-1} , psu) of section $n-1$ and vertically averaged river discharge rate (RD_{n-1} , $m^3 s^{-1}$) through the water column in section n as Equation 3 (Prichard 1965). The river flow (Q_o) leaving section n (Equation 4) is also estimated by a function of surface salinity (SS_{n+1} , psu) and bottom salinity (BS_{n+1} , psu) of section $n+1$ and vertically averaged river flow (RD_{n+1} , $m^3 s^{-1}$) in section $n+1$.

Table 2. The differential equations employed for the state variables. The symbols are described in Table 3.

-
- (1) *Picophytoplankton*

$$\frac{\partial PP}{\partial t} + \frac{\partial uPP}{\partial x} + \frac{\partial wPP}{\partial z} = \frac{\partial}{\partial z} D \frac{\partial PP}{\partial z} + PP(G-R-HFCGz-r_m-r_{ex}-r_s)$$
- (2) *Nanophytoplankton*

$$\frac{\partial NP}{\partial t} + \frac{\partial uNP}{\partial x} + \frac{\partial wNP}{\partial z} = \frac{\partial}{\partial z} D \frac{\partial NP}{\partial z} + NP(G-R-ZIGz-r_m-r_{ex}-r_s)$$
- (3) *Microphytoplankton*

$$\frac{\partial MP}{\partial t} + \frac{\partial uMP}{\partial x} + \frac{\partial wMP}{\partial z} = \frac{\partial}{\partial z} D \frac{\partial MP}{\partial z} + MP(G-R-ZZGz-r_m-r_{ex}-r_s)$$
- (4) *Heterotrophic Bacteria*

$$\frac{\partial HB}{\partial t} + \frac{\partial uHB}{\partial x} + \frac{\partial wHB}{\partial z} = \frac{\partial}{\partial z} D \frac{\partial HB}{\partial z} + HB(G-R-HFCGz-r_m)$$
- (5) *Heterotrophic Flagellates + Ciliates*

$$\frac{\partial HFC}{\partial t} + \frac{\partial uHFC}{\partial x} + \frac{\partial wHFC}{\partial z} = \frac{\partial}{\partial z} D \frac{\partial HFC}{\partial z} + HFC(G-R-ZIGz-(f_{er}+f_{sf})HFGz-r_m)$$
- (6) *Microzooplankton*

$$\frac{\partial ZI}{\partial t} + \frac{\partial uZI}{\partial x} + \frac{\partial wZI}{\partial z} = \frac{\partial}{\partial z} D \frac{\partial ZI}{\partial z} + ZI(G-R-ZZGz-(f_{er}+f_{sf})ZIGz-r_m)$$
- (7) *Mesozooplankton*

$$\frac{\partial Z2}{\partial t} + \frac{\partial uZ2}{\partial x} + \frac{\partial wZ2}{\partial z} = \frac{\partial}{\partial z} D \frac{\partial Z2}{\partial z} + Z2(G-R-ZZM-(f_{er}+f_{sf})ZZGz-r_m)$$
- (8) *Particulate Organic Carbon*

$$\frac{\partial POC}{\partial t} + \frac{\partial uPOC}{\partial x} + \frac{\partial wPOC}{\partial z} = \frac{\partial}{\partial z} D \frac{\partial POC}{\partial z} + (f_{er}+f_{sf})(HFC \cdot HFCGz + ZI \cdot ZIGz + Z2 \cdot ZZGz) + r_m(PP+NP+MP+HB+HFC+ZI+Z2) - POC(r_l+r_w)$$
- (9) *Dissolved Organic Carbon*

$$\frac{\partial DOC}{\partial t} + \frac{\partial uDOC}{\partial x} + \frac{\partial wDOC}{\partial z} = \frac{\partial}{\partial z} D \frac{\partial DOC}{\partial z} + r_{ex}(PP+NP+MP) + r_l POC - HB \cdot G$$
- (10) *Ammonium*

$$\frac{\partial NI}{\partial t} + \frac{\partial uNI}{\partial x} + \frac{\partial wNI}{\partial z} = \frac{\partial}{\partial z} D \frac{\partial NI}{\partial z} - NIT + \{(HB \cdot R + HFC \cdot R + ZI \cdot R + Z2 \cdot R) - PR(PP \cdot G + NP \cdot G + MP \cdot G)\} / f_{C,N}$$
- (11) *Nitrite + Nitrate*

$$\frac{\partial N2}{\partial t} + \frac{\partial uN2}{\partial x} + \frac{\partial wN2}{\partial z} = \frac{\partial}{\partial z} D \frac{\partial NI}{\partial z} + NIT - DENIT - (1-PR)(PP \cdot G + NP \cdot G + MP \cdot G) / f_{C,N}$$
- (12) *Orthophosphate*

$$\frac{\partial P}{\partial t} + \frac{\partial uP}{\partial x} + \frac{\partial wP}{\partial z} = \frac{\partial}{\partial z} D \frac{\partial P}{\partial z} + (HB \cdot R + HFC \cdot R + ZI \cdot R + Z2 \cdot R - PP \cdot G - NP \cdot G - MP \cdot G) / f_{C,P}$$
-

Table 3. Symbols and units of physical, biological and chemical processes incorporated in the model.

Physical and biochemical Processes	Symbol	Unit
Residual velocity in X, Z direction	u, w	$m s^{-1}$
Diffusion coefficient	D	$m^2 s^{-1}$
Picophytoplankton:		
Gross production	$PPG(t)$	$g C m^{-3} d^{-1}$
Respiration	$PPR(t)$	$g C m^{-3} d^{-1}$
Nanophytoplankton:		
Gross production	$NPG(t)$	$g C m^{-3} d^{-1}$
Respiration	$NPR(t)$	$g C m^{-3} d^{-1}$
Microphytoplankton:		
Gross production	$MPG(t)$	$g C m^{-3} d^{-1}$
Respiration	$MPR(t)$	$g C m^{-3} d^{-1}$
Grazing by heterotrophic flagellates+ciliates	$HFCGz(t)$	$g C m^{-3} d^{-1}$
Grazing by microzooplankton	$Z1Gz(t)$	$g C m^{-3} d^{-1}$
Grazing by mesozooplankton	$Z2Gz(t)$	$g C m^{-3} d^{-1}$
Sinking rate of phytoplankton	r_s	$m d^{-1}$
Exudation rate of phytoplankton	r_{ex}	d^{-1}
Mortality rate of auto- and heterotrophs	r_m	d^{-1}
Heterotrophic Bacteria		
Gross production	$HBG(t)$	$mg C m^{-3} d^{-1}$
Respiration	$HBR(t)$	$mg C m^{-3} d^{-1}$
Excretion	$f_{C,N} \text{ or } f_{C,P} HBR(t)$	$mg N \text{ or } P m^{-3} d^{-1}$
Heterotrophic Flagellate		
Gross production	$HFCG(t)$	$mg C m^{-3} d^{-1}$
Respiration	$HFCR(t)$	$mg C m^{-3} d^{-1}$
Excretion	$f_{C,N} \text{ or } f_{C,P} HFCR(t)$	$mg N \text{ or } P m^{-3} d^{-1}$
Microzooplankton		
Gross production	$Z1G(t)$	$mg C m^{-3} d^{-1}$
Respiration	$Z1R(t)$	$mg C m^{-3} d^{-1}$
Excretion	$f_{C,N} \text{ or } f_{C,P} Z1R(t)$	$mg N \text{ or } P m^{-3} d^{-1}$
Mesozooplankton		
Gross production	$Z2G(t)$	$mg C m^{-3} d^{-1}$
Respiration	$Z2R(t)$	$mg C m^{-3} d^{-1}$
Excretion	$f_{C,N} \text{ or } f_{C,P} Z2R(t)$	$mg N \text{ or } P m^{-3} d^{-1}$
Grazing by fish	$Z2M$	$mg C m^{-3} d^{-1}$
C:N and C:P ratios	$f_{C,N}, f_{C,P}$	unitless
Fraction of egestion by grazers	f_{eg}	unitless
Fraction of sloppy feeding by grazers	f_{sf}	unitless
Leaching rate of POC	r_l	d^{-1}
Grazing loss rate of POC	r_w	d^{-1}
Nitrification	$NIT(t)$	$g N m^{-3} d^{-1}$
Denitrification	$DENIT(t)$	$g N m^{-3} d^{-1}$

$$Q_i = \frac{BS_{n-1}}{BS_{n-1} - SS_{n-1}} RD_{n-1} , \quad (3)$$

$$Q_o = -\frac{BS_{n+1}}{BS_{n+1} - SS_{n+1}} RD_{n+1} \quad (4)$$

and

The surface and bottom salinities in the sections $n-1$ and $n+1$ were estimated based on 20 years data for the York River estuary (Wojcik 1981). Vertically averaged river discharge rates in section $n-1$ were predicted by running a 1-D hydrodynamic model developed by J. Shen at Virginia Institute of Marine Science under 6 different river discharge rates at the fall line of the York River system. In order to account for effects of river discharge rates at the fall line (RD_{fl}), the vertically averaged river discharge rates in section $n-1$ (Equation 5) were predicted by using the correlation ($r^2 = 0.98$) between the prediction and river discharge rate at fall line (RD_{fl}) as input data in the hydrodynamic model. The vertically averaged river discharge rate in section $n-1$ was assumed to equal that in section $n+1$.

$$RD_{n-1} = 1.384RD_{fl} + 2.62 \quad (5)$$

Vertical advection is governed by the upward velocity (w) in the vertical axis (z) as shown in the third terms on the left hand side of the equations. The upward velocity was determined by dividing the interface area (m^2) between surface mixed and bottom layers into the upward flow (Q_{up} , $m^3 s^{-1}$) which is determined by subtracting outgoing flow (Q_o) from incoming flow (Q_i) (see Fig. 2).

Turbulent mixing is governed by the empirical equation for the diffusion coefficient (D) in Equation 6 (Denman and Gargett 1983).

$$D = 0.25 \epsilon N^{-2} \quad (6)$$

The rate of dissipation of turbulent kinetic energy, ϵ is expressed as Equation 7 and the buoyancy frequency, N^2 ($s^{-1} = \text{radians } s^{-1}$) as Equation 8, where ω_* is turbulent frictional velocity ($m s^{-1}$), κ is von Karman's constant, z_1, z_2 are water depths of surface and bottom layers, u_* is bed shear velocity ($0.01 m s^{-1}$), g is the acceleration due to gravity, ρ_w is the density of water, $\partial\rho/\partial z$ is the vertical density gradient. In order to take into account the effects of bottom friction, u_* (bed shear velocity) was incorporated into the equation employed by Denman and Gargett (1983) and typical values (i.e. $0.01 m s^{-1}$) provided by Dr. S. Kim at VIMS were chosen for model simulation.

$$\epsilon = \frac{\omega_*^3}{\kappa z_1} + \frac{u_*^3}{\kappa z_2} \quad (7)$$

$$N^2 = \frac{g}{\rho_w} \cdot \frac{\partial\rho}{\partial z} \quad (8)$$

The turbulent frictional velocity, ω_* (Equation 9), is a function of windstress (τ), air and water densities ($\rho_a=1.2 \text{ kg m}^{-3}$, ρ_w , respectively), a drag coefficient (C_{10} , 1.3×10^{-3}), and the mean windspeed 10 m above the sea surface (U_{10}). Water densities are determined by Equation 10, where k is a constant, 7.5×10^{-4} , and S is salinity (Hamilton 1977).

$$\omega_* = \sqrt{\frac{\tau}{\rho_w}} = \sqrt{\frac{\rho_a C_{10} U_{10}^2}{\rho_w}} \quad (9)$$

where

$$\rho_w = \rho_a (1 + kS) \quad (10)$$

3. Mathematical Structure for Biological and Chemical Processes

Phytoplankton population densities are determined by advective transport, turbulent mixing, gross growth rate, respiration rate, sinking rate, mortality (senescence) rate, exudation rate, and grazing rate by herbivores (Table 2). Gross growth, G (Equation 11) is limited by light and nutrients acting on the potential maximum growth rate, which is itself dependent on body size and temperature.

$$G = G_M \cdot L_{lim} \cdot N_{lim} \quad (11)$$

Moloney and Field (1989) presented a significant relationship between body mass (pg C) and maximal nutrient uptake rates of phytoplankton (Equation 12). The effect of temperature on the maximal growth rates is also considered since Eppley (1972) documented that there is a significant relationship between temperature and an upper physiological limit to phytoplankton growth in conditions where neither light nor nutrient were in limited supply. The temperature effect is modeled as a function of the surface water temperature, $T(t)$ and a constant k_{cal} was defined as a calibration parameter.

$$G_M = 3.6M^{-0.25} \cdot \frac{T(t)}{k_{cat}} \quad (12)$$

Light limitation is determined by f , k_d , z , I_m and I_o as shown in Equation 13 (DiToro et al. 1971), where f is the photoperiod as a fraction of a day (e.g., 0.5 at the equinoxes), k_d is the light attenuation coefficient (m^{-1}), z is the depth (m), I_m and I_o are incident average and optimal light (Ein/day), respectively. Light attenuation (k_d) was measured over an annual cycle and used as input data. Daily k_d values were interpolated based on the field data. I_o can differ between size classes of phytoplankton and was determined in the process of calibration for the York River ecosystem model.

$$LtLim = \frac{e \cdot f}{k_d \cdot z} \left(e^{\frac{I_m}{I_o} e^{-k_d z}} - e^{-\frac{I_m}{I_o}} \right) \quad (13)$$

Nutrient limitation is determined using the Monod (1942) model (Equation 14). Equation 15 gives the derivation for the half saturation constant for each limiting nutrient. The half saturation constant (K_N) for nitrogen is calculated using Moloney and Field (1991) equations based on cell mean size (biovolume, μm^3) which can be converted to cell mass (M, C pg). K_P is determined by dividing K_N by the N:P ratio.

$$NtLim = Min \left(\frac{N}{K_N + N}, \frac{P}{K_P + P} \right) \quad (14)$$

where

$$K_N = 2M^{0.38}, \quad K_P = \frac{K_N}{N:P} \quad (15)$$

Estimation of respiration is based on an empirical equation, a function of surface water temperature ($T(t)$) and phytoplankton gross growth (G) as given in Equation 16 (Biebl and McRoy 1971).

$$R = 0.5[0.5G(0.0104T(t)+0.3432)+e^{(0.1370T(t)-i0.09)}] \quad (16)$$

Sinking rates of primary producers are determined by allometric relationships (Moloney and Field 1989), as $0.029M^{0.42}$. Mortality (senescence) rate (r_m) and a constant fraction of DOC release (cf. Malone and Ducklow 1990) by phytoplankton (exudation rate, r_{ex}) were determined by model calibration since equations or kinetics for the processes have not well established.

Grazing by herbivores is based on an empirical, cell size relationship between grazer and prey, and a prey density function (given below). It is assumed that heterotrophs feed only on prey within a size range from 10 to 100 times smaller than themselves. The mathematical equations employed to describe the relationships are based on nonlinear, donor- and recipient-controlled feedback equations developed by Wiegert (1973) and applied by Wiegert and Wetzel (1979) and Wetzel and Christian (1984). Trophic interactions between prey (or resource, i) and predator (or recipient, j) are regulated by feedback terms composed of four density related parameters: A_{ij} , the resource (donor) density or concentration below which uptake by the recipient is limited;

G_{ij} , the resource density or concentration at which the donor resource is not available to the recipient population; A_{ij} , the recipient density or concentration above which uptake of a resource is less than maximum (limited); G_{ij} , the maximum maintainable recipient density or concentration for a population when other resources are not limiting. It was assumed that the observed range in population densities during the sampling over an annual cycle included threshold and limit levels of each compartment in the ecosystem model of the York River model. Donor-controlled (fb_{ij}) and recipient-controlled feedback (fb_{ij}) terms were determined by standing stocks of donor (X_i) and recipient (X_j) compartments, and the density parameters (Equation 17).

$$fb_{ij} = \left[1 - \frac{X_i - G_{ij}}{A_{ij} - G_{ij}} \right], \quad fb_{ij} = \left[\frac{X_i - A_{ij}}{G_{ij} - A_{ij}} \right] \quad (17)$$

The feedback terms are constrained to range from 0 to 1 (maximum feedback control) and are dimensionless.

The recipient-controlled feedback must be corrected to allow for uptake or consumption of a population at maximum density such that uptake or consumption by the recipient from donor compartment meets metabolic losses. The metabolic correction term (C_{ij}) accounts for respiration (R_{het}), egestion (f_{eg}) and sloppy feeding (f_{sf}) of grazers as in Equation 18, where G_{ZM} is the maximum grazing rate (explained below).

$$C_{ij} = 1 - \frac{R_{het}}{G_{ZM} [1 - (f_{eg} + f_{sf})]} \quad (18)$$

The correction term is incorporated into the total multiplicative feedback terms, TF_{ij} , combining both donor- and recipient-controlled controls as Equation 19, where fb_{ij}' is

prime values of fb_{ij} , and determined as $1-fb_{ij}$. Nomenclatures i and j follow the numbers of state variables shown in Table 2 in the description of energy flow below where “ i ” is the donor and “ j ” is the recipient compartments respectively.

$$TF_{ij} = 1 - [fb_{ij} \cdot (1 - fb_{jj} \cdot C_{ij})] \quad (19)$$

Heterotrophic bacterial production is determined by gross growth, respiration, and grazing (Table 2). Bacterial growth (G_b) was a function of bacterial maximum growth rates (G_{Mb}), bacterial density (X_t) and total multiplicative feedback control (TF_{ij}) on DOC uptake by bacteria:

$$G_b = G_{Mb} \cdot X_t \cdot (1 - TF_{ij}) \quad (20)$$

where G_{Mb} was derived as for phytoplankton growth maximum rate (Equation 12).

Respiration rate (Equation 21) is estimated by a function of basal respiration (br_b , $0.5d^{-1}$), bacterial density, recipient-controlled feedback term (fb_{ij}) and a fraction (40%) of bacterial gross growth, G_b (see Eldridge and Sieracki, 1993).

$$R_b = br_b \cdot X_t \cdot fb_{ij} + 0.4G_b \quad (21)$$

The “assimilation efficiency” of bacteria is assumed to be 100%.

The other heterotrophs represented in the model have a similar structure for controlling factors: advective transport, turbulent mixing, gross growth, grazing by higher-level consumers, respiration, egestion and sloppy feeding. Gross growth, G_{het} (Equation 22) is determined by a function of flux preference (TP_{ij}), maximum grazing

rate (G_{Z_M}), predator compartments (X_j), and total multiplicative feedback (TF_{ij}) on energy flow from prey to grazer or predator.

$$G_{het} = TP_{ij} \cdot G_{Z_M} \cdot X_j (1 - TF_{ij}) \quad (22)$$

G_{Z_M} was determined by cell size of each size class; $63M_{het}^{-0.25}$ and TP_{ij} is a function of feeding preference (P_{ij}), flux preference value (PD_j) and the donor-controlled feedback term (fb_{ij}) as Equation 23.

$$TP_{ij} = P_{ij} \cdot PD_j (1 - fb_{ij}) \quad (23)$$

Feeding preference was considered since each predator has two classes of potential prey (autotrophs vs. heterotrophs) as shown in Fig. 3.

Respiration of grazers (R_{het}) is estimated by a function of basal respiration rate (br_{het} , 0.4 d^{-1}), grazer density (X_j), recipient-controlled feedback of the grazer-predator (fb_{ij}) and fraction (30%) of gross growth (G_{het}) of grazer-predator (Equation 24)

$$R_{het} = br_{het} \cdot X_j \cdot fb_{ij} + 0.3 G_{het} \quad (24)$$

Grazers egest a proportion of ingested matter as faeces as well as respiration; 10 % of ingestion is assumed to be egested as faeces (c.f. Barthel 1983, Miller and Landry 1984).

POC dynamics were determined by inputs from advective transport, turbulent mixing, mortality (senescence) rate of plankton, egestion rate of grazers, rate of sloppy feeding and losses due to leaching rate of POC and uptake by higher-level consumers

(Table 2). Sloppy feeding and grazing loss to zooplankton were defined as calibration parameters.

DOC concentrations were regulated by advective transports, turbulent mixing, exudation of phytoplankton, lysis of POC (leaching) and uptake by bacteria. Leaching rate was determined by calibrations within the range of literature values.

Ambient nutrient concentrations are determined by advective transport, turbulent diffusion and phytoplankton uptake rates and excretion rates of heterotrophs, as shown in Table 2. Uptake rates of nutrients by phytoplankton are calculated by dividing gross growth rates (G) by C:nutrient ratios; $G(C:Nt)^{-1}$. Assuming that phytoplankton prefer ammonium (NH_4^+) as their source of N, the preference (PR) was determined as a function of concentrations of ammonium (NH_4) and nitrite + nitrate (NO_x) concentrations and the half saturation constant (K_N) for nitrogen (Equation 25).

$$PR = [NH_4] \frac{[NO_x]}{(K_N + [NH_4])(K_N + [NO_x])} + \frac{[NH_4] \cdot K_N}{([NH_4] + [NO_x])(K_N + [NO_x])} \quad (25)$$

Excretion rates of heterotrophs are determined by respiration rates (R_{het}) and C:nutrient ratios; $R_{het}(C:Nt)^{-1}$. For the nitrogen pool, it was assumed that heterotrophs only excrete ammonium; however, nitrification of ammonium is a source for nitrite+nitrate, as well as input through turbulent mixing. Nitrification (NIT) was determined by a temperature-dependent mechanism as in Equation 26 (Jaworski et al. 1972), where the *time* is 1 day, k_t is $k_{20}^{(temp - 20)}$, where k_{20} = nitrification rate at 20 °C (0.068 day⁻¹), θ = constant for temperature adjustment of nitrification rate (1.188).

$$NIT = [NH_4^+] \exp(k_t \text{ time}) \quad (26)$$

Denitrification was assumed to be 10 % of nitrite+nitrate concentrations.

Model Validation and Sensitivity Analysis

Field data collected over an annual cycle (Section II) were used as validation data for the three size- structured phytoplankton populations and for nutrients. Bacterial abundance and DOC data collected (Aug. 96 – May 97) by G. Shultz at VIMS were used for model validation. The bacterial data were collected from a site close to the region of this study. In order to convert bacterial abundance to bacterial biomass, a conversion factor of 50 fg C μm^{-3} was used (Fagerbakke et al. 1996). Field data were not available for validation of heterotrophic flagellate + ciliate densities. The data for only heterotrophic flagellate densities collected by Kindler (1991) were used for the validation. EPA monitoring data collected at the station (WE4.2) nearby the mouth of the York River were used for model validation of micro- and meso-zooplankton. Abundances of these heterotrophs were converted to biomass using the conversion factors of 9.3 ng cell⁻¹ for microzooplankton and 9.3 $\mu\text{g cell}^{-1}$ for mesozooplankton (Moloney and Field 1991). POC data (May 1995 to March 1996) collected at the mouth of the York River by Dr. E. Canuel (VIMS) were used as validation data for POC concentrations.

Sensitivity analysis was performed to examine how sensitive model output was to specified changes in parameter values. Hypotheses proposed in the previous sections (Section I and II) were examined in the process of sensitivity analysis for the coefficients related to, or values of, parameters hypothesized to be major controlling factors on phytoplankton dynamics in the York River system after model calibration and validation. Each parameter was changed by $\pm 20\%$ in individual runs. Model sensitivity was estimated as the root mean square deviation (RMS) between the daily values of state variables from nominal model runs (N_k) and the outputs from sensitivity runs (S_k) for 3 year simulations ($n = 1095$ days) and was computed as Equation 27.

$$RMS = \sqrt{\frac{1}{n} \sum_{k=1}^n (N_k - S_k)^2} \quad (27)$$

In order to determine the effects of parameter variation, the percent change in outputs was calculated based on comparison between RMS and the means of each state variable for the nominal runs.

RESULTS

Model Validation

1. Forcing Variables

Comparison of model predictions and field data for the principal forcing variables show generally good agreement although variation in mean daily irradiance was

especially prominent and not captured by the model (Fig. 4). Field data for mean daily irradiance and surface temperature were collected at VIMS, Gloucester Point, VA. Salinity difference between surface and bottom waters was calculated from EPA monitoring data (station WE4.2) collected from June 1994 to October 1994. The equation for salinity difference used in this model was previously verified based on field data (June–September, 1985) by Eldridge and Sieracki (1993).

2. State Variables

The plankton ecosystem model was simulated for 3 years and model predictions of state variable concentrations for the third year were used for validation. The simulated state variables for nominal model runs were compared to field measurements. Good agreement was generally shown in terms of range and temporal distributions (Fig. 5 and 6) Model output for total chlorophyll generally followed field data except for peaks during February and March (Fig. 5A). Simulated microphytoplankton densities matched very closely field observations (Fig. 5B). For nanophytoplankton, simulation output was similar to that of field concentrations except for the peak during January and February (Fig. 5C). Simulated picophytoplankton concentrations generally followed the pattern of field measurement (Fig. 5D).

Modeled heterotrophic bacterial biomass in a unit volume (m^3) was close to that of measured bacterial biomass (Fig. 5E). Minimum concentrations during winter predicted by the model corresponded to field observations. It is difficult to validate simulated heterotrophic flagellate + ciliate biomass since few data for the protozoan biomass were available for the York River. However, the range of predicted protozoan

Fig. 4. Comparison of predicted values by the model to field data for surface daily PAR (A) and temperature (B) collected at VIMS, Gloucester Point, Virginia from August 1996 to July 1997. Salinity difference between surface and bottom waters was calculated from EPA monitoring data (Station WE4.2) collected from June 1994 to October 1994.

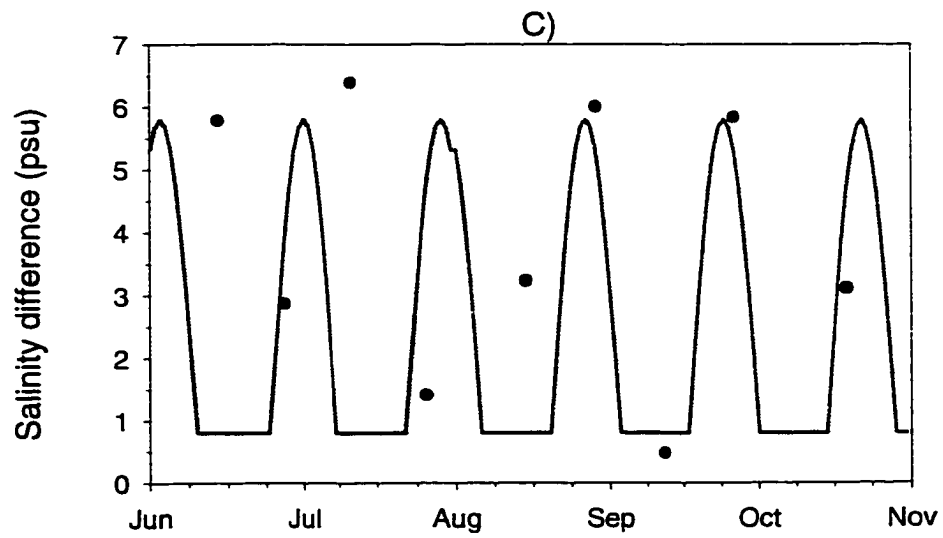
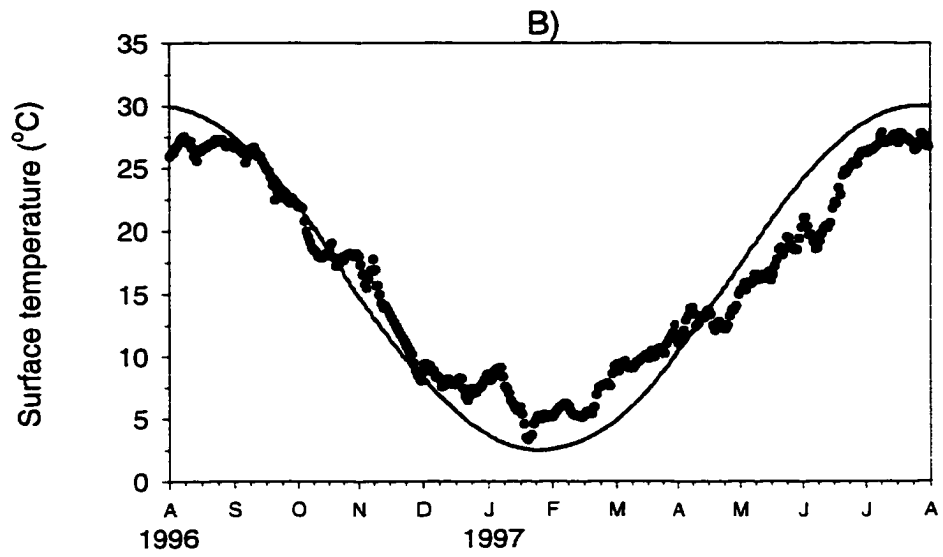
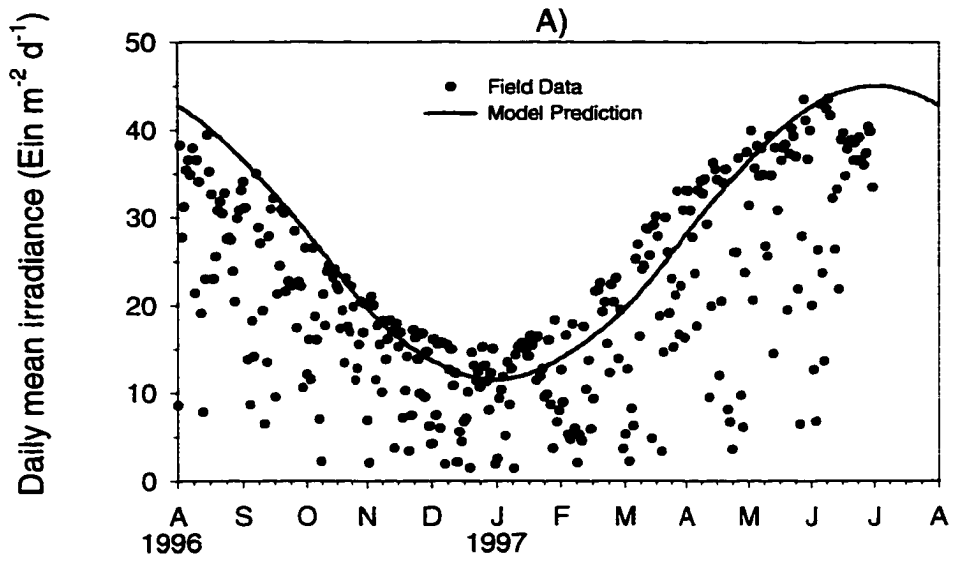


Fig. 5. Validation results for size fractionated chlorophyll *a* (total, micro, nano and pico) and heterotrophic bacteria, heterotrophic flagellate + ciliate in the mesohaline zone of the York River estuarine system. Field chlorophyll *a* data were collected from August 1996 to June 1997. Heterotrophic bacteria data were collected by Gary Schultz (VIMS) and flagellate biomass (Kindler, 1991) alone is shown in Fig. 5F. EPA monitoring data were used for micro- and meso-zooplankton biomass.

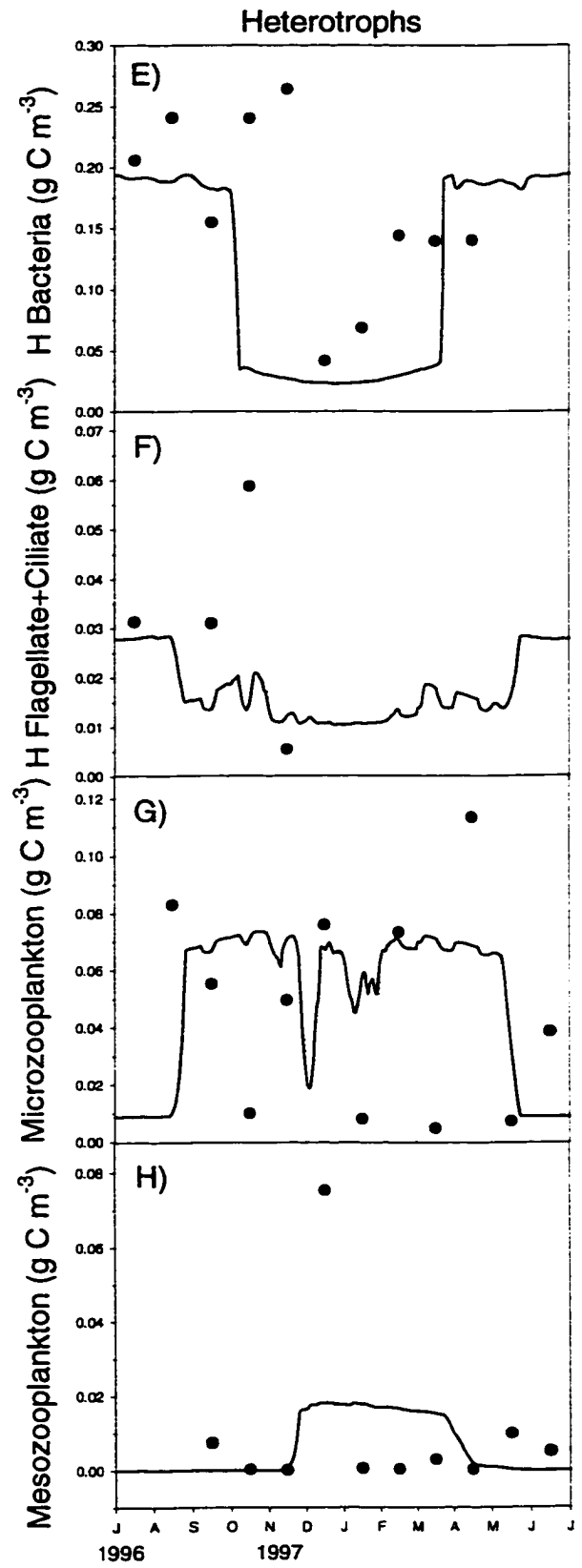
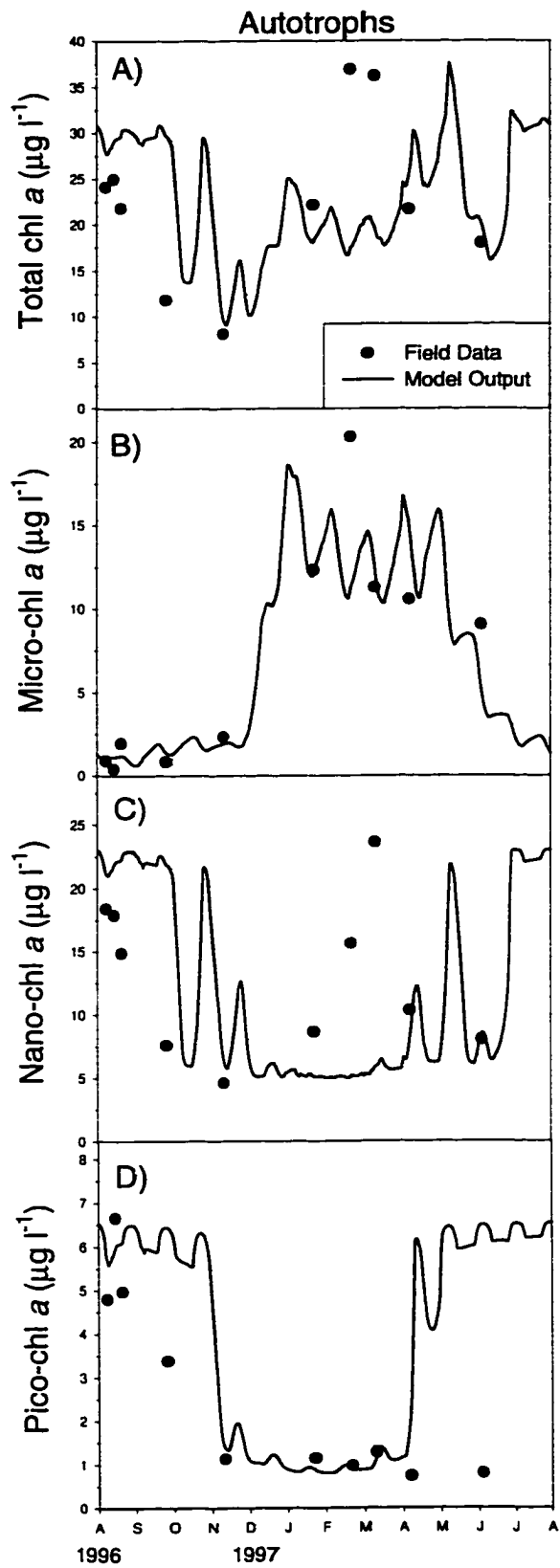
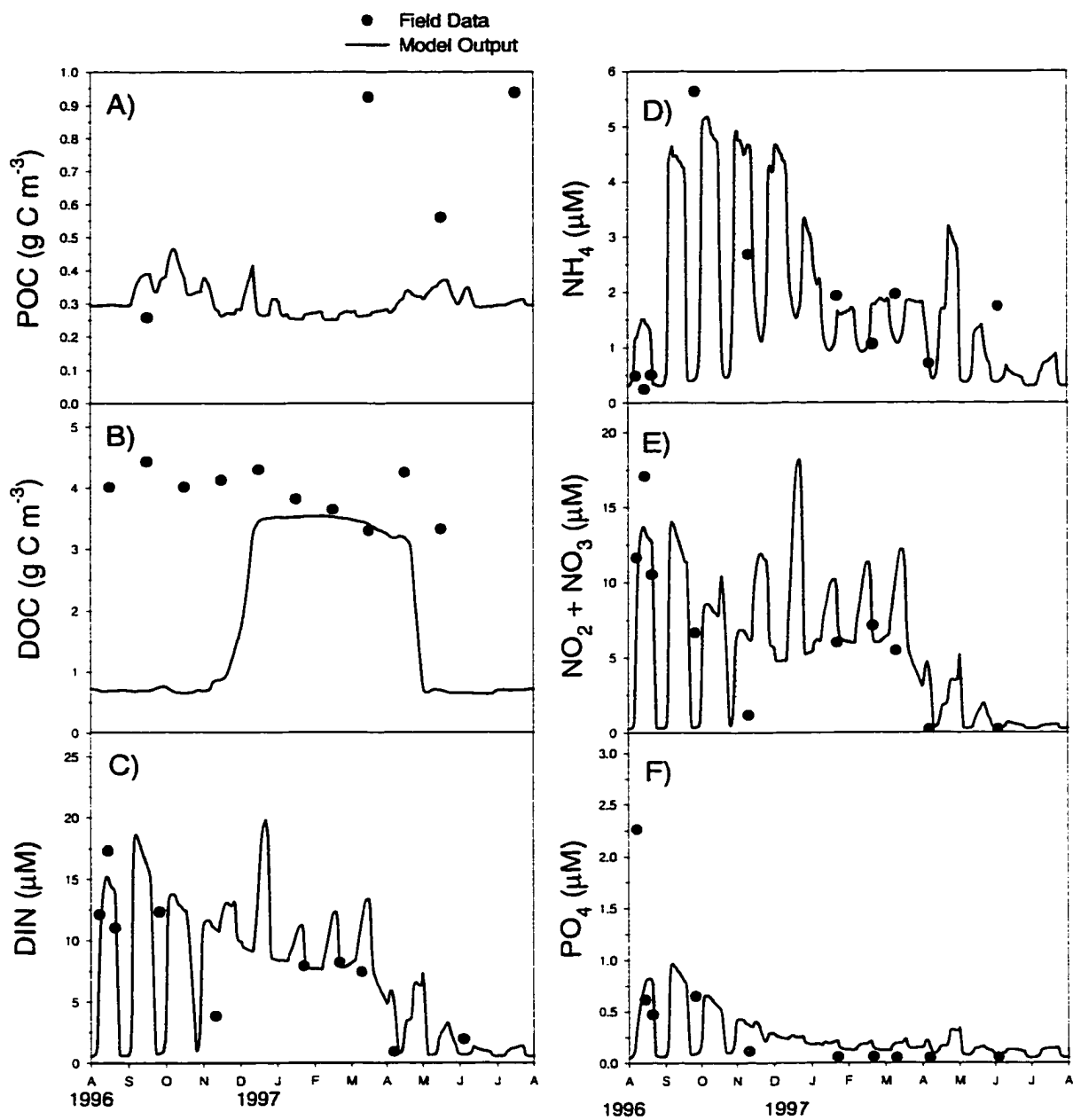


Fig. 6. Validation results for particulate organic carbon (POC), dissolved organic carbon (DOC) and nutrients (dissolved inorganic nitrogen, ammonium, nitrite+nitrate and orthophosphate) in the mesohaline zone of the York River estuarine system. POC was collected from May 1995 to March 1996 by Elizabeth Canuel and DOC collected by Gary Schultz (VIMS). Field nutrient data were also used (Sin et al. 1998).



biomass (Fig. 5F) was within that of heterotrophic flagellate biomass alone measured by Kindler (1991) although there is a possibility that the model underestimated the protozoan biomass. Simulated concentrations of microzooplankton were distributed within the range of measured concentrations which fluctuated greatly over the annual cycle (Fig. 5G). The ecosystem model did not simulate the peak of mesozooplankton concentrations during December but the range was similar to field concentrations (Fig. 5H).

As for protozoan biomass, it was difficult to validate POC concentrations since few data were available for comparison but it appears that the model underestimates York River concentrations based on several field data points (Fig. 6A). Measured DOC concentration did not vary greatly over an annual cycle whereas simulated DOC concentrations revealed a seasonal pattern; low concentrations during the warm season and high during the cold season (Fig. 6B). Modeled dissolved inorganic nitrogen (DIN), ammonium, and nitrate + nitrite concentrations showed good agreement with field data (Fig. 6C, 6D, 6E). The pattern of the simulated orthophosphate concentrations generally followed measured concentrations except the observed August 1996 peak (Fig. 6F). In general, model results for nutrients fluctuated greatly with a frequency less than a month which was not captured in field data.

Model Sensitivity Analysis

1. Model Sensitivity: parameter variation

To investigate potential mechanisms determining plankton dynamics in the model, a parameter was considered as 'sensitive parameter' related to controlling factors

for a state variable if a 20 % change in the parameter produced ≥ 10 % change in 3 years average concentration of the state variable relative to the nominal run.

Tables 4 and 5 present RMS of sensitivity runs for ± 20 % change in selected parameters and the % change of average state variable. Most state variables generally were not sensitive to this range in parameter values except for mesozooplankton, $X(7)$.

Picophytoplankton, $X(1)$ was marginally sensitive to changes in certain parameter values demonstrating a range of 3 to 5 % change in average concentrations relative to the nominal model run (Table 4). Nanophytoplankton, $X(2)$ were generally insensitive to changes in parameters related to metabolic processes although they appeared sensitive to a change in cell size, $xM(2)$; % change ≈ 10 %. In contrast to small cells, large cells (microphytoplankton, $X(3)$) were sensitive to change in cell size, $xM(3)$ and bed shear velocity (*shrvel*) exhibiting 14 and 12 % change in average concentration respectively.

Heterotrophic bacteria, $X(4)$ and protozoa (flagellate+ciliate, $X(5)$) were insensitive to changes in parameters (Table 4) having changes less than 2 %. Microzooplankton, $X(6)$ responded to change in bed shear velocity (*shrvel*) as microphytoplankton did. Changes in mortality, sloppy feeding and egestion rates showed % changes close to 10 % whereas change in cell size, *hetM(3)* resulted in a minor change in concentration. Unlike other heterotrophs, mesozooplankton were highly sensitive to each parameter tested. They showed high sensitivity (≥ 20 %) to loss terms such as mortality (*rm(7)*), sloppy feeding (*fsf(3)*), egestion (*eg(3)*), and loss to higher consumers (*Z2M*). Change in cell size also produced changes close to 20 %.

POC was sensitive to changes in the loss term, leaching rate (*rl*) but not to changes in the loss rate (*rla*) by grazing or to bed shear velocity (Table 5). DOC was

Table 4. The results of sensitivity analyses ($\pm 20\%$ change in parameter values) for biological components in the York River ecosystem model. Symbols for state variables and parameters are also given in Appendix I; % changes $\geq 10\%$ marked by *.

State Variable	Parameter	-20 %	+20 %	Average RMS	% Change
<i>X(1):</i>	<i>xlo(1): optimum light (I_n)</i>	0.21	0.13	0.17	4.4
<i>Picophytoplankton</i>	<i>xM(1): cell mass (M)</i>	0.14	0.15	0.15	3.7
	<i>rm(1): mortality rate (r_m)</i>	0.18	0.24	0.21	5.3
	<i>rex(1): exudation rate (r_{ex})</i>	0.18	0.24	0.21	5.3
	<i>p_{ij}(1): grazer preference (p_{ij})</i>	0.11	0.13	0.12	3.1
	<i>shrvel: bed shear velocity (u_*)</i>	0.12	0.13	0.13	3.2
<i>X(2):</i>	<i>xlo(2): optimum light (I_n)</i>	0.13	0.15	0.14	1.2
<i>Nanophytoplankton</i>	<i>xM(2): cell mass (M)</i>	1.26	0.86	1.06	9.0
	<i>rm(2): mortality rate (r_m)</i>	0.04	0.06	0.05	0.5
	<i>rex(2): exudation rate (r_{ex})</i>	0.06	0.08	0.07	0.6
	<i>p_{ij}(2): grazer preference (p_{ij})</i>	0.35	0.23	0.29	2.5
	<i>shrvel: bed shear velocity (u_*)</i>	0.43	0.07	0.25	2.1
<i>X(3):</i>	<i>xlo(3): optimum light (I_n)</i>	0.11	0.08	0.09	1.3
<i>Microphytoplankton</i>	<i>xM(3): cell mass (M)</i>	1.96	0.08	1.02	14.5*
	<i>rm(3): mortality rate (r_m)</i>	0.45	0.41	0.43	6.1
	<i>rex(3): exudation rate (r_{ex})</i>	0.45	0.41	0.43	6.1
	<i>p_{ij}(3): grazer preference (p_{ij})</i>	0.15	0.15	0.15	2.1
	<i>shrvel: bed shear velocity (u_*)</i>	1.71	0.02	0.86	12.3*
<i>X(4):</i>	<i>hetM(1): cell mass (M)</i>	0.003	0.004	0.003	2.7
<i>Bacteria</i>	<i>rm(4): mortality rate (r_m)</i>	0.0002	0.0002	0.0002	0.2
<i>X(5):</i>	<i>hetM(2): cell mass (M)</i>	0.0004	0.0003	0.0003	1.9
<i>Flagellate+Ciliate</i>	<i>rm(5): mortality rate (r_m)</i>	0.0001	0.0001	0.0001	0.32
	<i>fsf(1): fraction of sloppy feeding (f_{sf})</i>	0.002	0.0002	0.0002	1.1
	<i>feg(1): fraction of egestion (f_{ex})</i>	0.002	0.0002	0.0002	1.1
<i>X(6):</i>	<i>hetM(3): cell mass (M)</i>	0.0008	0.0008	0.0008	1.6
<i>Microzooplankton</i>	<i>rm(6): mortality rate (r_m)</i>	0.003	0.006	0.004	8.7
	<i>fsf(2): fraction of sloppy feeding (f_{sf})</i>	0.004	0.006	0.005	9.8
	<i>feg(2): fraction of egestion (f_{ex})</i>	0.004	0.006	0.005	9.8
	<i>shrvel: bed shear velocity (u_*)</i>	0.017	0.0001	0.008	16.9*
<i>X(7):</i>	<i>hetM(4): cell mass (M)</i>	0.001	0.001	0.001	17.2*
<i>Mesozooplankton</i>	<i>rm(7): mortality rate (r_m)</i>	0.002	0.002	0.002	28.1*
	<i>fsf(3): fraction of sloppy feeding (f_{sf})</i>	0.002	0.002	0.002	29.8*
	<i>feg(3): fraction of egestion (f_{ex})</i>	0.002	0.002	0.002	29.8*
	<i>Z2M: grazing by fish (Z2M)</i>	0.001	0.001	0.001	20.5*

Table 5. The results of sensitivity analyses ($\pm 20\%$ change of parameter values) for chemical components (POC, DOC and nutrients) in the York River ecosystem model. Symbols for state variables and parameters are also given in Appendix I; % changes $\geq 10\%$ marked by *.

State Variable	Parameter	-20 %	+20 %	Average RMS	% Change
<i>X(8): POC</i>	<i>rl: leaching rate (rl)</i>	0.029	0.050	0.039	12.8*
	<i>Rlo: grazing loss rate (rlo)</i>	0.017	0.022	0.019	6.3
	<i>shrvel: bed shear velocity (u_*)</i>	0.005	0.002	0.003	1.0
<i>X(9): DOC</i>	<i>rl: leaching rate (rl)</i>	0.084	0.064	0.074	4.0
	<i>shrvel: bed shear velocity (u_*)</i>	0.024	0.04	0.32	1.8
<i>X(10): NH₄</i>	<i>hCNrat: C:N ratio (C:N)</i>	0.002	0.004	0.003	12.8*
	<i>shrvel: bed shear velocity (u_*)</i>	0.053	0.031	0.042	2.4
<i>X(11): NO₂+NO₃</i>	<i>rdenit: denitrification</i>	0.006	0.007	0.007	8.7
	<i>shrvel: bed shear velocity (u_*)</i>	0.121	0.062	0.092	1.7
<i>X(12): PO₄</i>	<i>cprat: C:P ratio (C:P)</i>	0.0007	0.0009	0.0008	10.5*
	<i>shrvel: bed shear velocity (u_*)</i>	0.007	0.004	0.006	2.3

marginally sensitive to changes in leaching rate and bed shear velocity. Ammonium, $X(10)$ was sensitive to the change in C:N ratio for heterotrophs. Nitrite+nitrate was not sensitive to denitrification rate or to bed shear velocity. Orthophosphate concentration was sensitive to change in the C:P ratio but it was not sensitive to bed shear velocity.

2. Model Sensitivity: forcing variables

Average RMS and % change in the concentrations of the state variables are presented in Table 6 given $\pm 10 \text{ Ein m}^{-2} \text{ d}^{-1}$ change in incident radiation, $\pm 2 \text{ }^\circ\text{C}$ temperature change, and $\pm 20 \%$ changes in the light attenuation coefficient and top to bottom salinity difference. Picophytoplankton, $X(1)$, microzooplankton, $X(6)$, nitrite+nitrate, $X(11)$ and orthophosphate concentrations were sensitive to changes in incident daily irradiance. All state variables except microphytoplankton and POC were sensitive to changes in temperature and light+temperature. Small phytoplankton ($X(1)$ and $X(2)$), microzooplankton and nutrients ($X(6)$, $X(10)$, $X(11)$, $X(12)$) were sensitive to changes in k_d (light attenuation coefficient). Nano- and micro-phytoplankton, mesozooplankton, POC and nutrients were sensitive to changes in top to bottom salinity difference (Table 6).

Figure 7 shows sensitivity results for pico-, nano- and micro-phytoplankton given $\pm 10 \text{ Ein m}^{-2} \text{ d}^{-1}$ and $2 \text{ }^\circ\text{C}$ change in incident radiation and temperature respectively. Increase (or decrease) in daily irradiance increased (or decreased) pico- and nano-chlorophyll a concentrations whereas an increase of light level did not affect micro-chlorophyll a concentrations. Effects of change in top to bottom salinity difference on phytoplankton are presented in Fig. 8. Change in salinity difference did not affect pico-

Table 6. Average RMS and % change in concentrations of state variables when forcing functions (incident radiation, temperature and salinity) and light attenuation coefficient (k_d) were changed. These sensitivity analyses were performed given a $\pm 10 \text{ Ein m}^{-2} \text{ d}^{-1}$ change in incident radiation and $\pm 2 \text{ }^\circ\text{C}$ temperature change, and $\pm 20\%$ changes in light attenuation coefficient and top to bottom salinity difference; % changes $\geq 10\%$ marked by *

State Variable	Forcing Variable: Incident Radiation		Temperature		Light & Temperature		k_d		Salinity Difference	
	RMS	%	RMS	%	RMS	%	RMS	%	RMS	%
<i>X(1): PP</i>	0.62	15.8*	0.42	10.7*	1.05	26.8*	0.42	10.6*	0.26	6.6
<i>X(2): NP</i>	0.62	5.2	2.86	24.2*	2.97	25.2*	2.84	24.0*	2.56	21.6*
<i>X(3): MP</i>	0.37	5.2	0.51	7.3	0.67	9.6	0.58	8.3	2.47	35.1*
<i>X(4): HB</i>	0.003	2.6	0.025	21.9*	0.030	25.6*	0.009	8.1	0.009	7.8
<i>X(5): HFC</i>	0.001	5.9	0.003	17.5*	0.003	18.5*	0.001	5.7	0.0009	5.1
<i>X(6): Z1</i>	0.012	23.3*	0.019	38.9*	0.020	41.4*	0.005	10.5*	0.004	8.1
<i>X(7): Z2</i>	0.0002	3.8	0.004	62.2*	0.004	61.8*	0.000	1.2	0.0007	10.8*
<i>X(8): POC</i>	0.009	3.0	0.018	5.7	0.024	7.7	0.019	6.2	0.045	14.6*
<i>X(9): DOC</i>	0.08	4.3	0.30	16.3*	0.33	17.8*	0.14	7.5	0.099	5.4
<i>X(10): NI</i>	0.11	6.0	0.31	17.5*	0.36	20.3*	0.20	11.4*	0.35	19.8*
<i>X(11): N2</i>	0.58	10.8*	0.85	15.7*	1.40	25.7*	0.91	16.7*	1.12	20.6*
<i>X(12): P</i>	0.03	12.7*	0.050	20.7*	0.068	27.9*	0.049	20.3*	0.056	22.9*

Fig. 7. Sensitivity results for pico-, nano-, and micro-chlorophyll *a* (mg m^{-3}). The effects of change in light and temperature were examined given $10 \text{ Ein m}^{-2} \text{ d}^{-1}$ increase and decrease in incident radiation and $2 \text{ }^\circ\text{C}$ increase and decrease in temperature.

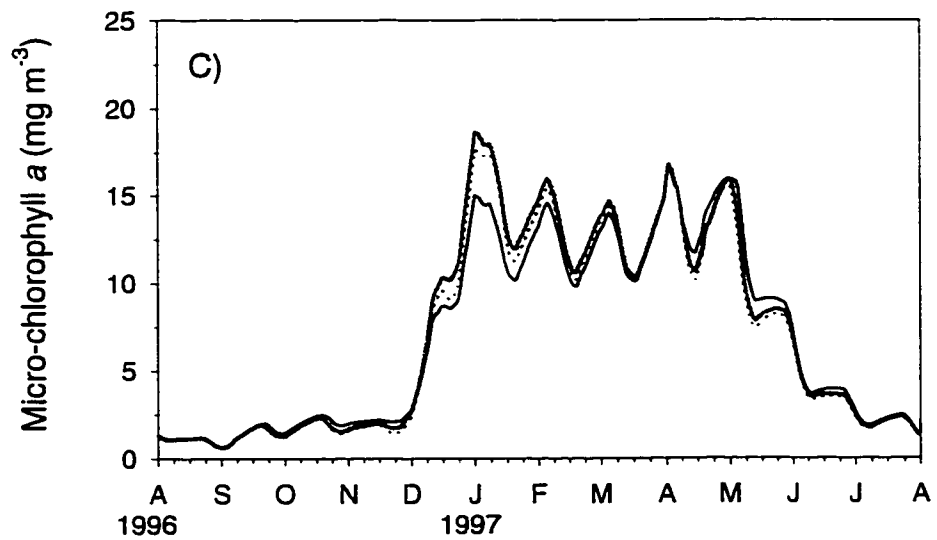
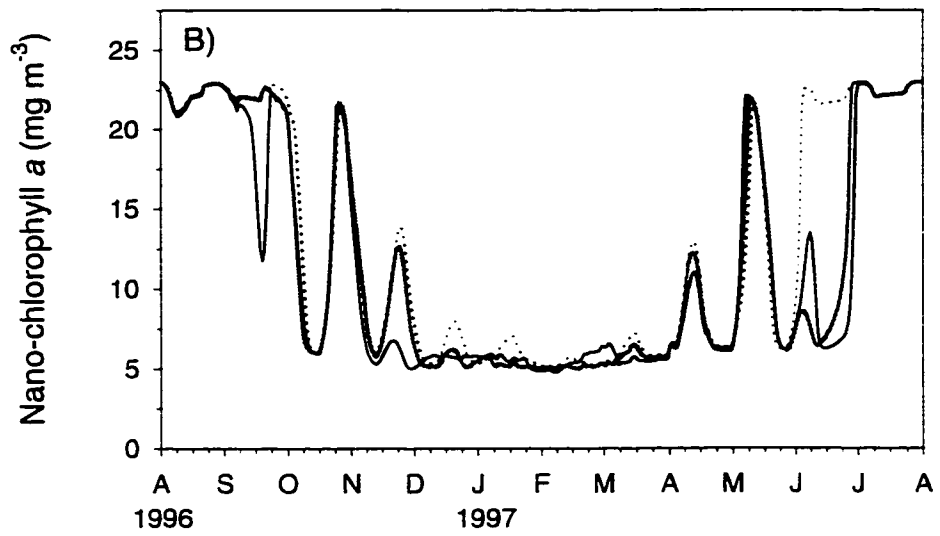
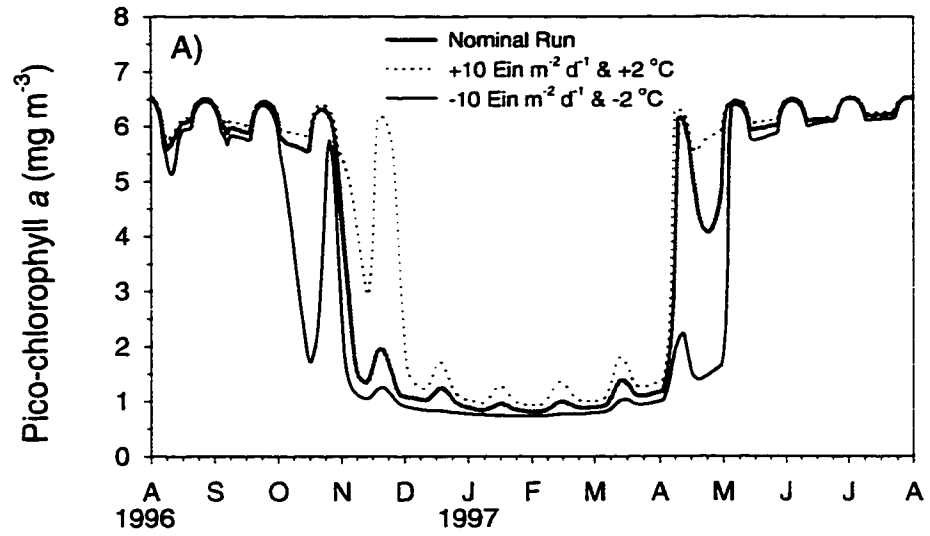
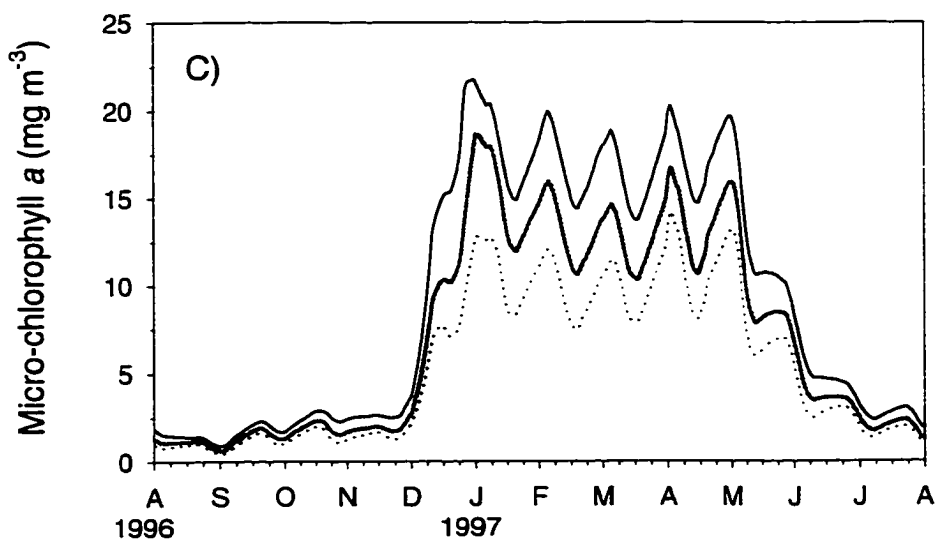
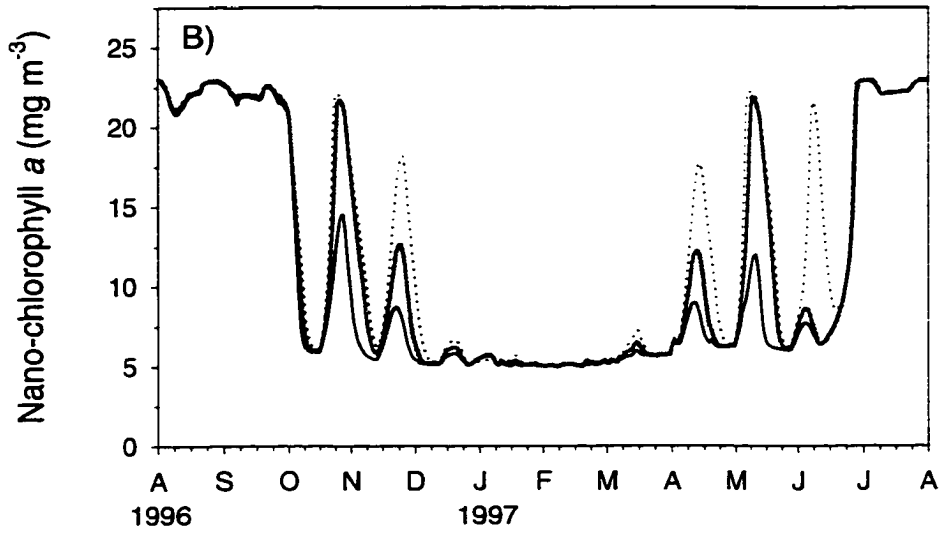
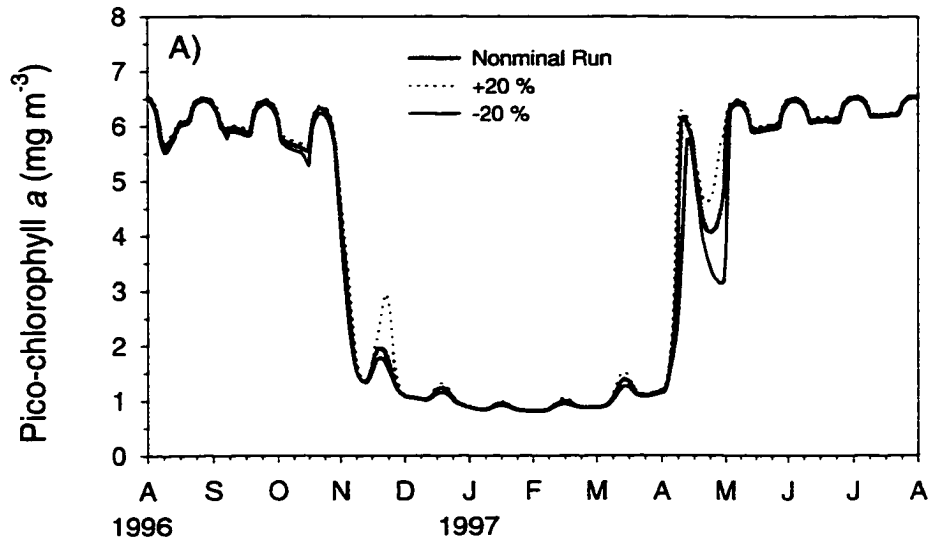


Fig. 8. Sensitivity results for pico-, nano-, and micro-chlorophyll *a* (mg m^{-3}). The effects of change in top to bottom salinity difference were examined given 20 % increase and decrease in top to bottom salinity difference.



phytoplankton concentrations but it affected nano- and microphytoplankton concentrations. A 20 % increase in salinity difference increased nanophytoplankton concentrations whereas increase in salinity difference decreased microphytoplankton concentrations. Responses of nutrients to change in the salinity difference are presented in Fig. 9. Ammonium and orthophosphate responded negatively to change in the salinity difference especially during summer (Fig. 9A, 9B) whereas nitrite + nitrate responded positively to the change especially during winter-spring (Fig. 9C).

3. Model Sensitivity: physical processes

Effects of a change ($\pm 20\%$) in the mixed layer depth and removal of physical processes including diffusion, vertical advection and diffusion-advection are given in Table 7. Nano-, micro-phytoplankton, micro-, meso-zooplankton, nitrite+nitrate, and orthophosphate were sensitive to change in the mixed layer depth as they were sensitive to change in diffusion when diffusion processes were removed from the model. Removal of vertical advection affected all state variable concentrations. Overflows in heterotrophic compartments prevented the model from running when the horizontal advection term was removed from the model. All state variable concentrations except pico-phytoplankton and heterotrophic bacteria were changed when the physical processes of diffusion and advection were removed from the model.

Figure 10 shows the model outputs for phytoplankton when the physical processes of advection and diffusion were removed from the model. Concentrations of picophytoplankton did not change greatly but nanophytoplankton concentrations were slightly increased. Winter-spring blooms of microphytoplankton completely disappeared

Fig. 9. Sensitivity results for ammonium, nitrite+nitrate and orthophosphate (μM). The effects of change in top to bottom salinity difference were examined by comparing nutrient concentrations between a nominal run and sensitivity runs given 20 % increase and decrease in top to bottom salinity difference.

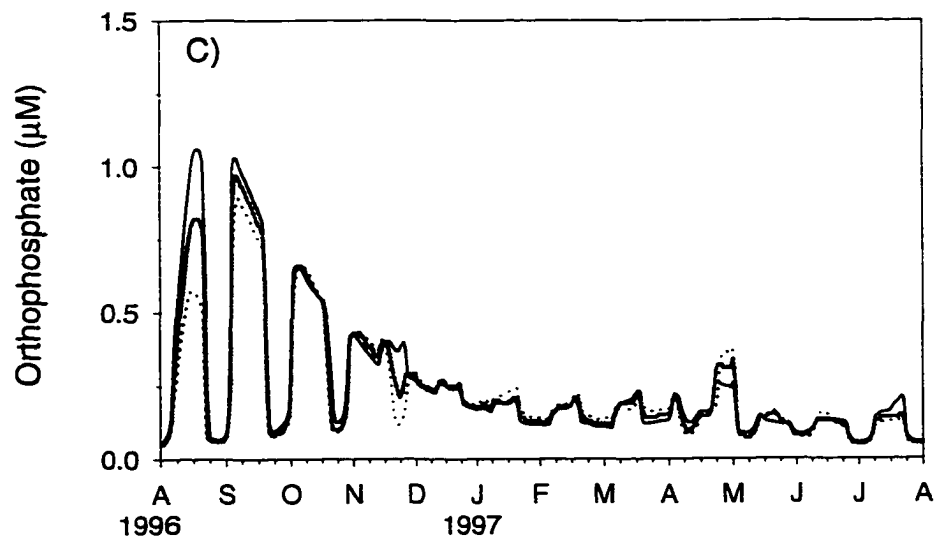
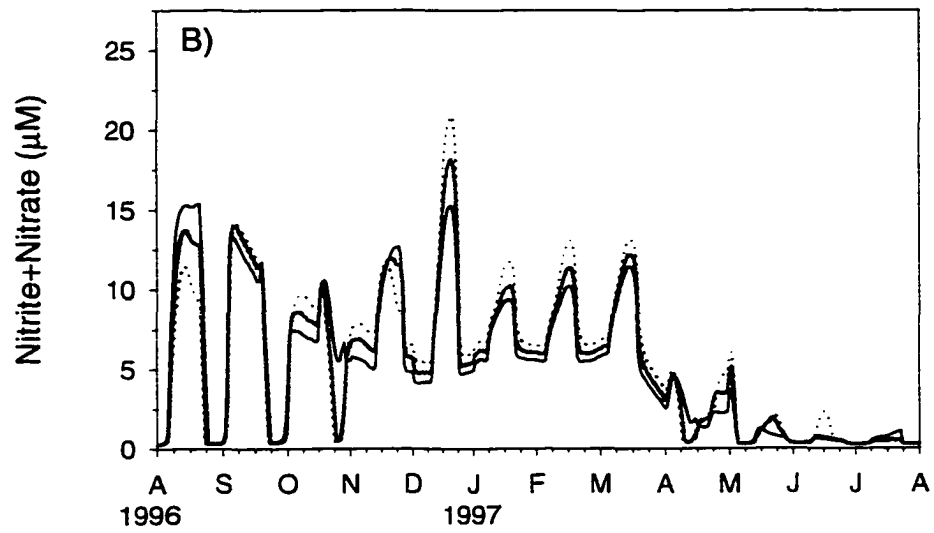
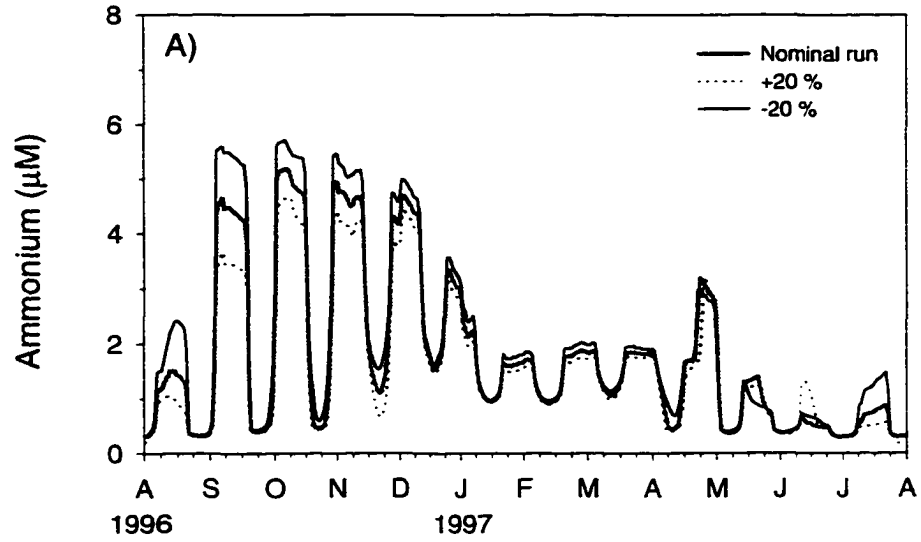
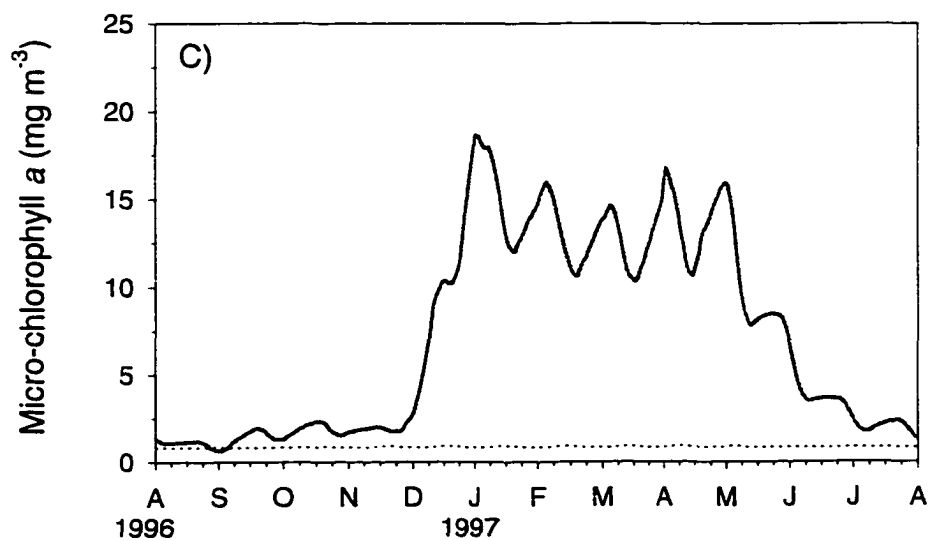
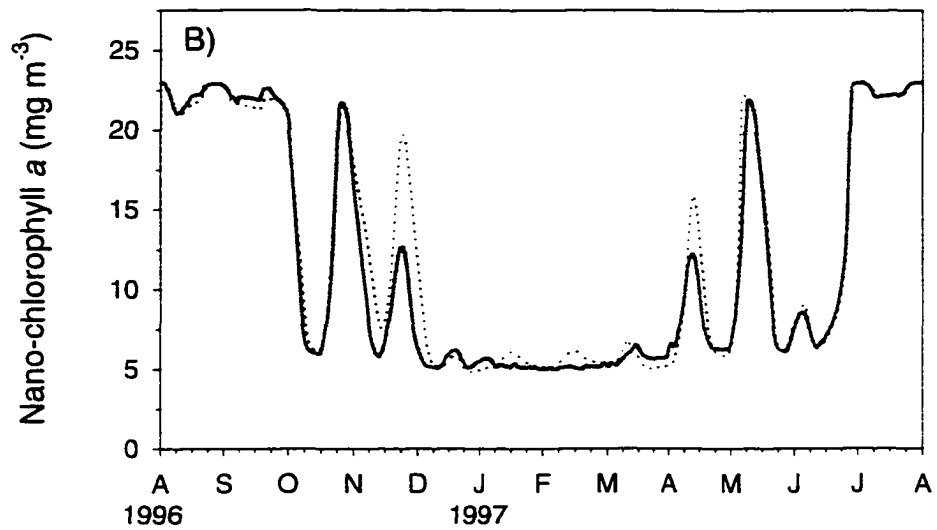
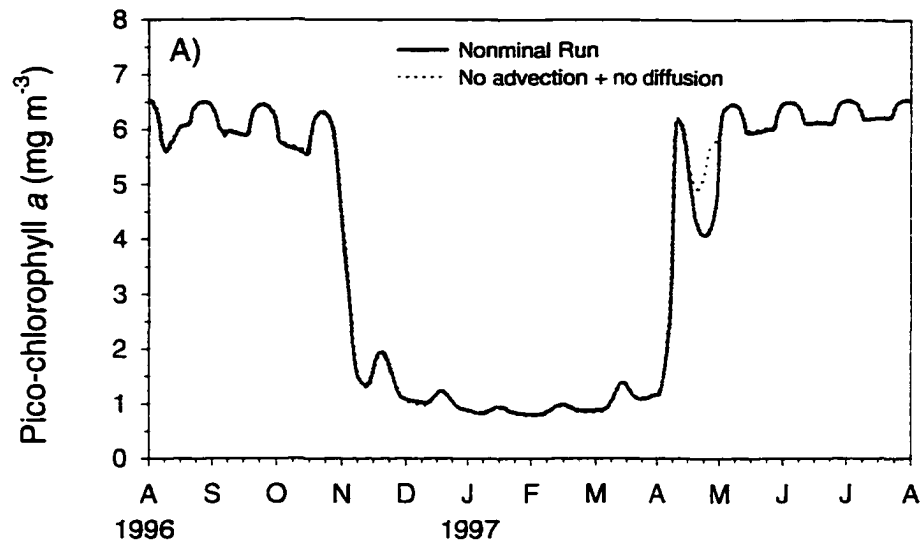


Table 7. Average RMS and % change in concentrations of state variables when the mixed layer depth, z_1 was changed ($\pm 20\%$) and physical processes were removed from the model; no diffusion, no vertical advection and no diffusion and advection; % changes $\geq 10\%$ for mixed layer depth and $\geq 100\%$ for others marked by *.

Physical Process: State Variable	<u>Mixed Layer Depth</u>		<u>Diffusion</u>		<u>Vertical Advection</u>		<u>Diffusion-Advection</u>	
	RMS	%	RMS	%	RMS	%	RMS	%
<i>X(1): PP</i>	0.39	9.9	0.22	5.5	3.32	84.5	0.18	4.5
<i>X(2): NP</i>	2.82	23.8*	1.18	10.0	10.5	89.1	1.51	12.8
<i>X(3): MP</i>	0.90	12.8*	8.15	115.9*	8.39	119.3*	8.31	118.1*
<i>X(4): HB</i>	0.010	8.4	0.009	8.0	0.14	118.8*	0.005	4.7
<i>X(5): HFC</i>	0.001	5.6	0.002	9.3	0.016	91.2	0.002	11.2
<i>X(6): Z1</i>	0.007	14.6*	0.025	49.9	0.055	112.5*	0.023	46.0
<i>X(7): Z2</i>	0.001	15.3*	0.003	38.0	0.010	155.2*	0.004	53.8
<i>X(8): POC</i>	0.030	9.8	0.015	4.9	0.28	89.1	0.049	15.7
<i>X(9): DOC</i>	0.16	8.9	0.096	5.3	2.18	119.1*	0.36	19.8
<i>X(10): NI</i>	0.17	9.8	0.17	9.9	2.16	123.1*	1.54	87.6
<i>X(11): N2</i>	0.66	12.1*	0.64	11.8	6.55	120.8*	5.24	96.6
<i>X(12): P</i>	0.042	17.3*	0.03	12.8	0.30	124.5*	1.22	502.8*

Fig. 10. Sensitivity results for pico-, nano-, and micro-chlorophyll a (mg m^{-3}). The effects of advection + vertical diffusion were examined by comparing chlorophyll a concentrations between a nominal and sensitivity run when no advection + vertical diffusion were incorporated.



when advection and diffusion mechanisms were removed from the model. Effects of the physical processes on nutrients are illustrated in Fig. 11. Oscillations of nutrients in the nominal model run observed during the warm season in 1996 disappeared and 1996's summer peaks of the nutrients also disappeared. Relatively high concentrations of orthophosphate were observed during winter-spring (Fig. 11C).

In order to investigate the role of diffusion as a factor influencing phytoplankton and nutrient dynamics, we examined the relationship between vertical eddy diffusivity (D) and chlorophyll a and nutrient concentrations (Fig. 12, Fig. 13). Biomass of small cells was related negatively to the coefficients at the scale of neap-spring tidal cycle (Fig. 12A, 12B) whereas biomass of large cells was slightly positively related to the coefficients (Fig. 12C). Ammonium showed apparently positive relationship with vertical eddy diffusivity throughout the annual cycle (Fig. 13A). Nitrite + nitrate and orthophosphate showed a positive relationship with the eddy diffusivity during the warm season whereas they were negatively related during the cold season (Fig. 13B, 13C). This result suggests vertical diffusion plays an important role in the nutrient dynamics of surface water.

The distributions of horizontal incoming and vertical upward flows were compared with those of chlorophyll a to investigate effects of advection on phytoplankton densities (Fig. 14). In general, stocks of small cells are negatively related to the flows (Fig. 14A, 14B) whereas those of large cells are slightly positive related to the flows (Fig. 14C).

4. Model Sensitivity: boundary conditions

Fig. 11. Sensitivity results for ammonium, nitrite+nitrate and orthophosphate (μM). The effects of advection + vertical diffusion were examined by comparing nutrient concentrations between a nominal and sensitivity run when advection + vertical diffusion were removed from the ecosystem model.

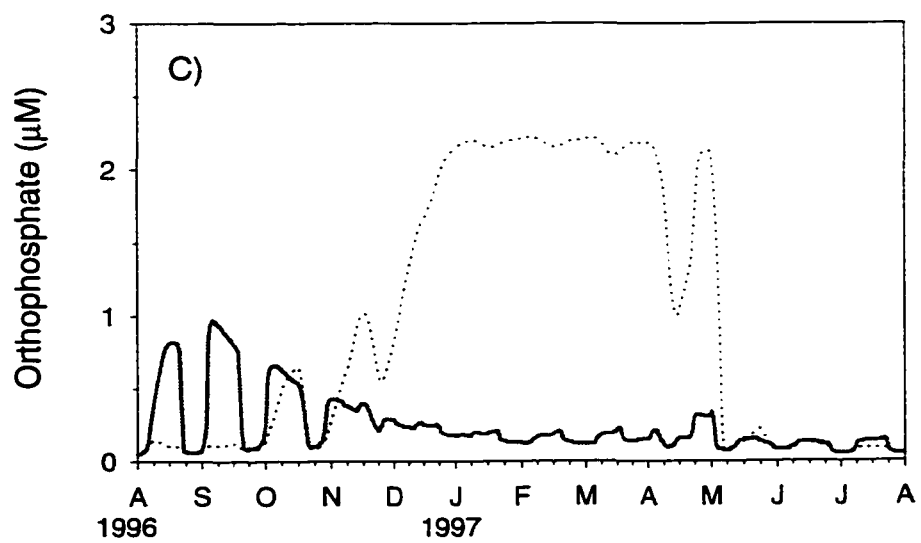
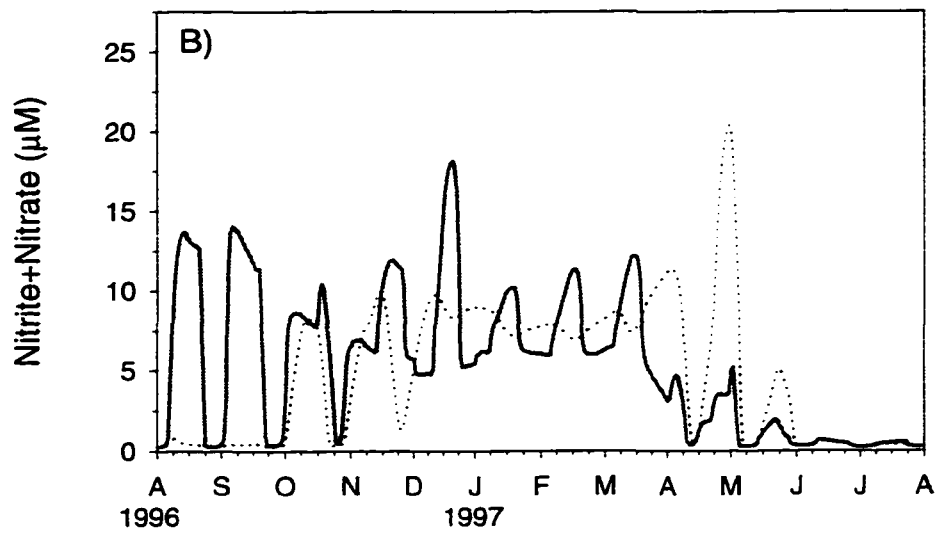
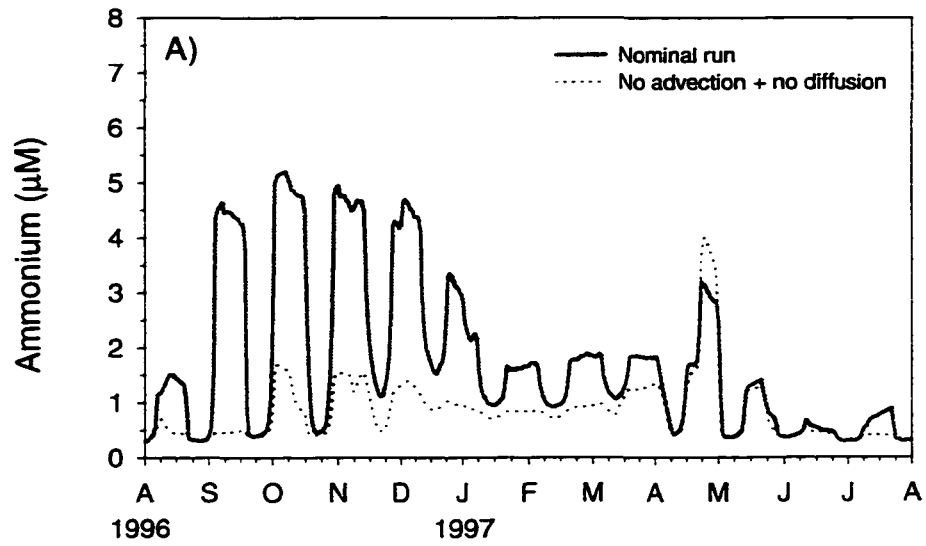


Fig. 12. The distributions of diffusion coefficient and chlorophyll *a* (pico-, nano-, and micro-sized) from the nominal model run of the ecosystem model.

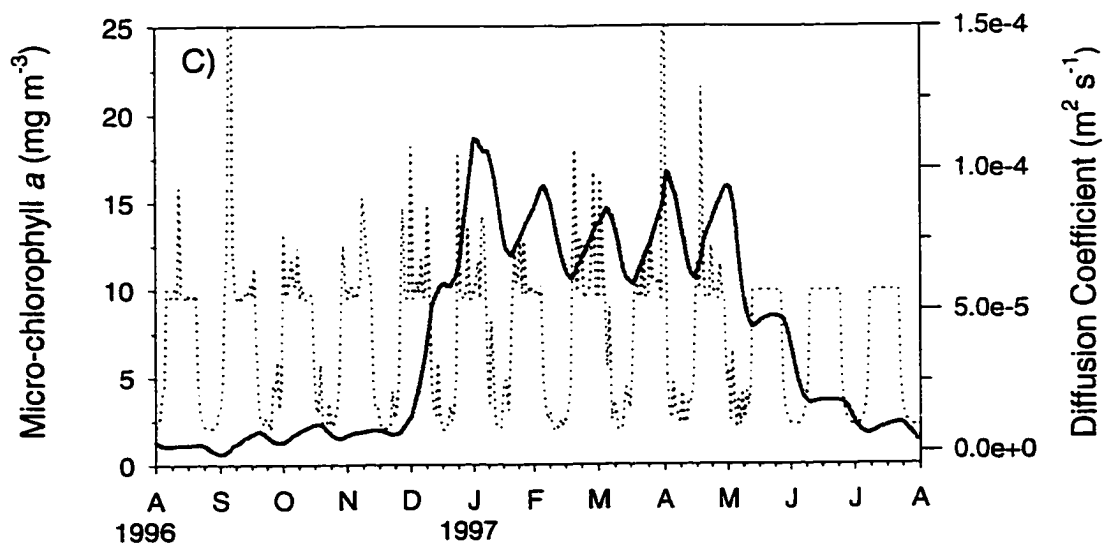
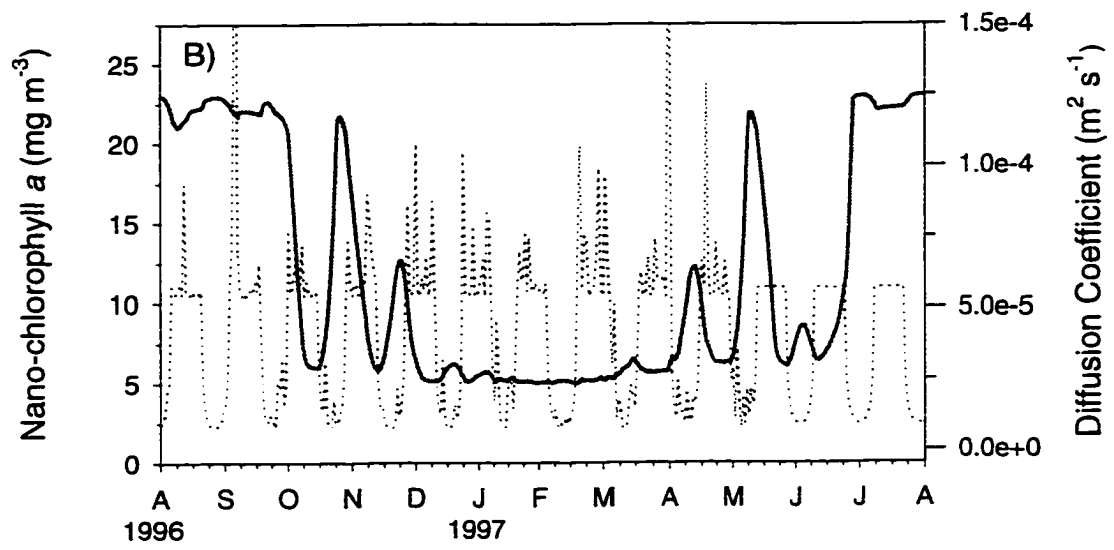
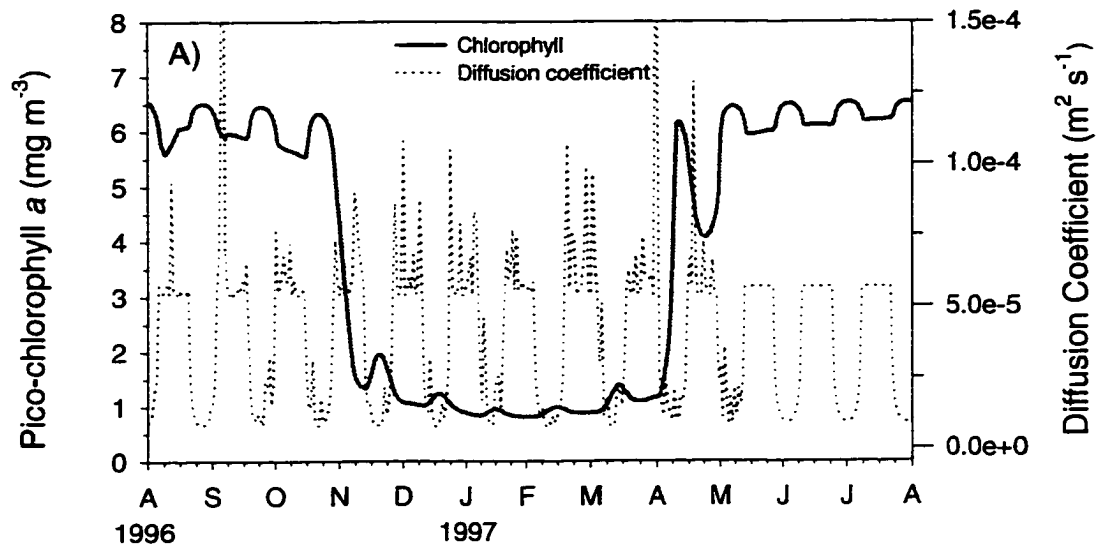


Fig. 13. The distributions of diffusion coefficient and nutrients (ammonium, nitrite + nitrate, and orthophosphate) from the nominal model run of the ecosystem model.

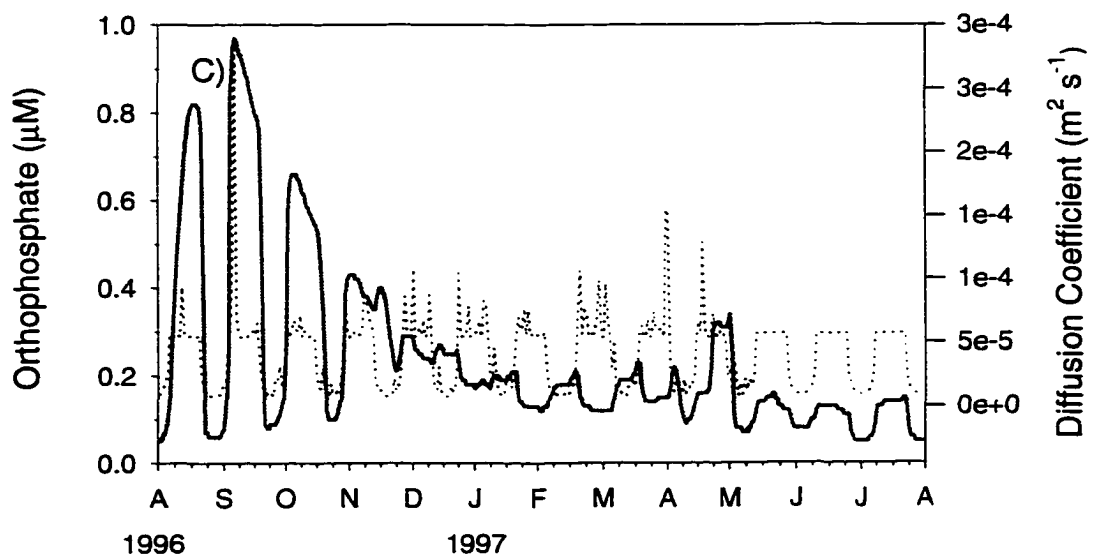
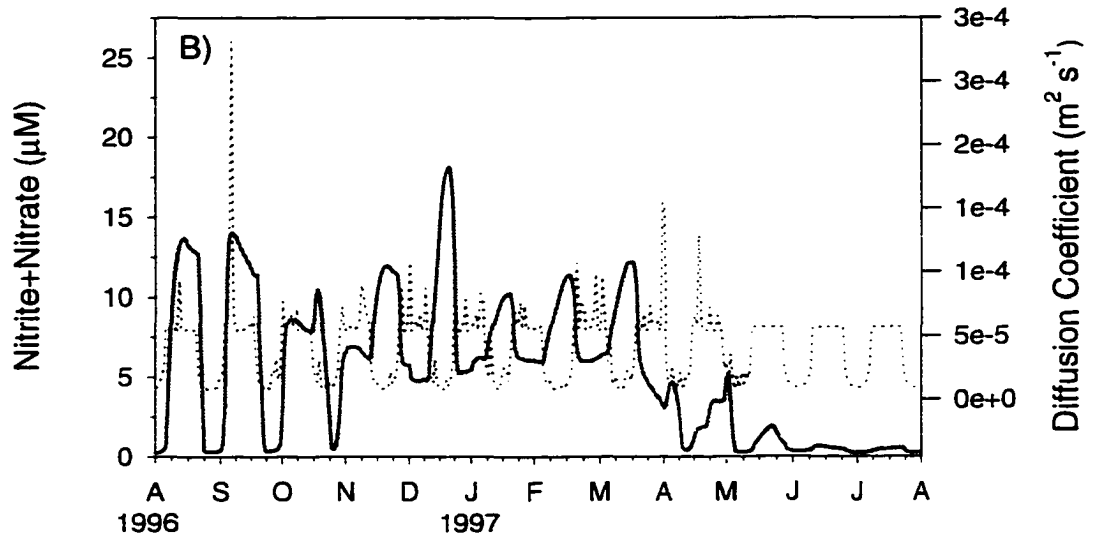
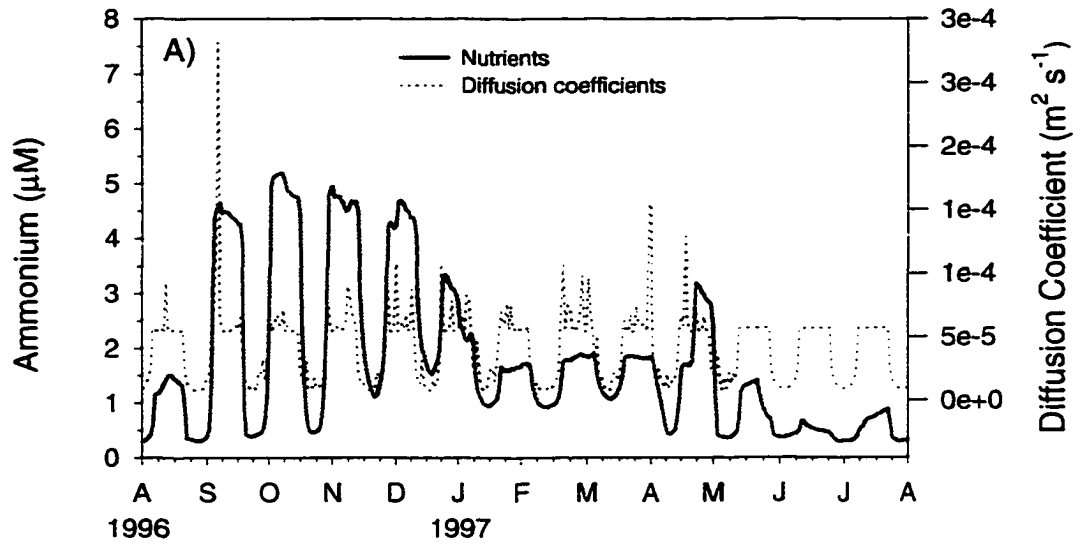
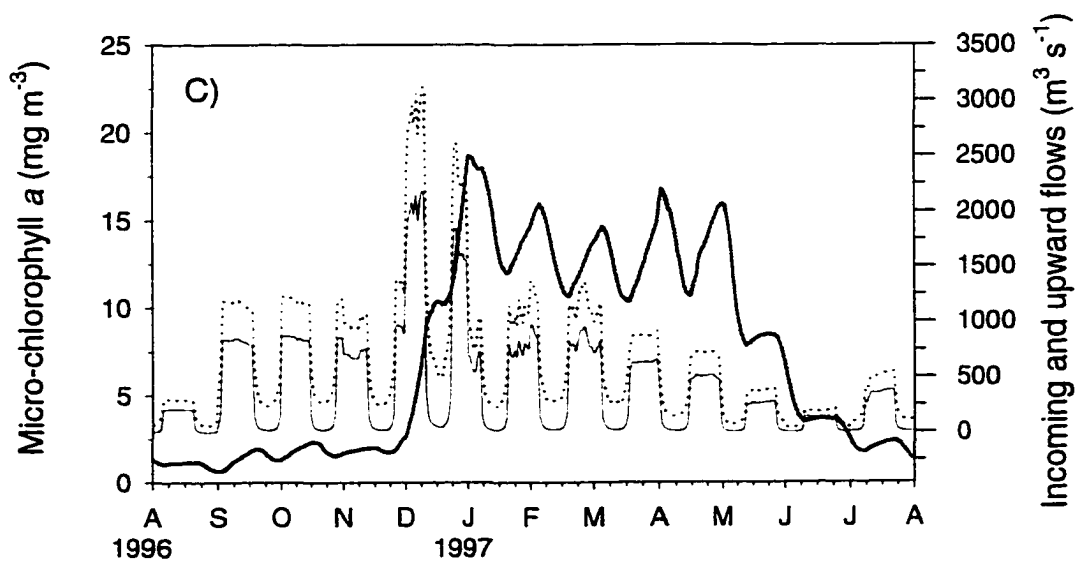
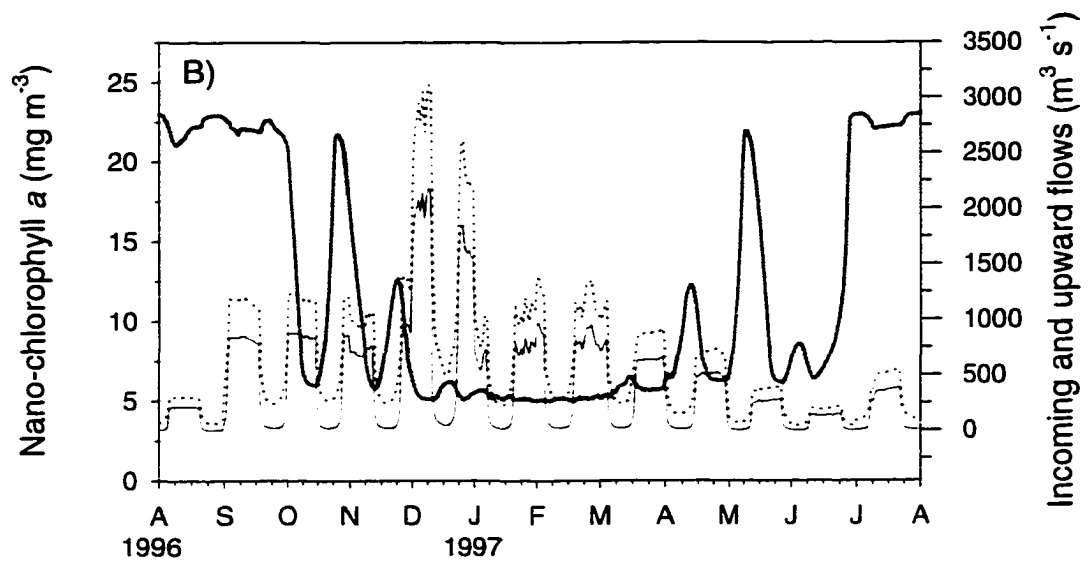
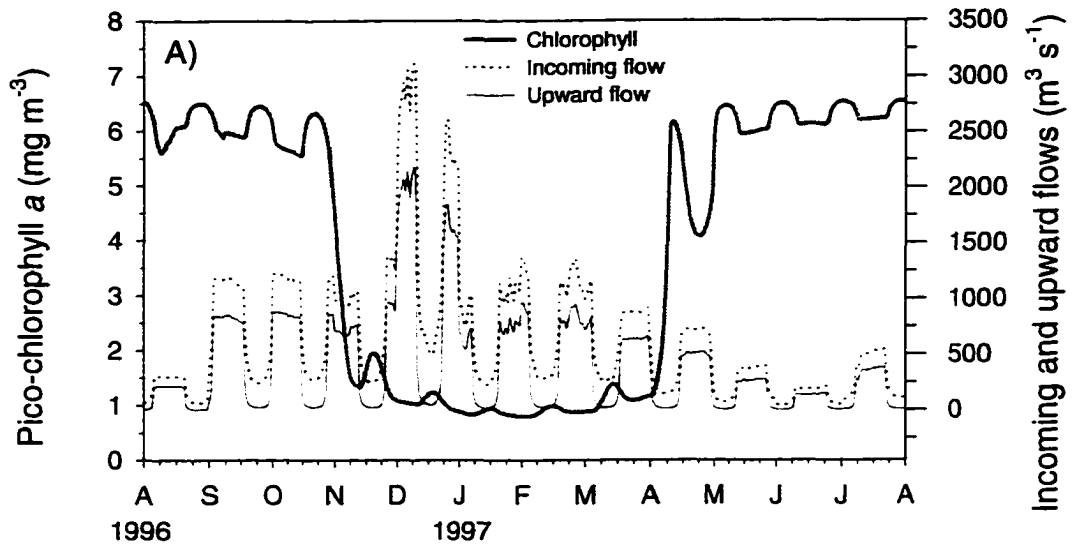


Fig. 14. The distributions of incoming (horizontal) and upward flows and chlorophyll a (pico-, nano-, and micro-sized) from the nominal model run of the ecosystem model.



Percent changes in the concentrations of state variables are presented in Table 8 given $\pm 10\%$ and $\pm 20\%$ changes in incoming source water from upriver and from bottom water respectively. Only picophytoplankton, microzooplankton and POC were sensitive to the changes in picophytoplankton densities in the incoming source water from upriver. All state variables except pico-, microphytoplankton and mesozooplankton were insensitive to change in nanophytoplankton densities in incoming source water from upriver. Microphytoplankton and orthophosphate were sensitive to change in microphytoplankton densities in coming source water from upriver. Only nitrite+nitrate concentrations were sensitive to change in incoming source. None of state variables were sensitive to the incoming source for pico-phytoplankton from bottom water whereas microzooplankton and orthophosphate were sensitive to change in the incoming source for nano-phytoplankton from bottom water. Micro-phytoplankton were sensitive to change in their incoming source from bottom water. Ammonium and orthophosphate were also sensitive to change in their incoming source from bottom water.

DISCUSSION

The microbial food web has become considered a principal component influencing water column processes and has been incorporated into modeling efforts of plankton food webs since the 'microbial loop' concept was introduced by Pomeroy 1974 and Azam et al. (1983). Complexity of the plankton food web has been addressed using allometric relationships, i.e., the size-dependence of plankton metabolic processes (e.g.

Table 8. Percent change in concentrations of state variables when boundary conditions (incoming source from upriver (*xin*) and bottom water (*xbt*)) were changed. These sensitivity analyses were performed given $\pm 10\%$ and $\pm 20\%$ changes in the incoming source from upriver and from bottom water respectively; % changes $\geq 10\%$ marked by *.

Boundary Variable:	<i>xin</i> (1)	<i>xin</i> (2)	<i>xin</i> (3)	<i>xin</i> (11)	<i>xbt</i> (1)	<i>xbt</i> (2)	<i>xbt</i> (3)	<i>xbt</i> (10)	<i>xbt</i> (12)
<i>X</i> (1): <i>PP</i>	41.7*	3.39	0.24	0.24	0.41	0.68	0.09	0.06	0.06
<i>X</i> (2): <i>NP</i>	2.41	70.4*	2.16	1.61	0.04	3.94	0.48	0.49	1.16
<i>X</i> (3): <i>MP</i>	2.70	9.84	136.3*	0.55	0.04	3.39	24.4*	0.24	5.21
<i>X</i> (4): <i>HB</i>	5.81	10.7*	2.63	1.49	0.03	3.64	0.55	0.38	0.19
<i>X</i> (5): <i>HFC</i>	4.87	13.8*	2.12	0.36	0.07	3.20	0.42	0.10	0.29
<i>X</i> (6): <i>Z1</i>	10.4*	41.5*	7.51	0.13	0.28	19.6*	1.16	0.06	0.63
<i>X</i> (7): <i>Z2</i>	1.25	9.20	6.48	0.31	0.03	1.70	4.05	0.19	1.47
<i>X</i> (8): <i>POC</i>	11.8*	10.9*	4.65	0.20	0.09	1.05	0.59	0.07	0.22
<i>X</i> (9): <i>DOC</i>	5.62	16.2*	2.04	0.66	0.04	1.86	0.15	0.17	0.36
<i>X</i> (10): <i>NI</i>	4.89	13.9*	1.82	1.42	0.09	3.55	0.45	21.1*	0.42
<i>X</i> (11): <i>N2</i>	8.02	22.3*	9.56	60.3*	0.05	2.41	1.70	11.3	1.83
<i>X</i> (12): <i>P</i>	9.52	17.4*	10.7*	1.14	0.08	16.1	2.03	0.43	28.6*

Fenchel, 1974; Peters, 1983; Joint, 1991). Incorporation of such general size scale relationships for planktonic dynamics have provided a straight forward approach for plankton ecosystem modeling efforts (e.g. Moloney and Field, 1991, Painting et al., 1993, Tamsalu and Ennet, 1995). This approach simplifies the process to calibrate parameters for various size class components in a aquatic food web system, reducing the number of parameters to be evaluated (Ducklow 1994). However, the approach may greatly reduce the explanatory capability of the ecosystem model while it simplifies the problem of parameter estimation (Wetzel 1994). For the model given here, allometric relationships were employed for estimating maximum growth rate (Equation 12), half saturation constants (Equation 15) and sinking rate of phytoplankton to differentiate the processes based on cell size. The size dependence of parameters governing the photosynthesis-light relations has not been well established to date. For this model, different values of optimal light intensity (I_o) were used for each size class of phytoplankton (see Appendix D) to account for any size dependence of the parameters. Lower light optima were selected for large cells (c.f. Laws, 1975) and the values were determined by model calibration.

The York River ecosystem model also employed density-dependent feedback control terms, a priori derivations based on testable underlying assumptions (e.g. Wiegart, 1979) which have been documented as far superior to empirical equations for studying trophic interactions among biotic compartments in the microbial food web (Wetzel, 1994). The ecosystem model uses these derivations rather than mechanistic or empirical equations for C flows between predators and prey, and also between heterotrophic bacteria and DOC.

Incorporation of physical processes is also essential in estuarine ecosystem process modeling since estuaries represent complex environments in which freshwater and tidal energy inputs interact to affect biological and/or ecological processes. The relationships between physical processes and plankton population dynamics in coastal estuarine systems have received increasing attention recently (Peterson and Festa, 1984, Cloern, 1991, Eldridge and Sieracki, 1993, Videgar et al., 1993). The ecosystem model presented here includes advection and diffusion by incorporating empirical equations to estimate residual velocities in x and z directions and diffusion terms reflecting spring-neap, tidally induced stratification and destratification.

The results of model validation (Fig. 4, 5, 6) indicated that the ecosystem model captures the dynamics of the principal components of the plankton community. Based on the results of model sensitivity analysis (Table 4, 5), the model is also relatively robust since it was not greatly sensitive to changes in most parameters. Therefore, the model could be used to examine various hypotheses suggested in the previous studies on phytoplankton dynamics in the York River estuary (Section I and II).

The EPA long-term data analyses (Section I) indicated that phytoplankton dynamics in the York River estuary may be controlled by abiotic mechanisms i.e., bottom-up control rather than trophic, biotic interactions i.e., top-down control. Results of model sensitivity analyses (Table 4) supported the conclusion since phytoplankton were not sensitive to changes in parameters related to trophic interactions and other biological processes including feeding preference (p_{ij}), mortality rate (rm) and exudation rate (rex). Microphytoplankton were sensitive to change in cell size ($xM(3)$) and bed shear velocity ($shrvel$). Mesozooplankton were sensitive to changes in parameters related

to biological processes suggesting that they may be controlled by biotic factors rather than abiotic mechanisms. Model sensitivity analysis for POC suggests that it is important to clarify the leaching rate (i.e., C flow between POC and DOC compartments).

Nutrients were sensitive to change in C:N ratio or C:P ratio indicating that it is important to use pertinent values for the ratios in the model.

Model sensitivity analyses of forcing variables (Table 6) suggest that small cells (pico-, nano-phytoplankton) may be regulated by light and temperature dependent metabolism since pico-phytoplankton were sensitive to change in incident radiation and temperature. Seasonal distributions of small cells (Fig. 5C, 5D) were also in phase with those of incident radiation and temperature (Fig. 4A, 4B) supporting the hypothesis. Results from sampling data in Section II showed a significant positive correlation between pico-sized chlorophyll *a* and temperature (Table 8). The small cells were also sensitive to changes in light attenuation.

Nano- and micro-phytoplankton, especially, were sensitive to changes in top to bottom salinity difference suggesting that larger cells may be regulated by physical processes such as tidal mixing (see Equation 8, 10). However, the response of phytoplankton to change in top to bottom salinity difference was different based on cell size (Fig. 8). Biomass of small cells, especially nano-sized, increased (Fig. 8A, 8B) when the salinity difference increased (+20 %) whereas biomass of large cells, micro-sized, decreased as the salinity increased (+20 %). This result suggests that growth of small cells may be enhanced by stratification whereas growth of large cells may be enhanced by destratification. This conclusion was reinforced when we examined the relationship between phytoplankton and diffusion coefficient distributions which was negative for

small cells and positive for large cells over the fortnight cycle (Fig. 12). The pattern for small cells is in contrast to the results observed in the EPA long-term data analyses (see Fig. 9 in Section D) whereas it agrees with the observation by Ray et al. (1989) in the mesohaline zone of the York River estuary. Ray et al. (1989) observed peak abundances of cyanobacteria and diatoms during periods of stratification and minima during periods of destratification. Using a numerical algal growth model controlled only by light limitation, Ray et al. (1989) concluded that cyanobacterial growth is limited by light availability in the surface water since vertical mixing increases the mixed layer depth and decreases light. A food web model (Eldridge and Sieracki, 1993) documented that changes in mixed-layer depth determines light availability regulating cyanobacterial growth rates in the mesohaline zone of the York River estuary. Therefore light availability coupled with the water column stratification-destratification cycle may be the major controlling factors for growth of small cells during the warm season in surface waters of the mesohaline zone. Based on long-term data analysis and a simulation model for the South San Francisco Bay, Cloern (1991) also documented that the temporal variation of phytoplankton biomass and production is largely driven by variation in physical forcings that control vertical tidal mixing. The model simulated the bloom dominated by nanophytoplankton which occurred under slow vertical mixing conditions as a result of rapid phytoplankton growth in the euphotic zone, coupled with slow sinking and vertical diffusion from surface water to the lower water column and sediment where grazing occurs. The models (Ray et al., 1989, Cloern, 1991, Eldridge and Sieracki, 1993), however, did not include nutrients which also serve as an important controlling factor for phytoplankton dynamics. Results of my study suggested that tidal mixing is a

major mechanism for supplying benthic-regenerated nutrients to the surface water during the warm season and the nutrients may be an important source for growth of small cells under elevated light levels during stratification (see Fig. 9, Fig. 12, Fig. 13). The importance of the water column stratification-destratification cycle for nutrient supply was also addressed by examining the correlations of bottom ammonium and orthophosphate vs. surface-bottom salinity difference in Section I of this dissertation.

Microphytoplankton were sensitive to change in bed shear velocity which determines the diffusion coefficient (Equation 7) as shown in Table 4 as well as change in top-bottom salinity difference. Stocks of large cells were positively related to horizontal and vertical flows (Fig. 14C). These results suggested that stocks of large cells may be determined by the physical processes of diffusion and advection. Effects of diffusion and advection on phytoplankton dynamics were investigated by removing the physical terms from the nominal model (Table 7, Fig. 10). Nano- and micro-phytoplankton, especially, were sensitive to the removal suggesting that populations of large cells may be controlled by physical processes including advection and diffusion in the lower part of the York River system. The model analysis suggested that winter-spring blooms of large cells are the consequence of physical processes including advection and diffusion rather than *in-situ* production considering their response to removal of the physical processes (Fig. 10) and nutrient input from upriver and bottom water (Table 8). Seasonal distributions of chlorophyll *a* from EPA long-term data showed that maximum chlorophyll *a* blooms develop in the region located more upriver than the modeled area of the estuary (see Fig. 3 of Section I). Bottom concentrations of chlorophyll were much higher than surface concentrations during winter-spring at the

lower reach of the York River (station WE4.2, Fig. 11 of Section II). The high bottom water concentrations of chlorophyll *a* may serve as a major source for winter-spring blooms of large cells by physical processes including advection and diffusion rather than by growth of large cells through nutrient uptake coupled with light availability. Possible mechanisms for the high bottom concentrations of chlorophyll *a* were discussed in Section II of this dissertation.

CONCLUSIONS

We developed a tidally-averaged ecosystem model that incorporated physical mechanisms including advection and diffusion with a neap-spring, fortnightly tidal cycle to investigate the controlling factors for size-structured phytoplankton dynamics in the mesohaline zone of the York River estuary. The realistic ecosystem model and analyses with the model supported the hypothesis established from analyses of EPA long-term datasets that phytoplankton dynamics appear controlled to large extent by resource limitation (bottom-up control) rather than zooplankton grazing (top-down control) in the York River estuary. Larger, mesozooplankton appear to be controlled by biotic mechanisms. The model analysis also showed that growth of small cells (pico-, nano-sized) may be regulated by light availability and temperature dependent metabolism on a seasonal basis. The simulated high-frequency fluctuations (days) of small cell population densities were phased with the neap-spring tidal cycle (fortnight) indicating that growth of cells over shorter time frames may be controlled by light availability coupled with

water column stratification–destratification, and supported by the input of benthic-regenerated nutrients into the surface water through vertical mixing especially during the warm season in the mesohaline zone. Their growth may be limited by light availability during destratification (tidal mixing) because vertical mixing increases the mixed layer depth and decreases light. In contrast to small cells, biomass accumulation of large cells may be a consequence of vertical and horizontal transport of cells through advection and diffusion from upriver and bottom water rather than *in-situ* production. This study suggests that it is important to refine the physical description in the ecosystem simulation model and to consider quality (size structure) as well as quantity (biomass) of phytoplankton to better understand phytoplankton dynamics in coastal estuarine environments.

LITERATURE CITED

- Azam, F., Fenchel, T., Field, J. G., Gray, J. S., Meyer-Reil, L. A. and Thingstad, F.. 1983. The ecological role of water-column microbes in the sea. *Mar. Ecol. Prog. Ser.*, 10: 257-263.
- Alpine, A. E. and J. E. Cloern. 1992. Trophic interactions and direct physical effects control phytoplankton biomass and production in an estuary. *Limnol. Oceanogr.* 37(5): 946-955
- Aksnes, D. L. and Lie, U. 1990. A coupled physical-biological pelagic model of a Shallow Sill Fjord. *Estuar. Coast. Shelf Sci.* 31:459-486.
- Armstrong, R. A. 1994. Grazing limitation and nutrient limitation in marine ecosystems: Steady state solutions of an ecosystem model with multiple food chains. *Limnol. Oceanogr.* 39(3):597-608.
- Barthel, K. G. 1983. Food uptake and growth efficiency of *Eurytemora affinis* (Copepoda:Calanoida). *Mar. Biol.* 74:269-274.
- Biebl, R. and McRoy, C. P. 1971. Plasmatic resistance and rate of respiration and photosynthesis of *Zostera marina* at different salinities and temperatures. *Mar. Biol.* 8:48-56.
- Boyer, J. P., R. R. Christian and D. W. Stanley. 1993. Patterns phytoplankton primary productivity in the Neuse River estuary, North Carolina, USA. *Mar. Ecol. Prog. Ser.* 97:287-297.
- Caraco, N. F., J. J. Cole, P. A. Raymond, D. L. Strayer, M. L. Pace, S. E. G. Findlay, and D. T. Fisher. 1997. Zebra mussel invasion in a large, turbid river: Phytoplankton response to increased grazing. *Ecology* 78(2): 588-602.
- Carpenter, S. R., and others. 1987. Regulation of lake primary productivity by food web structure. *Ecology* 68:1863-1876.
- Carpenter, S. R., J. F. Kitchell, and J. R. Hodgson. 1985. Cascading trophic interactions and lake productivity. *BioScience* 35:634-639.

- Christian, R. R. and R. L. Wetzel. 1978. Interactions between substrate, microbes, and consumers of *Spartina detritus* in estuaries, pp. 93-113. In: M. Wiley (ed.), *Estuarine Interactions*, Academic Press, N. Y.
- Cloern, J. E. 1996. Phytoplankton bloom dynamics in coastal ecosystems: a review with some general lessons from sustained investigation of San Francisco Bay, California. *Rev. Geophys.* 34(2):127-168.
- Cloern, J. E. 1991. Tidal stirring and phytoplankton bloom dynamics in an estuary. *J. Mar. Res.* 49:203-221.
- Cloern, J. E., Alpine, A. E., Cole, B. E., Wong, R. L. J., Arthur, J. F., Ball, M. D. 1983. River discharge controls phytoplankton dynamics in the Northern San Francisco Bay Estuary. *Estuar. Coast. Shelf Sci.* 16:415-429.
- Day, J. W., Jr., C. A. S. Hall, W. M. Kemp, and A. Yanez-Arancibia. 1989. *Estuarine Ecology*. p147-187. John Wiley & Sons, Inc.
- Denman, K. L. and A. E. Gargett. 1983. Time and space scales of vertical mixing and advection of phytoplankton in the upper ocean. *Limnol. Oceanogr.* 28(5):801-815.
- DiToro, D. M., O'Connor, D. J., Thomann, R. V. 1971. A dynamic model of phytoplankton populations in the Sacramento-San Joaquin delta. *Advan. in Chem. Series* 106:131-180.
- Ducklow, H. W. 1994. Modeling the microbial food web. *Microb. Ecol.* 28:303-319.
- Eldridge, P. M. and M. E. Sieracki. 1993. Biological and hydrodynamic regulation of the microbial food web in a periodically mixed estuary. *Limnol. Oceanogr.* 38(8):1666-16679.
- Eppley, R. W. 1972. Temperature and phytoplankton growth in the sea. *Fish. Bull.* 70:1063-1085.
- Fagerbakke, K. M., Heldal, M., and Norland, S. 1996. Content of carbon, nitrogen, oxygen, sulfur and phosphorus in native aquatic and cultured bacteria. *Aquat. Microbial Ecol.* 10:15-27.
- Fenchel, T. 1974. Intrinsic rate of natural increase: The relationship with body size. *Oecologia (Berlin)* 14:317-326.
- Gallegos, C. L., T. E. Jordan, and D. L. Correll. 1992. Event-scale response of phytoplankton to watershed inputs in a subestuary: Timing, magnitude, and location of blooms. *Limnol. Oceanogr.* 37(4):813-828.

- Haas, L. W. (1975). Plankton dynamics in a temperate estuary with observations on a variable hydrographic conditions. Doctoral dissertation, School of Marine Science, College of William and Mary, Gloucester Point, Virginia.
- Hamilton, P. 1977. On the numerical formulation of a time dependent multi-level model of an estuary, with particular reference to boundary conditions. In: M. Wiley (ed.), *Estuarine Processes: Vol II, Circulation, Sediments and Transfer of Material in the Estuary*, pp 347-364, Academic Press, Inc.
- Hayward, D., L. W. Haas, J. D. Boon, K. L. Webb, and, K. D. Friedland. 1986. Empirical models of stratification variations in the York River estuary, Virginia, USA, p. 346-367. In *Tidal mixing and plankton dynamics. Coastal Estuarine Studies. V. 17*. Springer.
- Hyer, P. V. 1977. Water quality model of York River, Virginia. Special Scientific Report No. 146. Virginia Institute of Marine Science.
- Jaworski, N. A., Lear, D. W., Villa, O., Jr. 1972. Nutrient management in the Potomac Estuary. *Nutrients and Eutrophication. ASLO Special Symp. Vol. I*, pp246-272.
- Joint, I. R. 1991. The allometric determination of pelagic production rates. *J. Plankton Res. 13(Suppl.):69-81*.
- Kindler, D. D. 1991. Contrasts between tidal freshwater and estuarine phytoplankton growth on intracellular and recycled nutrient pools over a summer-winter seasonal transition. M.A. Thesis. School of Marine Science, The College of William and Mary. Gloucester Point, Virginia.
- Kivi, K., S. Kaitala, H. Kuosa, J. Kuparinen, E. Leskinen, R. Lignell, B. Marcussen, and T. Tamminen. 1993. Nutrient limitation and grazing control of the Baltic plankton community during annual succession. *Limnol. Oceanogr. 38(5):893-905*.
- Laws, E. A. 1975. The importance of respiration losses in controlling the size distribution of marine phytoplankton. *Ecology. 56:419-426*.
- Madariaga, I. de, Gonzalez-Azpiri, L., Villate, F., and Orive, E. 1992. Plankton Responses to Hydrological Changes Induced by Freshets in a Shallow Mesotidal Estuary. *Estuar. coast. Shelf Sci. 35:425-434*.
- Malone, T. C. and H. W. Ducklow. 1990. Microbial biomass in the coastal plume of Chesapeake Bay: Phytoplankton-bacterioplankton relationships. *Limnol. Oceanogr. 35(2):296-312*.
- Malone, T. C. and M. B. Chervin. 1979. The production and fate of phytoplankton size fractions in the plume of Hudson River, New York Bight. *Limnol. Oceanogr. 24(4):683-696*.

- Malone, T. C., P. J. Neale and D. Boardman. 1980. Influences of estuarine circulation on the distribution and biomass of phytoplankton size fractions. In: v. Kennedy (Ed.), *Estuarine Perspectives*. Academic Press, New York, pp249-262.
- Malone, T. C., L.H. Crocker, S. E. Pike and B. W. Wendler. 1988. Influences of river flow on the dynamics of phytoplankton production in a partially stratified estuary. *Mar. Ecol. Prog. Ser.* 48:235-249.
- Miller, C. A. and Landry, M. R. 1984. Ingestion-independent rates of ammonium excretion by the copepod *Calanus Pacificus*. *Mar. Biol.* 78:265-270.
- Moloney, C. L. and Field, J. G. 1989. General allometric equations for rates of nutrient uptake, ingestion and respiration in plankton organisms. *Limnol. Oceanogr.* 34:1290-1299.
- Moloney, C. L. and Field, J. G., 1991. The size-based dynamics of plankton food webs. I. A simulation model of carbon and nitrogen flows. *J. Plankton Res.*, 13:1003-1038.
- Monod, J. 1942. *Recherches sur la croissance des cultures bacteriennes*. Paris: Herman et Cie.
- Newell, C. L. and Linley, E. A. S. 1984. Significance of microheterotrophs in the decomposition of phytoplankton: estimates of carbon and nitrogen flow based on the biomass of plankton communities. *Mar. Ecol. Prog. Ser.* 16:105-119.
- Odum, H. T. 1983. *Systems Ecology :An Introduction*. John Wiley & Sons, Inc.
- Painting, S. J., C. L. Moloney, and M. I. Lucas. 1993. Simulation and field measurements of phytoplankton-bacteria-zooplankton interactions in the southern Benguela upwelling region. *Mar. Ecol. Prog. Ser.* 100:55-69.
- Park, K., and A. Y. Kuo. 1993. A vertical two-dimensional model of estuarine hydrodynamics and water quality. Special Report in Applied Marine Science and Ocean Engineering No. 321, School of Marine Science, Virginia Institute of Marine Science, College of William and Mary, Gloucester Point, Virginia.
- Pennock, J. R., and Sharp, J. H. 1994. Temporal alternation between light-and nutrient-limitation of phytoplankton in a coastal plain estuary. *Mar. Ecol. Prog. Ser.* 111:275-288
- Pennock, J. R. 1985. Chlorophyll distributions in the Delaware Estuary: regulation by light-limitations. *Estuar. coast. Shelf Sci.* 21:711-725.

- Peters, R. H. 1983. The ecological implications of body size. Pp.1-329, Cambridge University Press, Cambridge.
- Peterson, D. H. and J. F. Festa. 1984. Numerical simulation of phytoplankton productivity in partially mixed estuaries. *Estuar. coast. Shelf Sci.* 19:563-589.
- Pomeroy L. R. 1974. The ocean's food web: a changing paradigm. *BioScience* 24:499-504.
- Pritchard, D. W. 1965. Lectures on estuarine oceanography. The Johns Hopkins University, Chesapeake Bay Institute and Department of Oceanography. Baltimore, Maryland.
- Ray, T. R., L. W. Haas, and M. E. Sieracki. 1989. Autotrophic picoplankton dynamics in a Chesapeake Bay sub-estuary. *Mar. Ecol. Prog. Ser.* 52:273-285.
- Tamsalu, R. and P. Ennet. 1995. Ecosystem modeling in the Gulf of Finland. II. The aquatic ecosystem model FINEST. *Estuar. coast. Shelf Sci.* 41:429-458.
- Tilman, D. 1982. Resource competition and community structure. Princeton University Press, Princeton, New Jersey.
- Vidergar, L. L., J. R. Koseff and S. G. Monismith. 1993. Numerical models of phytoplankton dynamics for shallow estuaries. Proceedings of the 1993 National Conference on Hydraulic Engineering, ASCE, San Francisco, CA, July, 1993, pp. 1025-1030.
- Wetzel, R. L. 1994. Modeling the microbial loop: An estuarine modeler's perspective. *Microb. Ecol.* 28:331-334.
- Wetzel, R. L. and Christian, R. R. 1984. Model studies on the interactions among carbon substrates, bacteria and consumers in a salt marsh estuary. *Bull. Mar. Sci.* 35:601-614.
- Wetzel, R. L. and Meyers, M. B. 1994. Ecosystem process modeling of submersed aquatic vegetation in the lower Chesapeake Bay. Final report 91993) to United States Environmental Protection Agency Region III, Chesapeake Bay Program Office: Virginia Institute of Marine Science.
- Wiegert, R. G. 1973. A general ecological model and its use in simulating algal-fly energetics in a thermal spring community, pp. 85-102. In: P. W. Geier, L. R. Clark, D. J. Anderson and H. A. Nix (eds.), *Insects: Studies in Population Management, Vol. 1. Occasional Papers, Ecol. Soc. Australia, Canberra.*
- Wiegert, R. G. 1979. Population models: experimental tools for the analysis of ecosystems. pp.239-275, In: Horn D. J., Mitchell R. and Stairs G. R. (eds.).

Proceedings of a colloquium on analysis of ecosystems. Ohio State Univ. Press, Columbus, Ohio

Wiegert, R. G. and R. L. Wetzel. 1979. Simulation experiments with a 14-compartment salt marsh model, pp. 7-39. In: R. F. Dame (ed.), *Marsh-Estuarine Systems Simulation*, Univ. So. Carolina Press, Columbia.

Wojcik, F. J. 1981. Monthly salinity data for the York River plotted by river mile by month. Data Report 17. Virginia Institute of Marine Science, School of Marine Science, College of William and Mary, Gloucester Point, Virginia.

Appendix I. Initial values for state variables and parameter values employed in the ecosystem model; symbol¹ represents state variables in the Fortran90 codes whereas symbol² denotes state variables used in the text of the dissertation.

Description	Symbol ¹	Symbol ²	Value	Source
<i>State Variables, initial conditions</i>				
Picophytoplankton	$X(1)$	$PP(t)$	6.0 mg Chla m ⁻³	Sin (unpublished)
Nanophytoplankton	$X(2)$	$NP(t)$	18.0 mg Chla m ⁻³	Sin (unpublished)
Microphytoplankton	$X(3)$	$MP(t)$	1.0 mg Chla m ⁻³	Sin (unpublished)
Heterotrophic bacteria	$X(4)$	$HB(t)$	0.18 g C m ⁻³	Kindler (1992)
Flagellates & ciliates	$X(5)$	$HFC(t)$	0.01 g C m ⁻³	Kindler (1992)
Microzooplankton	$X(6)$	$Z1(t)$	0.01 g C m ⁻³	EPA monitoring data
Mesozooplankton	$X(7)$	$Z2(t)$	0.002 g C m ⁻³	EPA monitoring data
Particulate organic carbon	$X(8)$	$POC(t)$	0.60 g C m ⁻³	Canuel (unpublished)
Dissolved organic carbon	$X(9)$	$DOC(t)$	2.65 g C m ⁻³	Schultz (unpublished)
Ammonium	$X(10)$	$NI(t)$	5.63 μM	Sin (unpublished)
Nitrite + Nitrate	$X(11)$	$N2(t)$	0.07 μM	Sin (unpublished)
Orthophosphate	$X(12)$	$P(t)$	2.26 μM	Sin (unpublished)
<i>Parameters</i>				
Time step	dt		0.0625 d	Calibration
Starting time	t_{zero}		1.0 d	Calibration
Ending time	t_{end}		1095.0 d	Calibration
Optimum light for picophytoplankton	$xlo(1)$	I_o	20.0 Ein m ⁻² d ⁻¹	Calibration
Optimum light for nanophytoplankton	$xlo(2)$	I_o	5.0 Ein m ⁻² d ⁻¹	Calibration
Optimum light for microphytoplankton	$xlo(3)$	I_o	1.0 Ein m ⁻² d ⁻¹	Calibration
Mass of picophytoplankton cell	$xM(1)$	M	0.088 pg	Moloney & Field (1991)
Mass of nanophytoplankton cell	$xM(2)$	M	16.0 pg	Moloney & Field (1991)
Mass of microphytoplankton cell	$xM(3)$	M	2800.0 pg	Moloney & Field (1991)
Mass of heterotrophic bacteria cell	$hetM(1)$	M	0.088 pg	Moloney & Field (1991)
Mass of heterotrophic flagellate+ciliate cell	$hetM(2)$	M	9.3 pg	Moloney & Field (1991)
Mass of microzooplankton cell	$hetM(3)$	M	9300.0 pg	Moloney & Field (1991)
Mass of mesozooplankton cell	$hetM(4)$	M	9.3×10 ⁶ pg	Moloney & Field (1991)
Denitrification rate	r_{denit}		0.1 d ⁻¹	Calibration
C:N ratio	$CNrat$	$C:N$	6.0	DiToro et al. (1971)
C:P ratio	$CPrat$	$C:P$	42.0	Redfield (1958)
C:N ratio for heterotrophs	$hCNrat$		5.0	Newell and Linley (1984)
C:Chla ratio	$cchl$		50.0	DiToro et al. (1971)
Mortality rate of phytoplankton	rm	r_m	1.0-10.0 %	Calibration
Exudation rate of phytoplankton	rex	r_{ex}	1.0-10.0 %	Calibration
Leaching rate of POC	rl	r_l	20 %	Calibration
Grazing loss rate of POC	rlo	r_{lo}	10 %	Calibration
Fraction of sloppy feeding	fsf	f_{sf}	10 %	Calibration
Fraction of egestion by grazers	feg	f_{eg}	10 %	Calibration
Mortality rate of mesozooplankton	$Z2M$	$Z2M$	25 %	Calibration
Air density	$airden$	ρ_a	1.2×10 ⁻³ g cm ⁻³	Park & Kuo (1993)
Drag coefficient	$dgcoeff$	C_{10}	1.3×10 ⁻³	Park & Kuo (1993)
Shear velocity	$shrvel$	u_*	0.01 m s ⁻¹	Calibration
Surface area of surface layer	$As(1)$		4.81×10 ⁶ m ²	Calculation
Surface area of bottom layer	$As(2)$		2.41×10 ⁶ m ²	Calculation
Water volume of surface layer	$wvol(1)$		40.40×10 ⁶ m ³	Calculation
Water volume of bottom layer	$wvol(2)$		18.32×10 ⁶ m ³	Calculation

Conversion factor for time	<i>sdconv</i>		86400.0	Calculation
Grazer preference for picophytoplankton	<i>p_{ij}(1)</i>	<i>P_{ij}</i>	0.2	Calibration
Grazer preference for nanophytoplankton	<i>p_{ij}(2)</i>	<i>P_{ij}</i>	0.2	Calibration
Grazer preference for microphytoplankton	<i>p_{ij}(3)</i>	<i>P_{ij}</i>	0.2	Calibration
Grazer preference for bacteria	<i>p_{ij}(4)</i>	<i>P_{ij}</i>	0.8	Calibration
Grazer preference for flagellate + ciliate	<i>p_{ij}(5)</i>	<i>P_{ij}</i>	0.8	Calibration
Grazer preference for microzooplankton	<i>p_{ij}(6)</i>	<i>P_{ij}</i>	0.8	Calibration
Donor threshold for picophytoplankton	<i>a_{ij}(1)</i>	<i>A_{ij}</i>	2.0 mg Chl <i>a</i> m ⁻³	Assumption
Donor threshold for nanophytoplankton	<i>a_{ij}(2)</i>	<i>A_{ij}</i>	8.6 mg Chl <i>a</i> m ⁻³	Assumption
Donor threshold for microphytoplankton	<i>a_{ij}(3)</i>	<i>A_{ij}</i>	2.0 mg Chl <i>a</i> m ⁻³	Assumption
Donor threshold for bacteria	<i>a_{ij}(4)</i>	<i>A_{ij}</i>	0.04 g C m ⁻³	Assumption
Donor threshold for flagellate + ciliate	<i>a_{ij}(5)</i>	<i>A_{ij}</i>	0.03 g C m ⁻³	Assumption
Donor threshold for microzooplankton	<i>a_{ij}(6)</i>	<i>A_{ij}</i>	0.009 g C m ⁻³	Assumption
Donor threshold for mesozooplankton	<i>a_{ij}(7)</i>	<i>A_{ij}</i>	0.002 g C m ⁻³	Assumption
Donor threshold for POC	<i>a_{ij}(8)</i>	<i>A_{ij}</i>	0.30 g C m ⁻³	Assumption
Donor threshold for DOC	<i>a_{ij}(9)</i>	<i>A_{ij}</i>	0.90 g C m ⁻³	Assumption
Donor threshold for ammonium	<i>a_{ij}(10)</i>	<i>A_{ij}</i>	0.50 μM	Assumption
Donor threshold for nitrite + nitrate	<i>a_{ij}(11)</i>	<i>A_{ij}</i>	0.71 μM	Assumption
Donor threshold for orthophosphate	<i>a_{ij}(12)</i>	<i>A_{ij}</i>	0.16 μM	Assumption
Donor limit for picophytoplankton	<i>g_{ij}(1)</i>	<i>G_{ij}</i>	0.70 mg Chl <i>a</i> m ⁻³	Assumption
Donor limit for nanophytoplankton	<i>g_{ij}(2)</i>	<i>G_{ij}</i>	4.60 mg Chl <i>a</i> m ⁻³	Assumption
Donor limit for microphytoplankton	<i>g_{ij}(3)</i>	<i>G_{ij}</i>	0.8 mg Chl <i>a</i> m ⁻³	Assumption
Donor limit for bacteria	<i>g_{ij}(4)</i>	<i>G_{ij}</i>	0.02 g C m ⁻³	Assumption
Donor limit for flagellate + ciliate	<i>g_{ij}(5)</i>	<i>G_{ij}</i>	0.01 g C m ⁻³	Assumption
Donor limit for microzooplankton	<i>g_{ij}(6)</i>	<i>G_{ij}</i>	0.007 g C m ⁻³	Assumption
Donor limit for mesozooplankton	<i>g_{ij}(7)</i>	<i>G_{ij}</i>	0.001 g C m ⁻³	Assumption
Donor limit for POC	<i>g_{ij}(8)</i>	<i>G_{ij}</i>	0.20 g C m ⁻³	Assumption
Donor limit for DOC	<i>g_{ij}(9)</i>	<i>G_{ij}</i>	0.6 g C m ⁻³	Assumption
Donor limit for ammonium	<i>g_{ij}(10)</i>	<i>G_{ij}</i>	0.21 μM	Assumption
Donor limit for nitrite + nitrate	<i>g_{ij}(11)</i>	<i>G_{ij}</i>	0.21 μM	Assumption
Donor limit for orthophosphate	<i>g_{ij}(12)</i>	<i>G_{ij}</i>	0.032 μM	Assumption
Recipient threshold for picophytoplankton	<i>a_{jj}(1)</i>	<i>A_{jj}</i>	5.50 mg Chl <i>a</i> m ⁻³	Assumption
Recipient threshold for nanophytoplankton	<i>a_{jj}(2)</i>	<i>A_{jj}</i>	20.6 mg Chl <i>a</i> m ⁻³	Assumption
Recipient threshold for microphytoplankton	<i>a_{jj}(3)</i>	<i>A_{jj}</i>	20.3 mg Chl <i>a</i> m ⁻³	Assumption
Recipient threshold for bacteria	<i>a_{jj}(4)</i>	<i>A_{jj}</i>	0.18 g C m ⁻³	Assumption
Recipient threshold for flagellate + ciliate	<i>a_{jj}(5)</i>	<i>A_{jj}</i>	0.05 g C m ⁻³	Assumption
Recipient threshold for microzooplankton	<i>a_{jj}(6)</i>	<i>A_{jj}</i>	0.065 g C m ⁻³	Assumption
Recipient threshold for mesozooplankton	<i>a_{jj}(7)</i>	<i>A_{jj}</i>	0.015 g C m ⁻³	Assumption
Recipient threshold for POC	<i>a_{jj}(8)</i>	<i>A_{jj}</i>	0.80 g C m ⁻³	Assumption
Recipient threshold for DOC	<i>a_{jj}(9)</i>	<i>A_{jj}</i>	3.0 g C m ⁻³	Assumption
Recipient threshold for ammonium	<i>a_{jj}(10)</i>	<i>A_{jj}</i>	5.0 μM	Assumption
Recipient threshold for nitrite + nitrate	<i>a_{jj}(11)</i>	<i>A_{jj}</i>	14.3 μM	Assumption
Recipient threshold for orthophosphate	<i>a_{jj}(12)</i>	<i>A_{jj}</i>	1.98 μM	Assumption
Maximum recipient density for picophytoplankton	<i>g_{jj}(1)</i>	<i>G_{jj}</i>	6.7 mg Chl <i>a</i> m ⁻³	Assumption
Maximum recipient density for	<i>g_{jj}(2)</i>	<i>G_{jj}</i>	23.6 mg Chl <i>a</i> m ⁻³	Assumption

nanophytoplankton				
Maximum recipient density for microphytoplankton	$g_{jj}(3)$	G_{ij}	22.3 mg Chl a m^{-3}	Assumption
Maximum recipient density for bacteria	$g_{jj}(4)$	G_{ij}	0.20 g C m^{-3}	Assumption
Maximum recipient density for flagellate + ciliate	$g_{jj}(5)$	G_{ij}	0.06 g C m^{-3}	Assumption
Maximum recipient density for microzooplankton	$g_{jj}(6)$	G_{ij}	0.075 g C m^{-3}	Assumption
Maximum recipient density for mesozooplankton	$g_{jj}(7)$	G_{ij}	0.02 g C m^{-3}	Assumption
Maximum recipient density for POC	$g_{jj}(8)$	G_{ij}	1.0 g C m^{-3}	Assumption
Maximum recipient density for DOC	$g_{jj}(9)$	G_{ij}	3.60 g C m^{-3}	Assumption
Maximum recipient density for ammonium	$g_{jj}(10)$	G_{ij}	14.3 μ M	Assumption
Maximum recipient density for nitrite + nitrate	$g_{jj}(11)$	G_{ij}	35.7 μ M	Assumption
Maximum recipient density for orthophosphate	$g_{jj}(12)$	G_{ij}	2.26 μ M	Assumption

•

PROJECT SUMMARY AND SYNTHESIS

**ECOSYSTEM ANALYSIS OF WATER COLUMN PROCESSES IN THE YORK
RIVER ESTUARY, VIRGINIA: HISTORICAL RECORDS, FIELD STUDIES AND
MODELING ANALYSIS**

The main objective of this dissertation research was to develop an ecosystem model and use the model as a tool to investigate principal factors controlling quantity and quality of phytoplankton and nutrient dynamics in the York River estuary. Modeling analysis along with the analyses of EPA long-term data and field data was useful in exploring water column processes in the York River estuary. It must be remembered that plankton dynamics in estuarine systems are complex due to the interactions between plankton and their environments which receive both freshwater and tidal inputs. In Section I of this dissertation, I use a spatially and temporally extensive data set to analyze variations in factors potentially limiting phytoplankton biomass and production in the York River estuary. By affecting residence time, nutrient input, light regime, and tidal mixing, river discharge rates regulate the magnitude, location and timing of phytoplankton blooms in the York River estuarine system. Thus, ecological processes in the York River system are predictable based on the river continuum concept. Phytoplankton growth in tidal fresh water is limited since the residence time (dependent on the river discharge rate) can be less than the cell doubling time. Temperature-dependent metabolism is also an important mechanism in this zone. In the transition zone or turbidity maximum zone, phytoplankton are limited mainly by light and internal processes dependent on temperature and estuarine circulation. In mesohaline regions, riverine nitrite + nitrate input during the winter results in winter-spring blooms at locations experiencing potential nitrogen limitation. Tidal mixing also influences summer phytoplankton dynamics in the mesohaline zone by supplying regenerated nutrients via a predictable cycle of water column stratification-destratification. In

general, phytoplankton dynamics appear controlled by resource limitation (bottom-up control) rather than zooplankton grazing (top-down control).

From analyses of data collected over an annual cycle, I believe that phytoplankton growth in the tidal freshwater zone may be limited by high flushing rates and regulated by light and temperature. The large contribution of microplankton to total phytoplankton biomass is thought to be due to the availability of sufficient nitrite + nitrate compared with other regions in the York River estuary. In the river-estuary transition zone, phytoplankton production is most likely limited by light availability since this region experiences a turbidity maximum during winter. Nanoplankton which dominate the phytoplankton community in the river-estuary transition zone throughout the year are most likely regulated by light. Growth of large cells in this zone is dependent on nitrite + nitrate input but only when light is not limiting. In the mesohaline zone total phytoplankton biomass follows a bimodal seasonal distribution with both summer and winter blooms. During summer small cells (picoplankton and nanoplankton) predominate, while during winter large cells (microplankton) dominate. This seasonal shift in size structure is thought to be due to the different preferences of phytoplankton size classes for "new" (nitrite + nitrate) vs. "old" (ammonium) nutrients in the water column. I conclude from these studies that spatial and seasonal variations in size structure of phytoplankton observed on the estuarine scale is determined both by the different preferences of micro-, nano-, and picoplankton for nutrients and by their different light requirements. These results further indicate that phytoplankton size structure in the York river estuary may be regulated primarily by resource limitation (bottom-up control) rather than zooplankton grazing (top-down control). Consequently,

this study supports the conclusions established from the EPA long-term data analyses on *phytoplankton and nutrient dynamics* and further demonstrates that analyses of size structure are necessary to better understand phytoplankton dynamics including the response of the total phytoplankton population to environmental changes in estuarine systems.

Based on the analyses of both the long-term data and an annual field datasets, I developed a tidally-averaged ecosystem model that incorporated physical mechanisms including advection and diffusion with a neap-spring, fortnightly tidal cycle to investigate the controlling factors for size-structured phytoplankton dynamics in the mesohaline zone of the York River estuary. The realistic ecosystem model and analyses with the model supported the hypothesis established from EPA long-term data analysis that phytoplankton dynamics appear controlled to large extent by resource limitation (bottom-up control) rather than zooplankton grazing (top-down control) in the York River estuary. Larger, mesozooplankton appear to be controlled by top-down mechanisms. The model analysis also showed that growth of small cells (pico-, nano-sized) may be regulated by light availability and temperature dependent metabolism on a seasonal basis. The simulated high-frequency fluctuations (days) of small cell populations were phased with the neap-spring tidal cycle (fortnight) indicating that growth of cells over shorter time frames may be controlled by light availability coupled with water column stratification-destratification, and supported by the input of benthic-regenerated nutrients into the surface water through vertical mixing especially during the warm season in the mesohaline zone. Their growth may be limited by light availability during destratification (tidal mixing) because vertical mixing increases the mixed layer depth

and decreases light. In contrast to small cells, biomass accumulation of large cells may be a consequence of vertical and horizontal transport of cells through advection and diffusion from upriver and bottom water rather than *in-situ* production. This study suggests that it is important to refine the physical description in the ecosystem simulation model and to consider quality (size structure) as well as quantity (biomass) of phytoplankton to better understand phytoplankton dynamics in coastal estuarine environments.

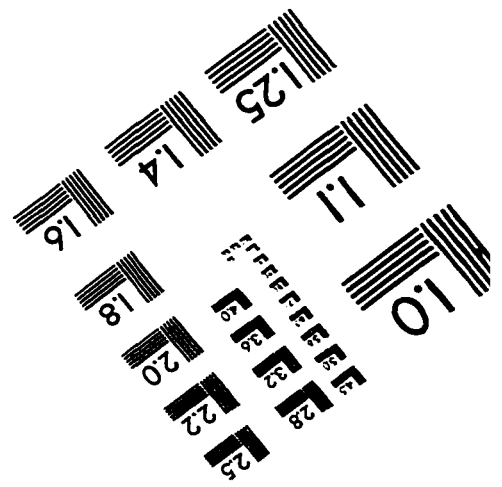
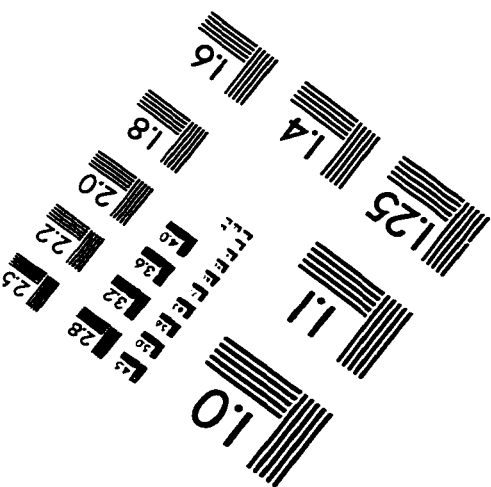
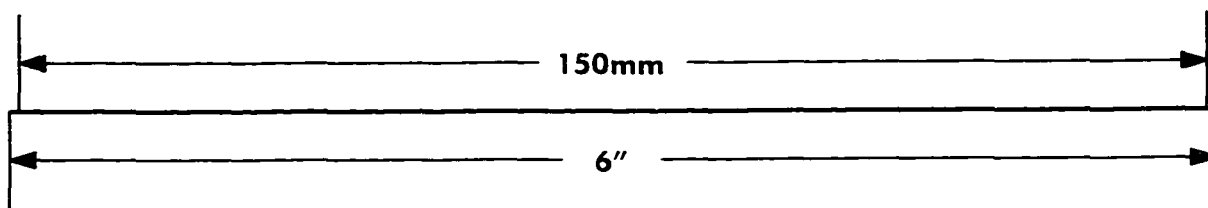
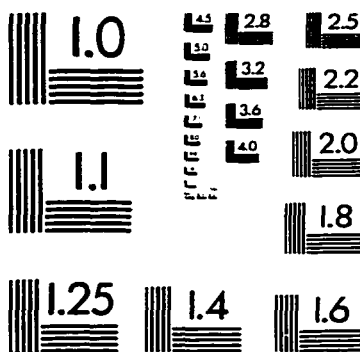
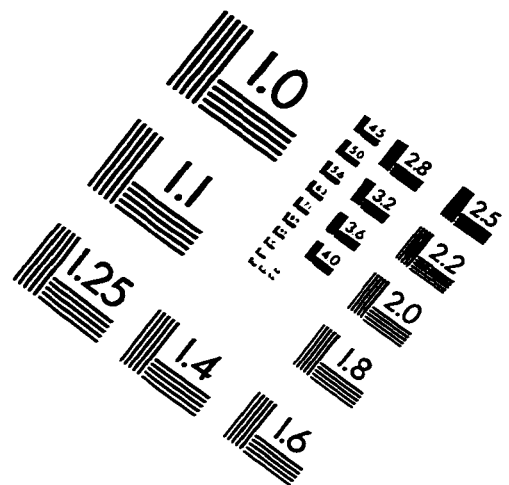
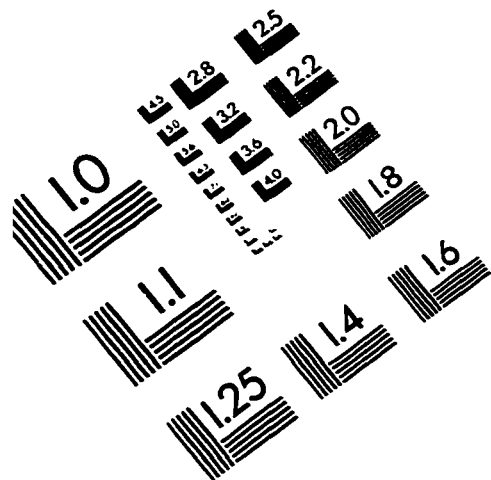
This dissertation research has provided an integrative tool for better understanding water column processes including phytoplankton and nutrients dynamics and their interactions with physical processes in the York River estuary.

VITA

Yongsik Sin

Born in Korea, 16 August 1966. Earned a B.S. in Oceanography from the Chonnam National University in February 1989 and a M.S. in Marine Science from the School of Marine Science, Virginia Institute of Marine Science, College of William and Mary in August 1992. Entered the Ph.D. program in the Biological Sciences Department at the School of Marine Science, College of William and Mary in September 1992. Fulfilled military obligations in Korea from March 1994 to February 1996 and returned to the graduate program in May 1996.

IMAGE EVALUATION TEST TARGET (QA-3)



APPLIED IMAGE . Inc
 1653 East Main Street
 Rochester, NY 14609 USA
 Phone: 716/482-0300
 Fax: 716/288-5989

© 1993. Applied Image, Inc.. All Rights Reserved